SOLAR DISTILLATION OF WATER USING U-TURN INCLINED METAL TUBES AS RECEIVER AND CONDENSER

Hieu Tri Le

A Thesis Submitted in Partial Fulfillment of the Requirements for the

Degree of Doctor of Philosophy of Mechanical Engineering

Suranaree University of Technology

Academic Year 2019

การกลั่นน้ำด้วยพลังงานแสงอาทิตย์โดยใช้ท่อโลหะเอียงวกกลับเป็นตัวรับความร้อนและเป็นคอนเดนเซอร์

นายเฮียว ฉี๋ เล่

SOLAR DISTILLATION OF WATER USING U-TURN INCLINED METAL TUBES AS RECEIVER AND CONDENSER

Suranaree University of Technology has approved this thesis submitted in partial fulfillment of the requirements for the Degree of Doctor of Philosophy.

Thesis Examining Committee

_____
(Assoc. Prof. Dr. Bundit Krittacom)

Chairperson

_____
(Asst. Prof. Dr. Atit Koonsrisuk)

Member (Thesis Advisor)

_____
(Asst. Prof. Dr. Keerati Suluksna)

Member

_____
(Asst. Prof. Dr. Krawee Treeamnuk)

Member

_____
(Asst. Prof. Dr. Pansa Liplap)

Member
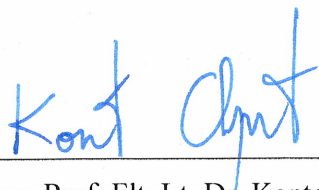
_____
(Assoc. Prof. Flt. Lt. Dr. Kontorn Chamniprasart)

Vice Rector for Academic Affairs

and Internationalization

_____
(Assoc. Prof. Dr. Pornsiri Jongkol)

Dean of Institute of Engineering

เฮียว ฉี่ เล่ : การกลั่นน้ำด้วยพลังงานแสงอาทิตย์โดยใช้ท่อโลหะเอียงวกกลับเป็นตัวรับ
ความร้อนและเป็นคอนเดนเซอร์ (SOLAR DISTILLATION OF WATER USING
U-TURN INCLINED METAL TUBES AS RECEIVER AND CONDENSER)
อาจารย์ที่ปรึกษา : ผู้ช่วยศาสตราจารย์ ดร.อาทิตย์ คูณศรีสุข, 143 หน้า.

การกลั่นน้ำกร่อยโดยใช้แสงอาทิตย์ สามารถช่วยให้น้ำกับ การเกษตร อุตสาหกรรม และ
มนุษย์ สำหรับวิทยาพนธ์นี้ได้นำเสนอการสร้างกลั่นน้ำด้วยแสงแดดรูปแบบใหม่ 3 รูปแบบ และ
รูปแบบทั่ว ๆ จะถูกศึกษาในวิทยาพนธ์นี้ โดยในการทดลองจะทดลองภายใต้สภาพแวดล้อมของ
จังหวัดนครราชสีมา ประเทศไทย โดยการกลั่นโดยใช้แสงอาทิตย์ที่ได้ศึกษาในวิทยาพนธ์นี้จะ
แตกต่างกับระบบกลั่นน้ำโดยใช้แสงอาทิตย์ทั่ว ๆ ไป โดยในระบบกลั่นน้ำในวิทยาพนธ์นี้จะเริ่มต้น
ด้วยให้น้ำจากถังเก็บน้ำไหลไปที่ท่อของอุปกรณ์กลั่นตัว เปรียบเสมือนกับแหล่งทิ้งความร้อนให้กับ
อุปกรณ์กลั่นตัว เพื่อที่จะเพิ่มอัตราการกลั่นตัวของน้ำที่ระเหยตัวอยู่ในภายในอ่างน้ำของเครื่องกลั่น
หลังจากที่น้ำผ่านอุปกรณ์กลั่นตัวแล้วจะไหลกลับเพื่อให้น้ำรับแสงอาทิตย์ เพื่อเพิ่มอุณหภูมิ
หลังจากนั้นจะไหลเข้าสู่ภายในอ่าง การทดลอง ได้ศึกษาอิทธิพลของ ความลึกของระดับน้ำที่ 0.5
เซนติเมตร 1 เซนติเมตร และ 2 เซนติเมตร รวมถึงอัตราการ ไหลของอัตราการปล่อยน้ำสู่เครื่องกลั่น
พบว่า ปริมาณน้ำสะอาดจากกลั่นเพิ่มมากขึ้น 34% จากการความลึกของน้ำเท่ากับ 0.5 เซนติเมตร
เมื่อเปรียบเทียบกับที่ความลึกเท่ากับ 2 เซนติเมตร รวมถึงพบว่า ปริมาณน้ำสะอาดที่ได้จากการกลั่น
เพิ่มมากขึ้น 28% จากอัตราการ ไหลของน้ำที่ไหลเข้าสู่เครื่องกลั่นเท่ากับ 1 ลิตรต่อชั่วโมง
เปรียบเทียบกับอัตราการ ไหลของน้ำเท่ากับ 0.5 ลิตรต่อชั่วโมง

สาขาวิชา วิศวกรรมเครื่องกล   ลายมือชื่อนักศึกษา _____
ปีการศึกษา 2562   ลายมือชื่ออาจารย์ที่ปรึกษา _____

HIEU TRI LE : SOLAR DISTILLATION OF WATER USING U-TURN
INCLINED METAL TUBES AS RECEIVER AND CONDENSER. THESIS
ADVISOR : ASST. PROF. ATIT KOONSRISUK, Ph.D., 143 PP.

SOLAR ENERGY/SOLAR STILL/SOLAR COLLECTOR/DISTILLATION OF
WATER/WATER PRODUCTION.

The solar water distillation distills brackish water, which can help the supply of pure water for agriculture, industry and human being. Three models of solar water distiller and a conventional solar still were fabricated and have been studied experimentally under weather conditions of Nakhon Ratchasima Province, Thailand. Unlike typical solar water distillers, the feed water flows through the condenser as a low-temperature fluid of the condenser to increase the condensation rate of the water evaporates from the basin in the distiller. The feed water then makes a U – turn and flow through the collector leading to an increase of the water temperature and flows into the basin. Effects of water feed rate and water depth in the basin were investigated in this study. The distiller was tested with water depths of 0.5 cm, 1 cm and 2 cm and feed rates of 0.5 L/h and 1 L/h. 34% increase of the fresh water produced was observed when the water depth was 0.5 cm compare to that of 2.0 cm water depth. Also, 28% increase of water production was obtained when the feed rate was 1 L/h compared to that of 0.5 L/h.

School of Mechanical Engineering   Student's Signature _____

Academic Year 2019   Advisor's Signature _____

AKNOWLEDEMENTS

TABLE OF CONTENTS

TABLE OF CONTENTS (Continued)

TABLE OF CONTENTS (Continued)

TABLE OF CONTENTS (Continued)

TABLE OF CONTENTS (Continued)

TABLE OF CONTENTS (Continued)

TABLE OF CONTENTS (Continued)

Page

LIST OF TABLES

LIST OF TABLES (Continued)

LIST OF FIGURES

LIST OF ABBREVITIONS AND SYMBOLS

A	=	Area	m^2
Cp	=	Specific heat capacity	J/kg K
d_w	=	Depth of water in solar still	m
d_o	=	outer diameter of copper tubes	m
d_{in}	=	inner diameter of copper tubes	m
Gr	=	Grashof number	
H	=	Hight	m
h	=	Heat transfer coefficient	W/m^2 K
h_e	=	Evaporative heat transfer coefficient	W/m^2 K
h_r	=	Radiative heat transfer coefficient	W/m^2 K
H_v	=	Latent heat of vaporization	W/m^2 K
I(t)	=	Intensity of solar radiation	W/m^2
k	=	thermal conductivity	W/m K
L_b	=	Length of basin liner	m
L_g	=	Length of glass	m
L_i	=	Length of insulation	m
L_{cd}	=	Length of condenser tubes	m
L_{co}	=	Length of collector tubes	m
L_{rt}	=	Lengnth of rectangular trough	m
M	=	mass	kg

LIST OF ABBREVIATIONS (Continued)

m_f	=	mass flow rate in each tube	kg/s
m	=	mass flow rate at valve	kg/s
m_{ew}	=	hourly yield from solar still	$kg/m^2\,h$
M_{ew}	=	Daily yiel from solar still	$kg/m^2\,day$
n	=	constant of Nutselt number	
N	=	Number of tubes	
p	=	Perimeter	m
P	=	Saturated partial pressure	N/m^2
Pr	=	Prandle number	
Q	=	Heat transfer rate	W
Q_c	=	Convective heat transfer rate	W
Q_e	=	Evaporative heat transfer rate	W
Q_r	=	Radiative heat transfer rate	W
Ra	=	Rayleigh number	
Re	=	Reynold number	
t	=	time	s
T	=	Temperature	^oC
v	=	wind velocity	m/s
V	=	Volume	m^3
α	=	Absorptivity	
ε	=	Emissivity	
ρ	=	Density	kg/m^3

LIST OF ABBREVIATIONS (Continued)

μ	=	Dynamic viscosity	N s/m^2
σ	=	Stefan – Boltzman constant	
σ_b	=	thickness of basin	
σ_i	=	thickness of insulation	
σ_{wc}	=	thickness of wood cover	
ŋ	=	Efficiency	
a	=	ambient	
ag	=	air gap between glass and collector tubes	
b	=	basin liner	
cd	=	condenser tubes	
co	=	collector tubes	
f	=	fluid flow in tubes	
f_icd	=	inlet fluid of condenser tubes	
f_ocd	=	outlet fluid of condenser tubes	
f_ico	=	inlet fluid of collector tubes	
f_oco	=	outlet fluid of collector tubes	
i	=	insulation	
ws	=	water in basin	
wc	=	wood cover	

CHAPTER I

INTRODUCTION

1.1   General introduction

There is nothing more essential in life than water, which is a key factor sustainable future. Although water covers approximately three-quarters of the Earth, a mere 0.014 percentage of water can be used directly for human being and other demands (Kabeel, 2006). Consequently, 844 million people globally lack access to safe water and by 2025, two-thirds of the world's population could be living under water stressed conditions (World Health Organization & UNICEF Joint Monitoring Program (JMP), 2015). The World Economic Forum reported that water crisis is the fourth global risk in terms of impact to society. The main driving forces for the increasing worldwide demand for water are explosion of world population, improving living standards, development of industries and expansion of irrigated agriculture. As the struggle to access to fresh water pose a grand challenge, this causes an uproar demand in desalination technology.

Technology of desalination is a water treatment process by which sea or brackish water is made into potable water. Additionally, water desalination is a well-established technology mainly for drinking-water supply in water scarce regions. Desalinated water can also be crucial in emergency situations where water sources have been polluted by saline incursions, such as in Thailand and Vietnam. Especially, it may be main source of potable water in many islands around the world. Moreover, it has contributed as an additional source of water for agriculture and industry. Desalination

technologies can be separated into three types: thermal desalination technologies, membrane-based desalination technologies and solar desalination technologies (Yacoub Yousef Ahmad Alotaibi, 2015). However, thermal and membrane techniques use electrical power, which associates with environmental issues because a large portion of this power is generated by gas or coal – nonrenewable energy source. It was estimated that the production of 1 million m^3/day requires 10 million tons of oil per year. Current statistics show that globally, fossil fuels account for over 85% our global energy consumption and the world will run out of them within 100 to 200 years. As a result, renewable energy sources (particularly solar energy) have gained more attraction. Utilizing solar energy resource is one of the best ways to reduce our reliance on fossil fuel.

Respectively speaking, solar energy plays an important role for a sustainable development in upcoming years as an alternative energy source with minimal environmental impact. It is a renewable source of energy, requiring low maintenance and easy to install despite of its dependence on sunlight. There are many techniques using solar energy, such as: solar photovoltaic, solar water heaters, air heaters, cookers, dryers and distillation devices, all of which have advanced notably in decades in terms of efficiency and reliability. The world market for solar energy has expanded significantly in the last decade with gratifying gains in technology of various types of solar collector have been achieved. The efficiency of these devices typically ranging from about 40 to 60 % for low and medium temperature applications (Thirugnanasambandam et al., 2010). Therefore, taking advantage of solar energy to distill saltwater is one of the good solutions for the age of water crisis.

The combination of desalination technique with solar energy has been conducted for long history. In fact, the method of using solar still was mentioned in the fourth century B.C (Tiwari et al., 2003) and the earliest research on it was conducted by Arab alchemists in the 16th century (Mauchot, 1869). Solar distillation of water received more interest after the First World War. One possible reason is solar desalination is suitable for remote, arid and semi-arid areas, where drinking water shortage is a major problem and solar radiation is high. The benefit of solar distiller is using its free of sun charge, simple design, maintenance and independent water production. However, entail with them are limitations such as: high initial cost and the intermittent nature of its source of energy, the sun.

1.2 Problem statement

In recent decades, extensive research has been studied on solar desalination systems to improve their productivity and to enhance their cost-effectiveness. Solar basin-type solar stills are potential renewable technology that use solar thermal energy to supply fresh water for human life. these systems have advantages: simple construction, low maintenance requirements, high flexibility and safety in operation. However, the intermittent availability of solar radiation hinders the performance of these systems. Because such systems are often characterized by relatively low production capacity, it is a challenging task to improve the productivity and efficiency of solar water stills.

This research makes a contribution to the growing field of scientific studies of renewable energy applications, and specifically to using solar energy in seawater desalination systems. The original method to enhance the performance of a small-scale

solar desalination system is presented in this study. The research introduces theoretical and experimental investigations of a dynamic solar water desalination using inclined metal tubes as condenser and receiver. It consists of a single basin with condenser tubes cover its top and receiver tubes. The water flows from the water tank will cool down in condenser tubes and then will be heated up in receiver tubes before flowing inside the solar still. This drop in temperature of condenser intensifies the condensation process and the high temperature of water accelerate the evaporation process, which lead to an increase in the productivity of the system.

In this project, a theoretical and experimental investigations were carried out on the performance of single basin solar still covered by tube bank. In the theoretical study, a dynamic mathematical model was developed in MATLAB which consists of a system of ordinary differential equations, to simulate the operation of the proposed system. Experimental tests have been conducted on the developed set-up in the University's Energy Laboratory. Experiments have been conducted under climate condition of Thailand. During these experiments, operational parameters were monitored and recorded. Subsequently, the experimental results obtained were used to examine the accuracy of the mathematical model.

1.3 Objectives

The present work endeavor to create a new technique for water distillation is proposed whereby black metal tubes, much like those used in solar water heater, are employed in place of transparent glasses in traditional distillation devices. The objectives are as follows:

- Conduct experimental study of the water distillation system, and improve its daily yield.

- Develop a theoretical model for the concept to simulate the performance of the propose distiller.

1.4   Scope of this study

Base on the design concept, the physical models of solar still was designed, fabricated and tested under condition weather of Thailand.

An attempt has been made to find the most suitable water depth and mass flow rate for maximizing yield of the solar still.

A mathematical model was developed that can be evaluated the performance of the system, by solving the balance equations from the thermodynamic model.

1.5   Thesis outline

The structure of the thesis is described as following:

Chapter 1 introduce problem statement, advantages of solar energy and desalination of sea water, objectives, scope and outline of thesis. The chapter concludes with the complete outline of the thesis report.

Chapter 2 provides a review of solar distillation of water, consist of principle operation of solar still, parameter effect to efficient of solar still and previous studies improved its productivity.

Chapter 3 depicts design concept, components and fabrication of solar still system, its operation and measured parameters. Based on balance equations and substitute equations, the theoretical model is also presented in this chapter.

Chapter 4 discusses experimental results of 3 models and parameters affect to the performance of solar still. Additionally, we also discuss about theoretical analysis.

Chapter 5 summarizes all main points from experiment and theoretical analysis, including future work.

CHAPTER II

LITERATURE REVIEW

The literature related to water desalination is presented here. Various designs for water desalination are presented. The parameters affect to productivity of solar still was introduced, including controlled and uncontrolled variables. Finally, research works have been done to improve the yield and efficiency of solar still was reviewed.

2.1 Solar distillation of water

Solar still is a device taking advantage solar energy, a source of one of renewable energy to convert brackish water to portable water. Solar distillers can remove effectively many substances and are used in drinking water production from seawater. The technology has been well known all around the world.

2.1.1 Basic principle of solar still process

Desalination is among oldest technology. However, historically its initial goal was to produce salt rather than fresh water purpose. Obtaining freshwater from seawater has only been developed only in the modern decades. The earliest study was conducted by Arab alchemists in the 16th century (Tiwari et al., 2003). Solar distillation is a thermal desalination method which bases on the principle of hydrologic cycle, known as the way to make rain. In 1872, Carlos Wilson designed the first conventional solar still was fabricated by Carlos Wilson in Northern Chile (Julio R. Hirschmann, 1975). It consisted of 64 water basins (a total of 4,459 square meters) made of blackened wood with sloping glass covers. This installation was used to supply

water (20,000 liters per day) to animals working in mining operations (Horace McCracken Joel Gordes 1985). A conventional solar still includes a black basin containing brackish water and glass covering its top. The sun's energy goes through a glass to evaporate water in the still and the produced water vapor subsequently condense on the inner surface of the glass.

Distillation process relates to two separate processes, which are evaporation and condensation. Solar still is always taking place in a closed system. The product can be either the condensate (in case of a solar distillation unit) or the concentrated residue which is not evaporated.

Evaporation, on the one hand is a phenomenon which occurs on the surface of fluid layer, where high energetic molecules leave the compound and thereby change into the gaseous phase (vapor). The higher the water temperature is, the more molecules are changing their state. When evaporation happens, the temperature of the liquid will reduce because of the energy removed from the vaporized liquid. Theoretically, evaporation takes place from the melting-point of a substance onwards, until its boiling point. Additionally, the process will be shorter if liquid absorb more energy. Meanwhile, impurities such as salts and heavy metals will be kept down.

The process of condensation is opposite of to evaporation process: the vapor condenses due to reaching its dew point at a surface which has a lower temperature than itself.

Figure 2.1 shows a schema of the energetic processes in a solar still. The process consists of two parts happen simultaneously:

1. Evaporation process or the heating up of the raw fluid

2. Transformation from the liquid to the gaseous phase.
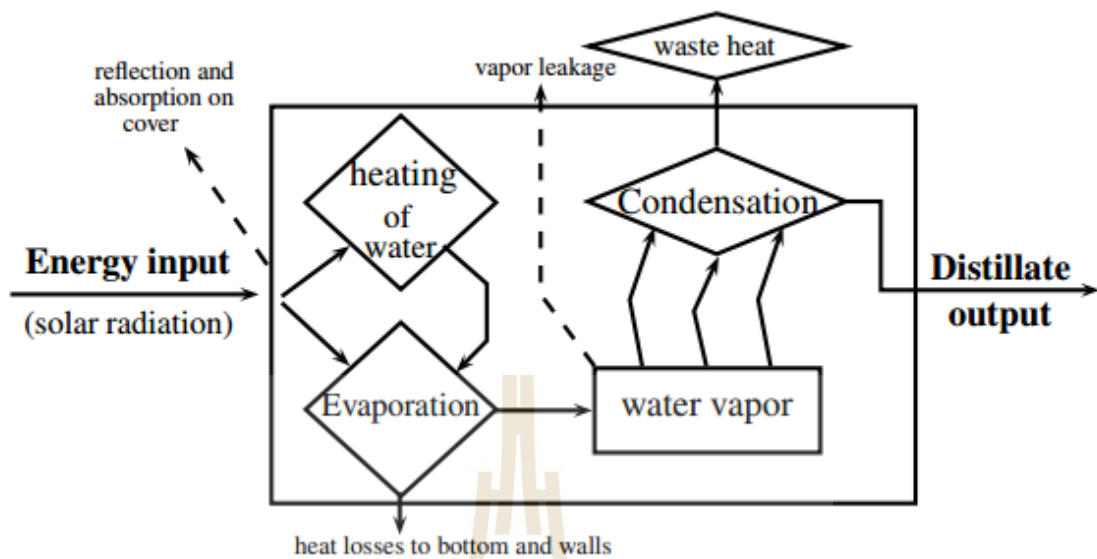
Figure 2.1 Energetic working principle of a single-basin solar still.

2.1.2   Single basin single slope solar still

The single basin type is the simples design and easy to fabricate. The schematic diagram of plastic conventional solar still is shown in Figure 2. Phadatareetal (2007) carried out an experimental study on the effect of water depth on a single basin single slope plastic solar still. From experimental results, Yield of distilled fresh water is 2.1 L/m2/day and its efficiency was 34% with a water depth of 2cm.

Many studies were performed to increase the output of conventional solar still. Abdallah et al. (2008) try to increase the amount of solar radiation absorptance of basin by installing a mirror on higher vertical side. The experimental result showed that the internal mirrors enhanced 30% the efficiency of the system. Velmuruganetal. (2008) modified the single basin solar still by using fins, sponges and wicks for improving its productivity. The cross-sectional view of the basin type solar

still integrated with fins is in Figure 2.3. It was observed that using wick-type still, sponges and fins raised productivity to 29.6%, 15.3% and 45.5% respectively.
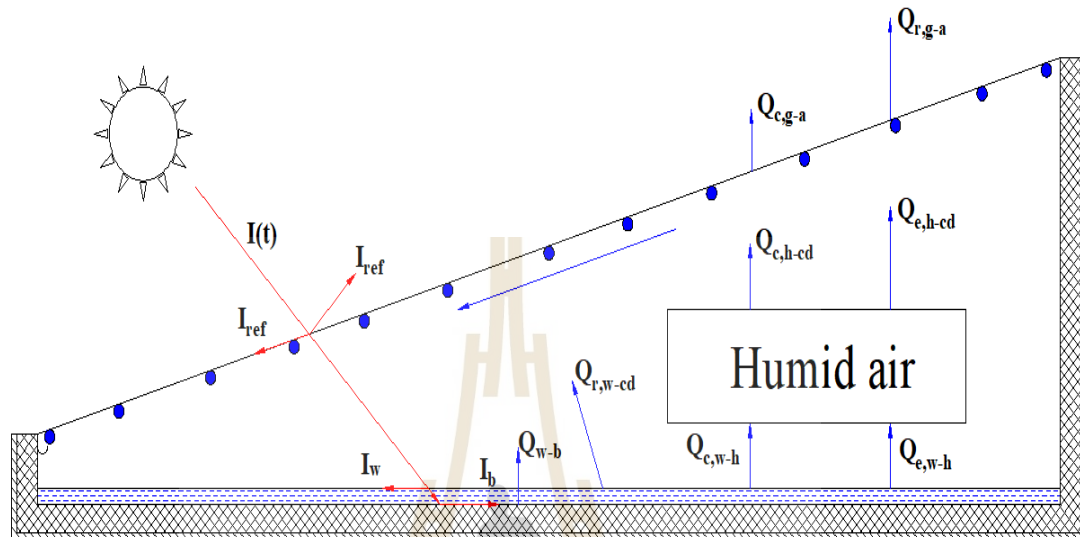
Figure 2.2 Single basin single slope solar still
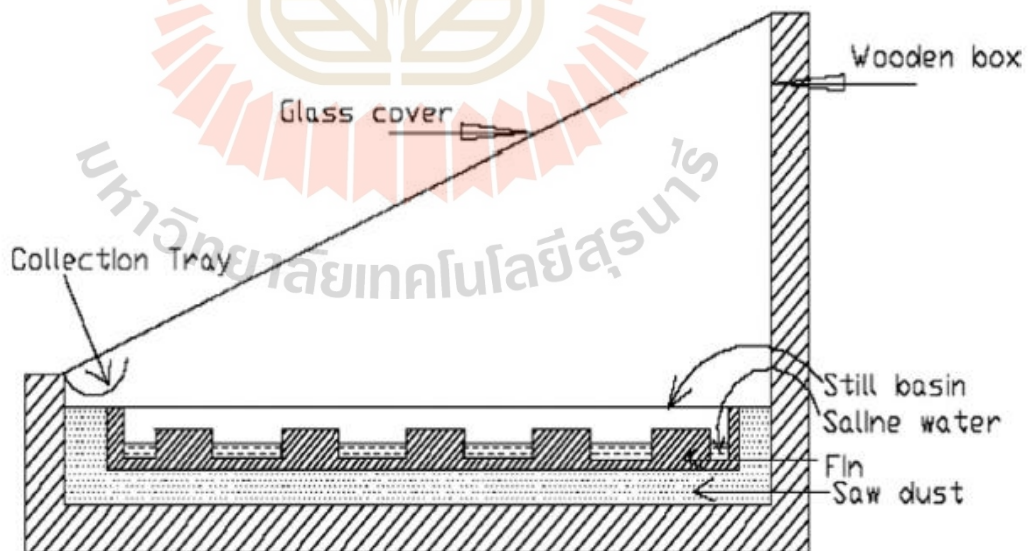
Figure 2.3 Cross-sectional view of solar still integrated with basin type fins

(Velmuruganetal. 2008)

2.1.3   Single basin double slope solar still

Figure 2.4 describe construction of a single basin double slope solar still. It also has basin liner, insulation and top of still is covered by two glass. Kalidasa Murugavel et al., (2011) fabricated and tested double slope solar still with different basin wick at minimum water depth 0.5 cm. He found that light black cotton cloth has highest productivity about 3.49 L/m^2 day.
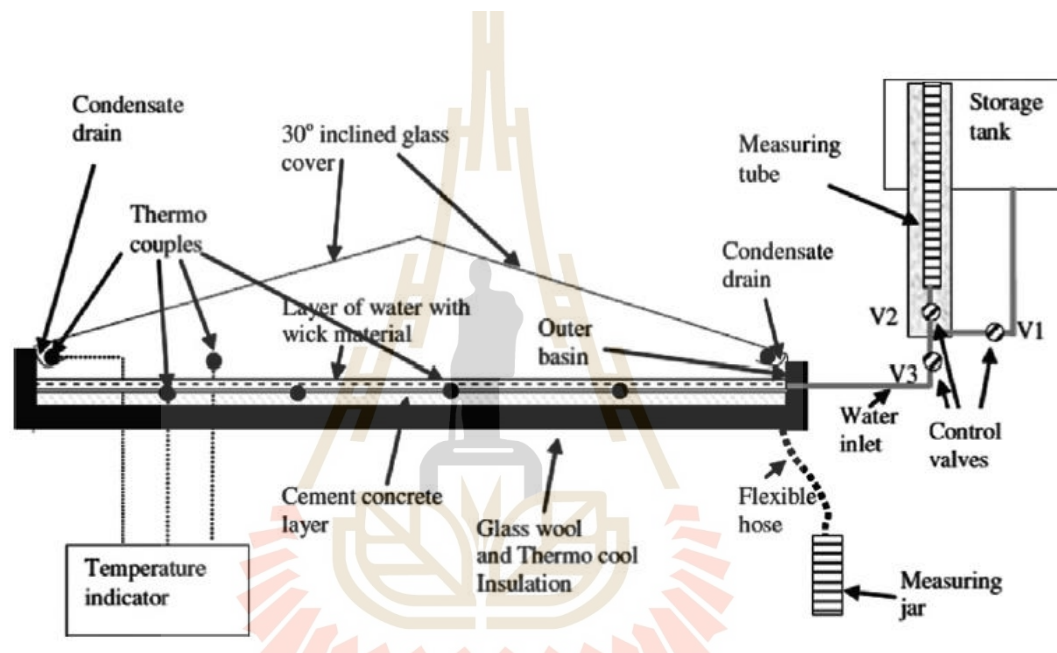
Figure 2.4 Single basin double slope solar still

2.1.4   Other designs of passive solar still

Some researchers designed the single basin type with different shapes of top cover such as: spherical solar still (Dhiman Naresh K., 1988), hemispherical solar still (Arunkumar et al., 2012), concave wick solar still (Shanmugan et al., 2008), tubular solar still (Arunkumar, 2012 and Amimul Ahsan et al., 2010) and pyramid solar still (Taamneh Yazan, 2012), which is illustrated in Figure 2.5 to figure 2.9. Various special

design of single basin passive solar still was reviewed and compared by Durkaieswaran et al., (2015).
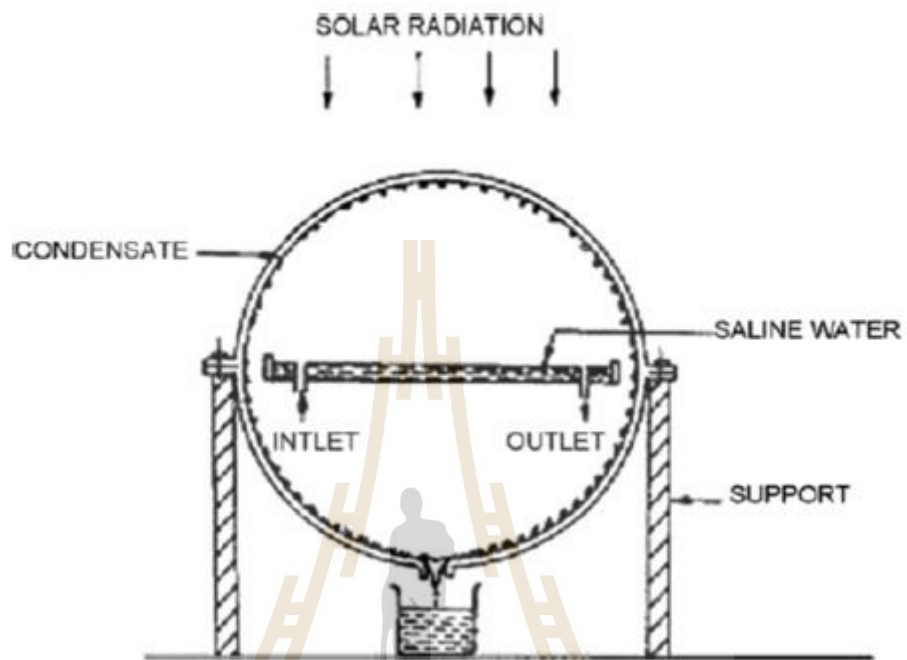
Figure 2.5 Schematic diagram of spherical solar still (Dhiman Naresh K., 1988)
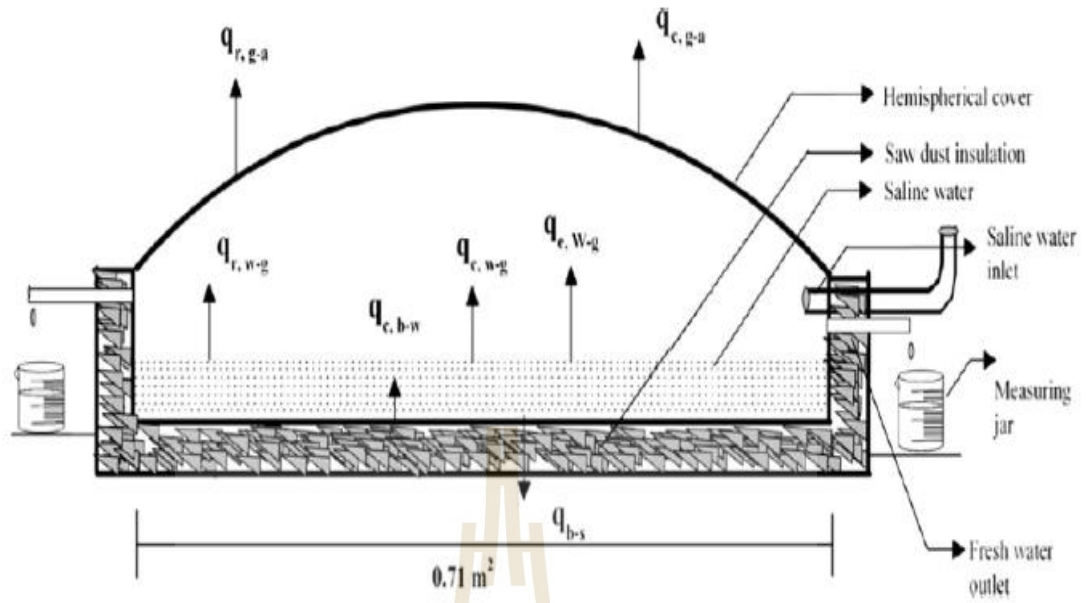
Figure 2.6 Cross sectional view of hemispherical solar still (Arunkumar et al., 2012)
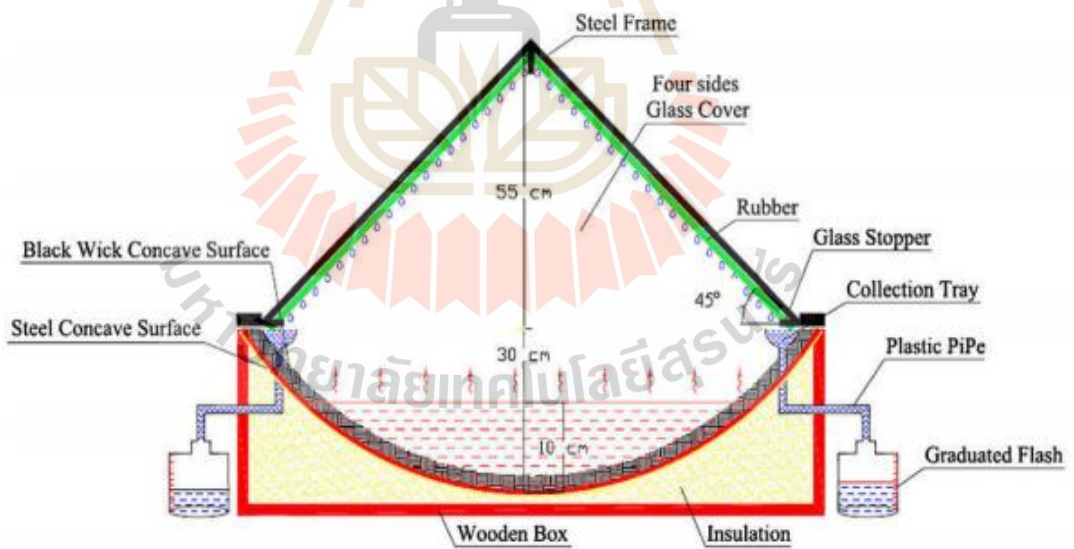
Figure 2.7 Concave solar still (Shanmugan et al., 2008)
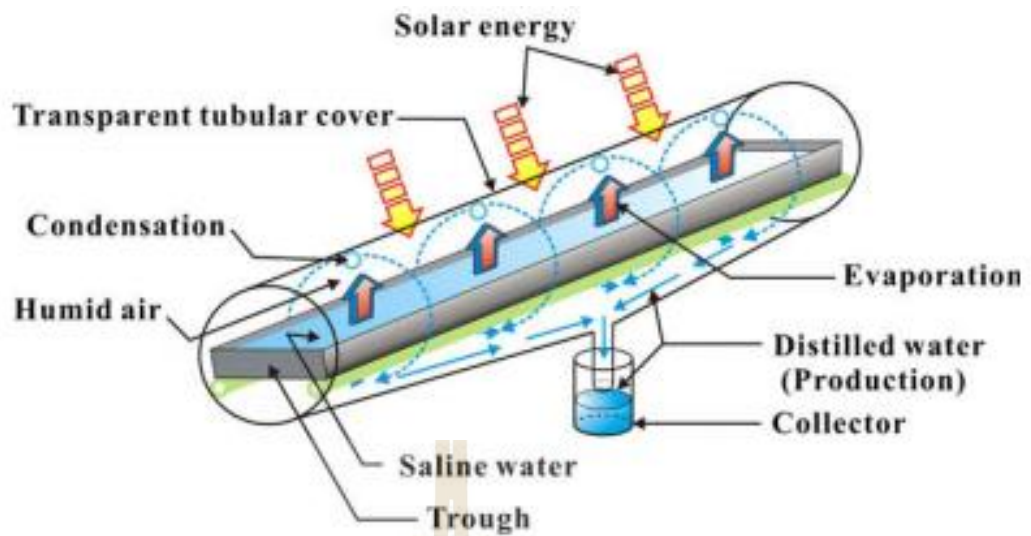
Figure 2.8 Mechanism of tubular solar still (Amimul Ahsan et al., 2010)
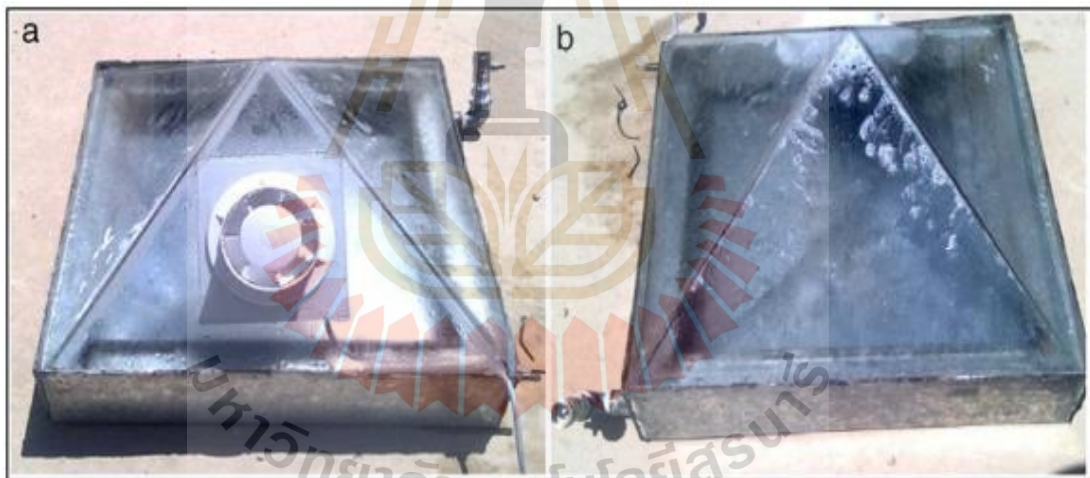
Figure 2.9 Depict of Pyramid solar still with fan (a) and without fan (b)

(Taamneh Yazan, 2012).

Table 2.1 Comparison of productivity of different solar still designs (Durkaieswaran et al., 2015)

No	Details	Productivity(L/m²/day)
1	Single basin single slope solar still	2.1
2	Single basin double slope solar still	3
3	Spherical solar still	2.2
4	Hemispherical solar still	3.5
5	Concave solar still	4
6	Tubular solar still	2.05
7	Pyramid solar still	2.485

2.1.5 Parameter affect to solar still

The estimation of a solar distiller is expressed as the quantity of water productivity. It is important to consider parameters influence on the productivity of solar still, which is reviewed by A. Muthu Manokar [9]. There are many parameters influence on the productivity of solar distiller. Controlled and uncontrolled variable impact to still are listed below:

- Solar radiation
- Temperature of ambient air
- Wind velocity

- Depth of water in the basin

- Material and tilt angle of top cover

2.1.5.1 Intensity of solar radiation

The radiant energy is the most important factor affecting still's operation. Researchers have studied the effect of solar radiation and concluded that it is proportional the productivity of solar still. The more solar energy absorbed by solar still, the more water was distilled.

2.1.5.2 Ambient temperature

Although Few research has investigated the influence of ambient temperature, it is noted that the higher temperature of surrounding air is, the better the performance of solar still is. The work of Nafey et, al. (2000) and Al -Hinai et al. (2002) supported this effect. 3% increase was noted when the ambient increased by 5°C in the former study, and a similar rise by 8.2% is witnessed in a latter study, in which the ambient air temperature raise 10%.

2.1.5.3 Wind velocity

In general, the wind outside of the distiller will cool down the cover's temperature. It will increase the difference between the temperature of condensing surface and brackish water, resulting in high productivity. This indicates the effect of wind velocity on the efficiency of the solar distiller. However, the effect of wind speed on productivity is very low. El-Sebaii (2000) studied the impact of wind speed on different designs of solar stills. He observed that the value of air velocity is independent from the still shape and heat capacity of the brine.

2.1.5.4 Brine level in the basin

The influence of water depth on the performance of solar still was investigated by Khalifa et al. (2009), Tiwari et al. (2007) and Tripathi et al. (2005). Their results showed an output increase as the water level decrease. Additionally, the depth of water is an independent variable of convective heat transfer coefficient between condenser and water.

2.1.5.5 Material and tilt angle of top cover

The productivity of solar distiller depends on the titl angle and material of top cover. Firstly, the solar radiation absorption of basin and water are influenced by the transparent cover. Secondly, the distance between the cover and the surface of the water correlate to the heat and mass transferred inside solar still. Tiwari et al., (2005) experimented to determine the optimization of cover. They suggested that the optimum title angle of glass under winter condition is 45 degree.

2.2   Design objectives for an efficient solar still

A lot of research works has been already done by many scientists to improve the productivity of solar still. Different designs of the active solar water distillation were reviewed by Sampathkumar, 2010. The production rate of solar stills can be elevated by raising the temperature difference between the glass cover and the water in the basin, which is known as the driving force of the evaporation/condensation process. Generally, most of designs focus on enhancing evaporation and condensation rate.

2.2.1   A high feed water temperature

The increased temperature of the water in basin can improve the evaporation rate. We can achieve a high temperature of water if more radiation is absorbed by the feed water and basin liner. Rehim and Lasheen, (2007) used a solar conical concentrator with a focal pipe and simple heat exchanger coupled with a solar desalination system. The results gained a high temperature compared to the conventional one. E1-Bahi and Inan, (1999) and Hiroshi Tanaka, (2006) increased the solar radiation incident on the basin liner by adding internal and/or external reflectors. What they found is that the efficiency increased on average by 48 percent.

Additionally, one more solution to rise the temperature of feed water is to preheat the feed water by circulating it through the solar collector, which has been widely adopted, such as: solar pond, flat plate collectors, parabolic trough collector, evacuated tube collector and evacuated tube heat pipe collectors. An investigation on the performance of an active system under operation of thermo-syphon mode was made in 1983 by Zaki et al.. He reported that the maximum increase of yield by 33 percent when the water in the single slope solar still was preheated in the flat plate collector. In addition, Rai and Tiwari, (1983) conducted an experiment with flat plate collector under forced condition. The sketch of a combination between conventional solar still and flat plat collector is shown in figure 2.10. The results indicated that the daily yield of a coupled single basin still is 24 percent higher than that of an uncoupled one. Comparing to forced circulation mode, natural circulation mode has more benefits in terms of simplicity, reliability and cost effectiveness.
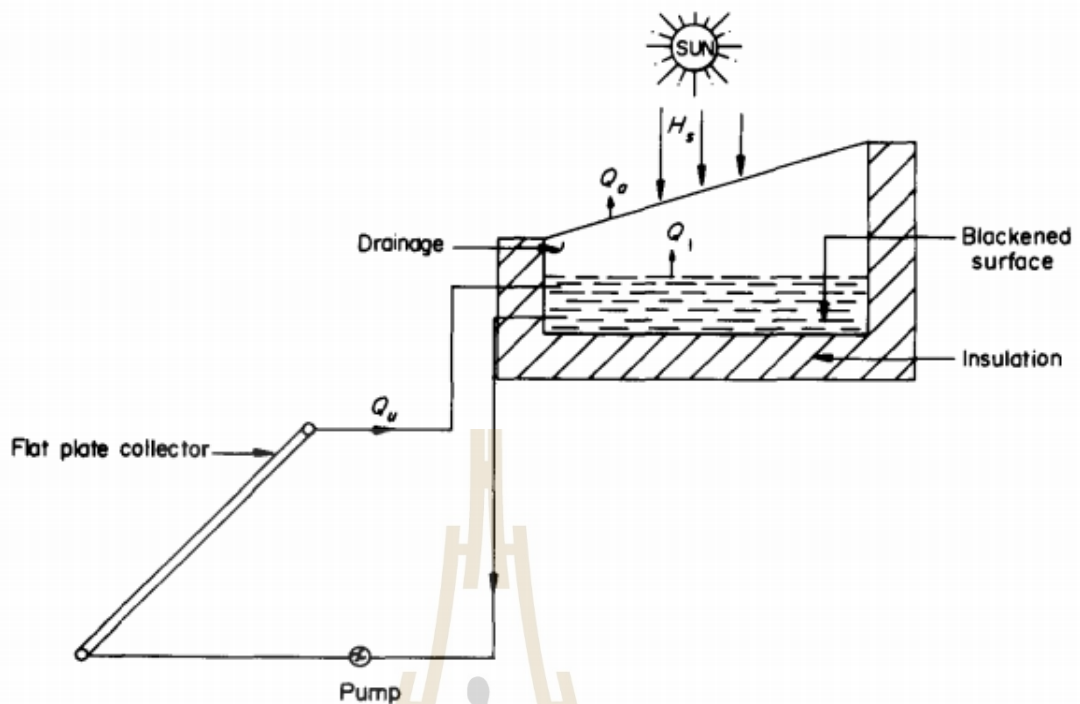
Figure 2.10 Sketch of single basin solar still coupled with flat plate collector

(Zaki et al., 1983).

According to Ragh Vendra Singh (2013), who presented a solar still integrated with evacuated tube collector in natural mode, later on drew the conclusion that the integration of evacuated tubes collector with solar still increases the water temperatures as well as yield. The energy and exergy efficiencies found to be 33.0% and 2.5% respectively. Meanwhile, Shiv Kumar (2014) studied with an evacuated tube collector under forced mode. He discovered that the daily yield obtained in summer and winter was 3.9 kg and 2.75 kg, respectively. The energy and exergy efficiencies are 33.8 percent and 2.6 percent during a typical summer day. The average annual yield per unit of solar collector area has been estimated to be higher than the natural mode. Tiwari et al. (2007) developed the thermal models for active solar stills coupling with different

solar collectors. The total daily yield of passive solar still, FPC, concentrating collector,

ETC and ETC with heat pipe is shown in Figure 2.11.

Figure 2.11 Photograph and schematic diagram of evacuated tube collector augmented

with solar still in force mode
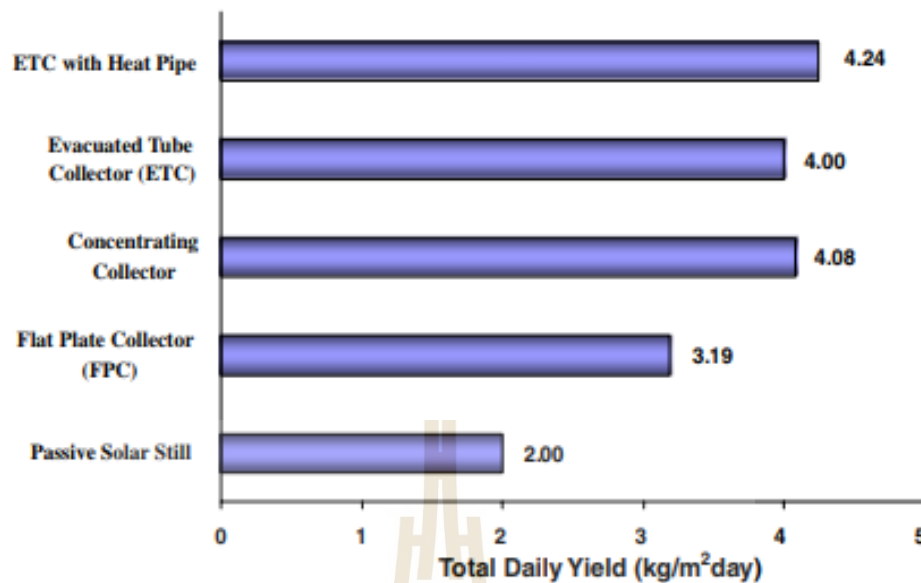
Figure 2.12 Total daily yield for active solar stills (Tiwari et al., 2007)

Moreover, heat losses from the basin walls should be kept low in order to insure the storage of the absorbed thermal energy. The insulation should have high thermal resistance. Hashim (2009) carried out experiment with five solar stills. One of them did not have insulation and four with different material of insulation (an air gap, plywood, hay, and glass wool). The study reported that the productivity of the solar stills with insulation materials were better than solar still without insulation. The effect of insulation thickness was researched by Khalifa and Hamood (2009). He found that a 60 mm thick insulation layer increased productivity by 80 percent compared with one of 30 or 100mm thickness.

2.2.2 A large temperature difference between basin water and condensing surface

The yield of a solar still significantly depends on the temperature gradient between water and condensing surface. Besides increasing the temperature of

brackish water, the previous study focused on reducing temperature of condensing surface. A study by Tiwari et al. (1984) acknowledged the effect of flow of water over the glass cover on the performance of single basin solar still. From that, He concluded that the daily productivity of the still is almost doubled. However, it is opposite with the increase of water flow. Lawrence et al. (1990) investigated the effect of heat capacity on the performance of solar still with water flow over the glass cover and realized that the reduction of glass temperature increases the condensation rate. Similarly, Abu-Hijleh et al. (1996) reduced condenser's temperature by using   a cooling water film. The results showed that the still efficiency raised by 6 percent. Nevertheless, combinations of film cooling parameters can lead to considerable reductions in still efficiency. Zurigat et al. (2004) introduced a regenerative solar still with provision of cooling water to flow in and out of the second effect. The results of the simulations showed that the productivity of regenerative solar still was 20 percent higher than conventional solar still. Arunkumar et al. (2013) studied a tubular solar still with flowing water and air over the cover. Its productivity was 2.05 l/day without the cooling flow and increased to 3.05 l/day and to 5 l/day with flow of cooling air and water respectively.

2.2.3 Utilize latent heat of vaporization

Reusing latent heat of condensation is a solution to enhance the output of solar water distillation, however, few experiments has conducted to utilize it. In solar still, most heat energy are lost to ambient through top cover. Some research was performed to reuse this heat loss to heat up the water in additional distillate, which known as multi stage, multi basin or multi-effect distillation. Originally, multi basin was proposed by Lobo and Araujo (1977). The design of double basin is illustrated in

figure 2.10 showing that the latent heat of vaporization from the lower still basin transfer to the water in the upper basin. Both experimental and theoretical study of a double basin of solar still carried out by Sodha et al. (1980). The result showed that the distillate production of such a still is 36 percentage higher than that of a single basin still.
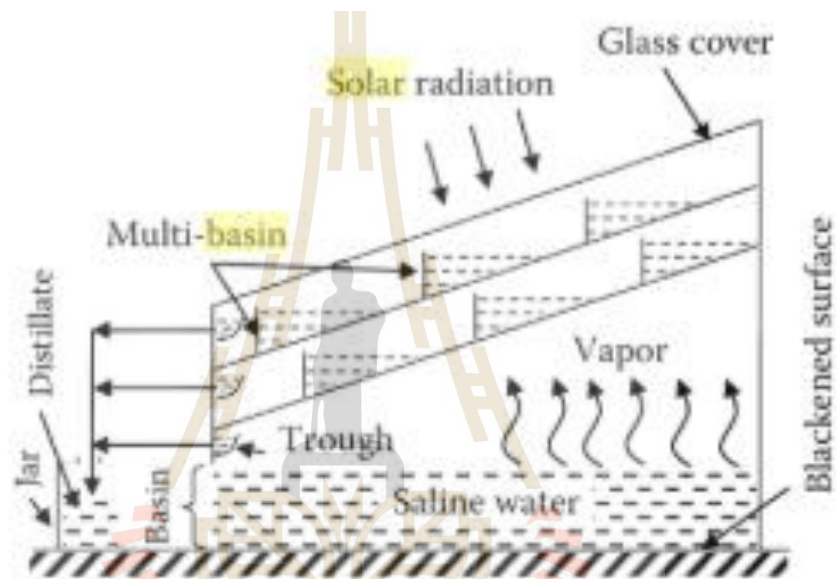
Figure 2.13 Multi – effect multi -basin solar still. (Lobo and Araujo, 1977).

CHAPTER III

EXPERIMENTAL PROCEDURE AND THEORETICAL

ANALYSIS

This thesis uses two methods, which are experimental and theoretical one. First, this chapter will begin with experimental procedure. Three models were illustrated, fabricated and tested under the atmospheric conditions of Nakhon Ratchasima Province, Thailand. The experiments were carried out to achieve a better understanding of the practical behavior of the system. Second, the theoretical analysis is presented, which is a system of energy balance equations applied to the proposed solar still.

3.1 Experimental procedure

In this section, three physical models are presented, which are Model 1, Model 2, and Model 3. First, Model 1 is proposed. After the experimental results of Model 1 were obtained, it was found that the productivity was lower than expected. So, the analysis was conducted and the explanations of low productivity was proposed. Then Model 1 was modified and called as Model 2.

In the second part of this section, the descriptions of Model 2 were presented. According to the experimental results, the productivity of Model 2 is higher than that of Model 1, but still less than the expected one. Then, a minor modification of Model 2 was conducted and Model 2 became "Model 2 with glass". The productivity was slightly higher. So, "Model 2 with glass" was modified and called as Model 3. The description of Model 3 was covered in the third part of this section.

3.1.1 Model 1

This section presents a detailed description of the first physical model of the proposed solar water desalination system in which the desalination process takes place and freshwater is produced.

3.1.1.1 Design concept of proposed solar still
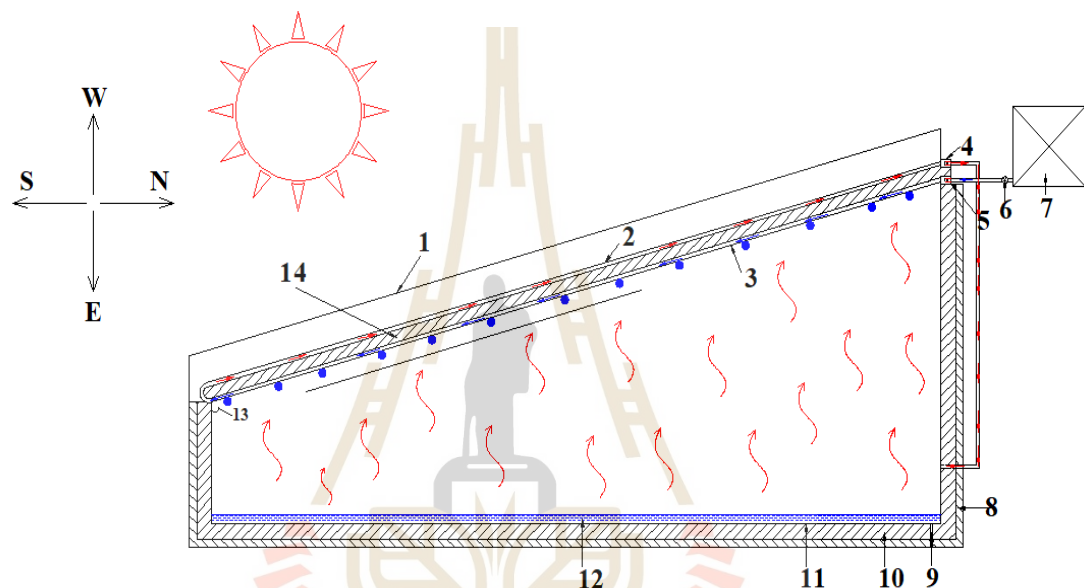
Figure 3.1 A cross sectional view of schematic diagram of solar still 1 - Glass cover; 2 – Receiver/Collector tubes; 3 – Condenser tubes; 4, 5 – rectangular copper boxes; 6 – valve; 7 – storage water tank; 8 – wood cover; 9 – drainage hold; 10 – aero foam insulation; 11 – basin wall; 12 – water in basin; 13 – distilled water collector; 14 - insulation between lower and upper tubes.

This study proposes a novel design of solar water distiller which illustrated in Figure 3.1. The proposed solar still consists of a basin liner, a tube bank and a storage water tank. The tube bank was bent into a U shape, which included of an

upper side and a lower side. The lower side is called condenser and the upper side is called receiver. Design concepts of distiller are as follow:

1. **Condenser tubes**

The water flows from the insulated storage tank (No. 7 in Figure 3.1) to the condenser tubes (No. 3 in Figure 3.1). As the water in the basin (No. 12 in Figure 3.1) evaporates and flows up, it is condensed on the surface of the condenser tubes. It was believed that this design can enhance the condensation rate because the temperature of the water flowing in the condenser tubes is relatively low.

2. **Receiver**

The water flowing in the condenser tubes get hotter (preheats) because it absorbed the laten heat from the condensation process and then it flows to the receiver (No. 2 in Figure 3.1) before flowing continuously to basin wall of solar still (No. 11 in Figure 3.1). The temperature of water will increase which rise its vapor pressure, results in an improved evaporation rate will be improved. The current research in renewable energy indicates a growing interest for solar collectors with tubes. The tube solar collector has more advantageous than the flat plate collectors for water heating purposes. In flat plate collectors, sun rays are perpendicular to the collector only at noon and thus a proportion of the sunlight striking the surface of the collector is always likely to be reflected. On the contrary, in tube collector, due to its cylindrical shape, the sun rays are perpendicular to the surface of the tubes for most of the day.

3. **No heat loss.**

In the conventional solar still, latent heat of vaporization/ condensation absorbed by glass and loss to ambient. Moreover, the basin water loss heat to ambient through bottom and sides of basin wall. Nevertheless, it is worth noting

that energy released when the vapor condenses will be utilized by condenser tubes to preheat water flow inside before entering the receiver. The heat loss from water to ambient through basin wall can prevented by insulator. As a result, the uniqueness of this concept is that there is approximately no heat loss to ambient in the proposed distiller. Furthermore, there is no hot water outlet from the system.

4. Other concepts

- There is no glass cover solar still in order to maintain the temperature inside to be low.

- Water is supplied from storage tank by making use of gravitational effect. Hence, no pumping power is required.

The differences between proposed solar still and a single basin solar still are illustrated in Table 3.1. Furthermore, the role of each components of Model 1 is summarized in Table 3.2.

Table 3.1 Comparison between conventional solar still (CSS) and proposed solar still
(PSS)

No.		CSS	PSS
1	Top cover	Top is covered by glass	Top is covered by U-tube bank
2	Function of top cover	Transmit solar energy to evaporate basin water	- Heat loss from water to surrounding air through top will be absorbed by condenser tubes - Condense water vapor and preheat feed water
3	Function of basin liner	Absorbed solar energy and transfer to water	Remain temperature of water and prevent heat loss from water to surrounding air through bottom.

Table 3.2 Function of components of proposed solar still

No.	Component	Function
1	Condenser tubes	- Condense water vapor - Absorb the latent heat of condensation in the condensation process

Table 3.2 Function of components of proposed solar still (Continued)

No.	Component	Function
2	Solar Receiver	- Increase the temperature of water to increase its vapor pressure
3	Basin liner	- Contain hot water flowing from receiver - Remain high temperature of water
4	Water tank	- Supply water with gravitational effect
5	Glass cover receiver	- Minimize convective and radiant heat loss from receiver. - Protect the receiver from outside environment.
6	Insulator	- Reduce heat loss from condenser tubes, receiver and basin liner to surrounding air.

3.1.1.2 Material for different parts of Model 1

Base on the design concept of the novel solar water distiller, materials of components of Model 1 was selected before fabrication.

- **Glass cover**

The role of glazing is to admit the maximum possible radiation and to minimize the upward loss of heat. The most commonly used material is glass because it can transmit up to 90 percent of the incident shortwave radiations while its transmittance to the longwave heat radiation, emitted by the upper tubes, is negligible. Plastic film and sheets may also be used for the purpose of glazing as they possess high transmittance to shortwave solar radiation, but transmission bands in the

middle of thermal radiation spectrum and dimensional changes in this temperature range restricts their use as a good glazing surface. So, we chose glass as the glazing material. Table 3.3 shows physical properties of a glass cover.

Table 3.3 Physical properties of glass cover

Properties	Symbol	Value	Unit
Thermal conductivity	k_g	0.78	W/m K
Specific heat	C_p	840	J/kg K
Density	ρ_g	2800	kg/m^3
Absorptivity	α_g	0.0475	
Transmissivity	τ_g	0.9	

- **Lower and upper tubes**

The most important part of the research is the collector of solar still. The function of the collector tube is to maximize to absorb possible solar radiation incident on it through the glazing. Several Materials commonly used for collector, in descending order of cost and conductance, are cooper, aluminum and steel. Additionally, a worth noting claim from Vimal Dimri et al. (2008) was that the use of copper metal against plastic increased the production of water by 18%. Therefore, we decided to use cooper for both upper and lower tubes. Both of them were painted black. Table 3.4 shows physical properties and size of cooper tube:

Table 3.4 Physical properties of cooper tube:

Properties	Symbol	Value	Unit
Thermal conductivity	k_{cd}	401	W/m K
Specific heat	C_p	390	J/kg K
Density	ρ	8933	kg/m^3
Absorptivity	ε	0.64	

- **Basin wall**

It is the part of the system keeping and transferring heat to the water. The basin wall can be made from plastic, metal sheets, copper, aluminum, steel or some other materials with a high thermal capacity. Compare to aluminum and copper, the thermal conductivity of steel is relatively lower, but its price is cheaper. According to a study of Gnanadason et al., (2014), a modified solar still made of copper ensures a higher evaporation rate and efficiency. In another study, Gnanadason et al., (2013) claimed that the efficiency was higher for solar still made up of copper compared to galvanized iron sheet. The bottom of the basin can be made of 4 mm-thick aluminum as an absorbent in the research of Tiwari et al., (1997) and B.I. Ismail (2009). In my research, the material of the basin wall in Model 1 is aluminum, while that in Model 2, Model 3 are stainless steel. Table 3.5 shows physical properties and the size of basin liner:

Table 3.5 Physical properties of aluminum

Properties	Symbol	Value	Unit
Thermal conductivity	k_b	237	W/m K
Specific heat	C_p	0.9	kJ/kg K
Density	ρ_b	2700	kg/m³

- **Insulation**

The insulating material is a crucial parameter design because proper insulation is necessary to prevent heat loss from the bottom and sides of the basin to environment. For better insulation, we used aero foam inside and wood cover. Table 3.6 shows physical properties and thickness of aero foam and wood cover:

Table 3.6 Physical properties of aluminum

Properties	Symbol	Value	Unit
Thermal conductivity of aero-foam	k_i	0.034	W/m K
Thickness of aero-foam	σ_i	0.025	m
Thermal conductivity of wood cover	k_{wc}	0.106	W/m K
Thickness of wood cover	σ_{wc}	0.01	m

3.1.1.3 Construction of Model 1

A cross sectional view of schematic diagram of solar still is shown in Figure 3.1. The experimental set up consists of a glass cover of collector (No. 1 in Figure 3.1), a U-type tube collector, basin wall (No. 11 in Figure 3.1), insulation (No. 9, 10 and 14 in Figure 3.1) and a distillate collection (No. 13 in Figure 3.1). The tube bank includes thirty U-type tubes welded continuously together. The tubes are made of copper of 8.5 mm inlet diameter copper and the receiver is coated with black paint to increase the solar radiation absorption. The gap between upper tube and lower tube is 20 mm. In order to prevent heat loss from condenser tubes to ambient and heat transfer between lower and upper tubes, there is an insulation layer which made from aero foam. The upper and lower tubes was welded with upper rectangular trough and lower rectangular trough respectively by using Oxy – Acetylene welding machine, which is described in Figure 3.2. Singh and Tiwari (2014) studied that the optimum glass's tilt angle should be the latitude of the location for improving annual output. Hence, the tilt angle of the U tube bank and the glass cover equals to the latitude of the Nakhon Ratchsima (15°). The basin liner is made of aluminum, 2 mm thickness. It is made by using TIG welder. It is additionally insulated on three sides and at the bottom by aero foam, to reduce heat loss from the solar still to the atmosphere. The basin liner and insulation are placed inside the wooden box. The condensed water is collected through the distillation trough. Silicon is used to prevent any leakage between U tube bank and basin liner. Dimension of different parts of Model 1 are described in Table 3.7, which also give dimension of conventional solar still, Model 2 and Model 3.

Brackish water is supplied from the storage tank, flows naturally along the condenser, collector and basin respectively. The brackish water is heated by

solar energy while flowing in the receiver. Then, the water flows to the basin of the system with high temperature and evaporate to vapor form. The water vapor will condense on surface of lower tubes. The fresh water droplets will flow into the distilled water collector due to the gravity.

Figure 3.2 Welding copper tubes

Figure 3.3 Pictorial view of Model 1

Table 3.7 Dimension of different parts of 3 Models and Conventional solar still (Css).

	Css	Model 1	Model 2 without glass	Model 2 with glass	Model 3
Length of condenser tubes (mm)	N/A	1,000	450	450	450
Inclined angle of condenser tubes	N/A	15º	45º	45º	45º
Length of receiver tubes (mm)	N/A	1,000	1,000	1,000	1,000

Table 3.7 Dimension of different parts of 3 Models and Conventional solar still (Css).

(Continued)

	Css	Model 1	Model 2 without glass	Model 2 with glass	Model 3
Inclined angle of receiver tubes	N/A	15º	15º	15º	15º
Number of tubes (tube)	N/A	30	40	40	40
Thickness glass cover (mm)	5	5	5	5	5
Angle of glass cover solar still	15º	N/A	N/A	90º	15º
Material of basin wall	Stainless steel	Aluminum	Stainless steel	Stainless steel	Stainless steel
Length of basin wall (mm)	1,000	1,000	500	500	1,000
Width of basin wall (mm)	380	380	380	380	380
Height of basin wall (mm)	150x420	150x420	150x650	150x150	150x150

Table 3.7 Dimension of different parts of 3 Models and Conventional solar still (Css).

(Continued)

	Css	Model 1	Model 2 without glass	Model 2 with glass	Model 3
Thickness of basin wall (mm)	1.5	2	1.5	1.5	1.5
Material of insulator	Aero-foam and wood	Aero-foam and wood	Aero-foam and wood	Aero-foam and wood	Aero-foam and wood
Insulator for water storage tank	N/A	N/A	Aero-foam	Aero-foam	Aero-foam and PE foam

3.1.1.4 Experimental procedure

Various parameters have to be measured simultaneously and periodically in order to investigate the performance of proposed solar still. In this work of Model 1, the emphasis has been on temperature and solar insolation measurements.
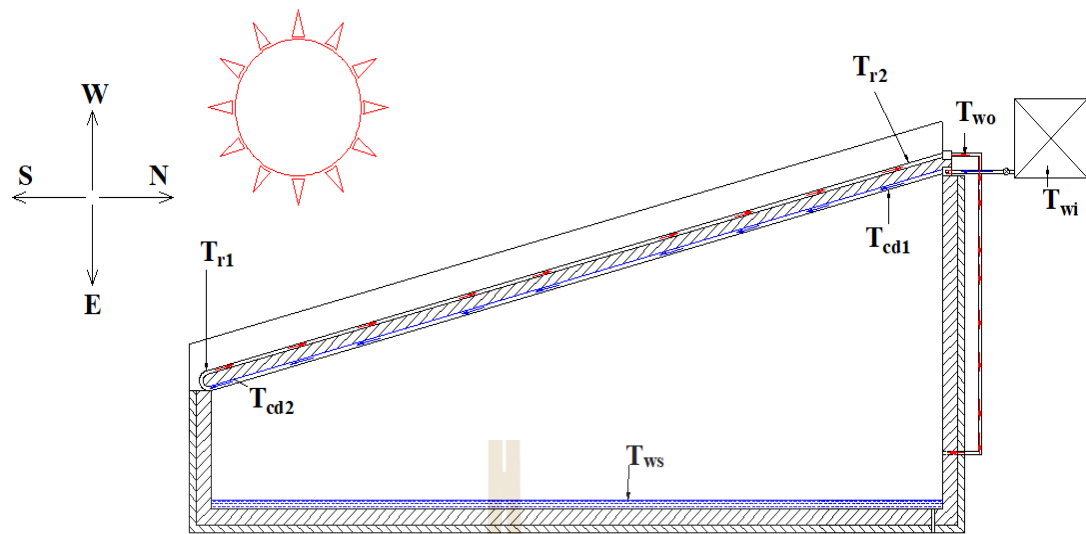
Figure 3.4 Measurement points of Model 1

The temperature of different parts in Model 1 was measured hourly by K-type digital thermometer from 10 o'clock to 16 o'clock, which is illustrated in Figure 3.4. The temperature of condenser's surface was measured at inlet position (T_{cd1}) and outlet position (T_{cd2}) and that of receiver's surface also measured at inlet position (T_{r1}) and outlet position (T_{r2}). Temperature of water in the storage tank (T_{wi}), temperature of water in the basin (T_{ws}) and temperature of outlet water of receiver (T_{wo}) are recorded.

The solar radiation was measured every hour on different experimental days by a pyranometer CMP3 supplied Kipp & Zonen. Distilled water will be collected and measured every hour.

Before starting experiment, mass flow rate of water is measured by a stop watch and a volume measuring cylinder. The mass of water in basin wall is zero when the experiment start.

After experiment finish, all water in solar still will flow out through drainage hole (9).

3.1.2 Model 2

In the previous section, I introduced the design concept and construction of Model 1. However, the productivity of Model 1 is significantly lower than expectation. Therefore, I modified Model 1 and called it as Model 2. After conducting experiments, I have more ideas of some minor modifications. As a result, two Models 2 was created, namely "Model 2 without glass cover solar still" and "Model 2 with glass cover". Their details are outlined in this section.

3.1.2.1 Model 2 without glass

The modifications from Model 1 to this Model and the reasons for this alteration are illustrated in Table 3.8.

Table 3.8 Modifications of Model 1 to be "Model 2 without glass" and their reasons

No.	Modification	Reasons
1	Tilt angle of condenser tubes was changed from 15° to 45°	To prevent water droplets to fall down to basin.
2	The connection between the condenser and receiver was changed from using a copper tube to rubber tube.	To reduce heat transfer from the receiver to the condenser
3	Material of basin wall was changed from aluminum to stainless-steel.	To reduce heat loss from water in basin to ambient.

Table 3.8 Modifications of Model 1 to be "Model 2 without glass" and their reasons

(Continued)

No.	Modification	Reasons
4	The connecting pipe between the receiver and the basin wall (No. 10 in Figure 3.5) was insulated.	To prevent heat loss from the hot feed water to surrounding air.
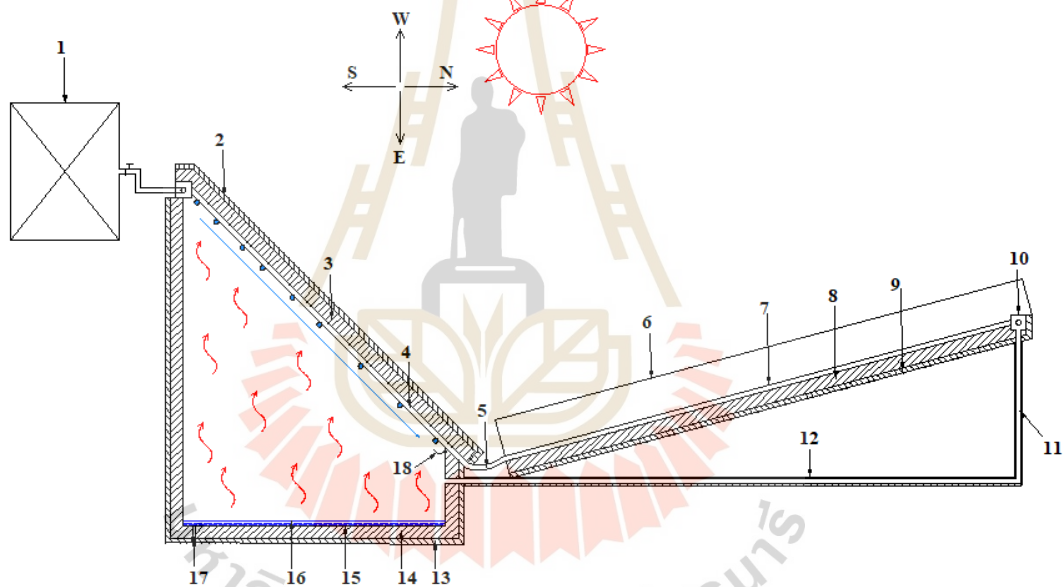
Figure 3.5 A cross sectional view of schematic diagram of Model 2 without glass. 1 - Storage water tank; 2 – wood cover of condenser; 3 – insulation of condenser tubes; 4 – condenser tubes; 5 – rubber tubes connect condenser and receiver tubes; 6 – glass cover of receiver; 7 – Receiver; 8 – Insulation of receiver; 9 – wood cover of receiver; 10 – rectangular box of receiver; 11 – connecting pipe; 12 – insulation of connecting pipe; 13 – wood cover of basin liner; 14 – Insulation of basin; 15 – basin wall; 16 – water in basin; 17 – Drainage hold; 18 - distilled water collector.

"Model 2 without glass" consists of three components as described in Figure 3.5. These are storage water tank (No. 1 in Figure 3.5), distiller and receiver. The distiller included basin wall (No. 13 in Figure 3.5) which is insulated with aero-foam (No. 14 in Figure 3.5) and wood layer (No. 13 in Figure 3.5). The top of still was covered by condenser tubes (No. 4 in Figure 3.5). The condenser tubes link to the receiver tubes (No. 7 in Figure 3.5) which was covered by glass (No. 6 in Figure 3.5). Both of the receiver and condenser tubes are insulated by aero-foam and wood layer. The tilt angle of condenser tubes is changed to 45 degree and faces to the North direction. Condenser tubes and collector tubes are connected together by rubber tubes. Water tank was insulated by aero-foam. The mass flow rate is controlled at 1 L/h.

3.1.2.2 Model 2 with glass

The experimental results show that there is an increase in the daily productivity of Model 2 without glass compared to Model 1. Nevertheless, it is still lower than the yield of a conventional solar still, which lead to some ideas to modify design of Model 2 without glass. The difference in the construction of Model 2 with glass is explained in table 3.9. A cross sectional view of Model 2 was described in Figure 3.6.

Table 3.9 Modifications of "Model 2 without glass" to "Model 2 with glasss" and their

reasons

| No.	Modification	Reasons
1	Three sides of the solar distiller were covered with glass	To improve evaporation process by increase solar radiation absorbed by the water in basin.
2	A valve (10) was set up on the connecting pipe to control mass flow rate flow to basin.	
3	Water tank was insulated with aero foam	To keep the water in tank in low temperature.
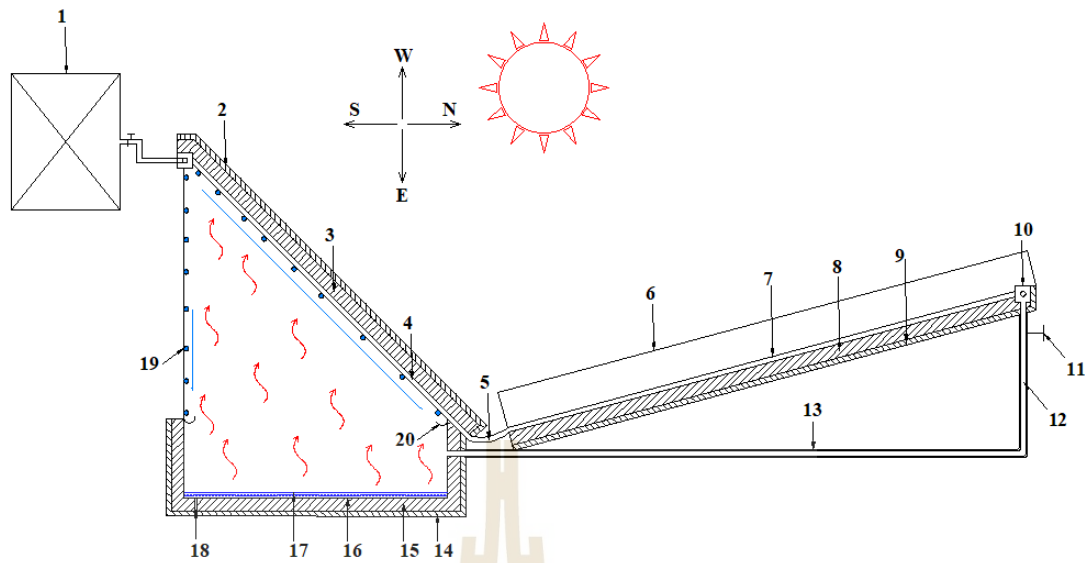
Figure 3.6 A cross sectional view of schematic diagram of Model 2 with glass cover.

1 - Storage water tank; 2 – wood cover of condenser; 3 – insulation of condenser tubes; 4 – condenser tubes; 5 – rubber tubes connect condenser and receiver tubes; 6 – glass cover of receiver; 7 – Receiver; 8 – Insulation of receiver; 9 – wood cover of receiver; 10 – rectangular box of receiver; 11 – valve control mass flow rate; 12 – connecting pipe; 13 – insulation of connecting pipe; 14 – wood cover of basin liner; 15 – Insulation of basin; 16 – basin wall; 17 – water in basin; 18 – Drainage hold; 19 – glass cover of solar still; 20 - distilled water collector.

3.1.2.3 Geometric dimension of Model 2

All components of these two Models 2 have the same dimension which are displayed in table 3.10. The basin liner of Model 2 is made from stainless steel, 1.5 mm thickness. The number of condenser and receiver tubes is forty.

Table 3.10 Dimension of different parts of Model 2

Glass cover of collector	- Thickness: 5 mm
	- Gap between glass and collector tubes: 25 mm
	- Size: 1000x450x5 mm
Glass cover of solar still	- Thickness: 5 mm
Condenser and collector tubes	- Inner diameter: 8.5 mm
	- Outer diameter: 9.5 mm
	- Length of receiver tubes: 1,000 mm
	- Length of condenser tubes: 450 mm
Box of condenser tubes and collector tubes	- Material: copper
	- Size: 400x30x30 mm
Insulation	- Thickness: 25 mm
Wood cover	- Thickness: 10 mm

3.1.2.4 Experimental procedure

The measuring instruments in Model 2 required are K-type thermocouples, data logger, solar intensity meter (Pyranometer), a humidity sensor for measuring relative humidity and a volumetric jar measure the amount of fresh water produced. Figure 3.7 illustrates a schematic of the experimental rig showing location of measuring points.
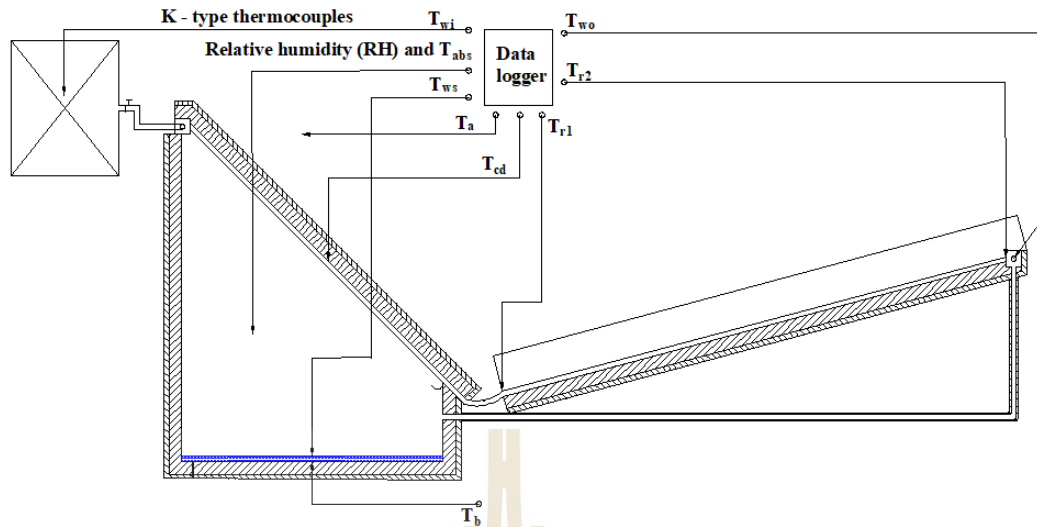
Figure 3.7 Measured parameters in solar still model 2 without glass
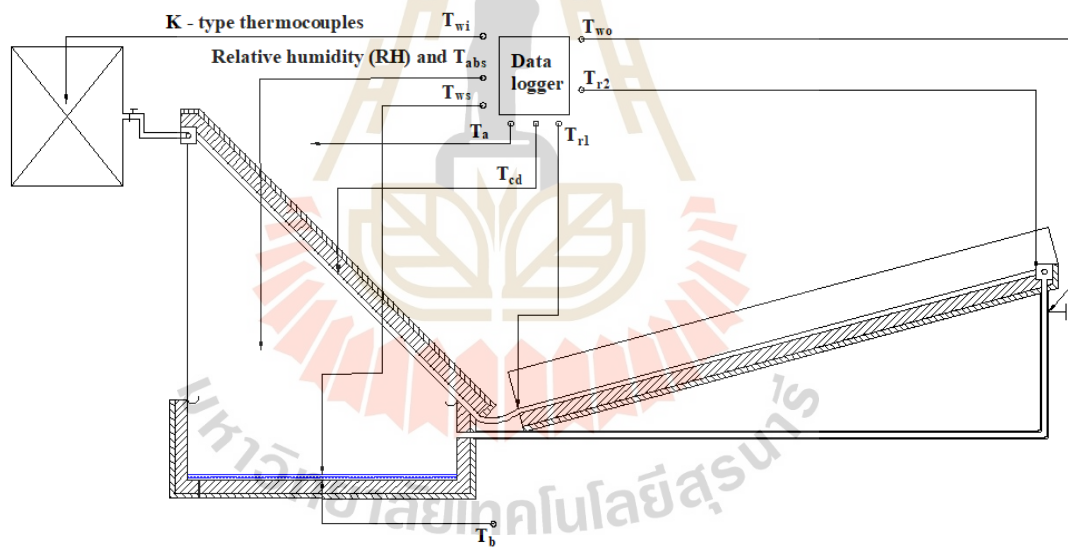
Figure 3.8 Measured parameters in solar still model 2 with glass

There should be seven temperature sensors. A thermocouple, T_{wi} is required to measure the temperature of the water in storage tank. One thermocouple measure temperature of condenser's surface. Two thermocouples T_{cl1} and T_{cl2} at inlet and outlet of the receiver tube are required to measure the temperature of its surface.

Another two thermocouples T_{wo} and T_{ws} are required to measure the temperature of hot brackish water out of the receiver and in solar still respectively. One other thermocouple T_b is required to measure temperature of basin. Finally, the humidity sensors measure the temperature of the humid air T_{abs} and relative humidity (RH) in solar still. All thermocouples initially were tested and calibrated to provide approximately the same reading by exposing them to the ambient temperature and compare them to a mercury-in-glass thermometer. All temperatures were recorded in 10 minutes by a data – logger which connected to a computer. The experiment was conducted between 10 o'clock and 18 o'clock.

The solar radiation was measured by a pyranometer CMP3 supplied by Kipp & Zonen. These data were recorded by a data – logger every 10 minutes and saved in computer.

Before starting experiment, mass flow rate of water is measured by a stop watch and a volume measuring cylinder. The mass flow rate is 1 L/hour. In both models of Model 2, the mass of water in basin is zero when the experiment began.

After the experiment finish, all water in solar still will flow out through drainage hole. The water storage tank was fulfilled and kept overnight.

3.1.3 Model 3

Experimental results and discussion in section 4.2.2 observed that using glass improved evaporation process and insulating water tank helped to reduce temperature of condenser's surface. This caused the increase of daily productivity. However, the yield of proposed is not as high as expectation, which led to the building of Model 3. Model 3 was then fabricated with modifications described in Table 3.11.

Table 3.11 Modifications in Model 3 and their reasons

No.	Modification	Reasons
1	Top of the solar still was covered by two roofs included a glass and condenser tubes	- To maximize solar radiation absorptivity. - To increase condenser's surface area.
2	Three holes were drilled on the side of basin liner.	- In order to remain water level in solar still unchanged by using overflow. - The water depth in solar still was controlled at 0.5, 1 and 2 cm.
3	A feed water reservoir was set up behind the storage tank	To make sure that the head of storage tank is constant.

3.1.3.1 Construction of Model 3

A cross sectional view of schematic diagram of solar still is illustrated in Figure 3.9. The solar still consists of a water storage tank (No. 2 in Figure 3.9), a basin wall (No. 12 in Figure 3.9), condenser and receiver tubes (No. 5 and No.6 in Figure 3.9, respectively), 2 glasses covers solar still and receiver (No. 1 and No.7 in Figure 3.9, respectively) and fresh water collectors (No. 16 in Figure 3.9). The number of condenser tubes equal to that of collector tubes (40 tubes). The tilt angle of the collector tubes and glass cover should be equal to the latitude of experimental place (Singh and Tiwari, 2014), so their angle is 15 degree. Meanwhile, the condenser tubes

incline 45 degree. The basin wall is made of stainless steel, 1.5 mm thickness. The basin wall, the connecting pipe, condenser tubes and collector tubes were insulated throughout with aero foam, 25 mm thickness. Polyethylene is used to insulate the water tank. A valve on the connecting pipe controls the mass flow rate of water flow to solar still. The silicon is used to prevent any leakage between the basin and top cover. Materials selection and dimension specification of Model 3 are shown in Table 3.12. The picture of model 3 is depicted in figure 3.11.
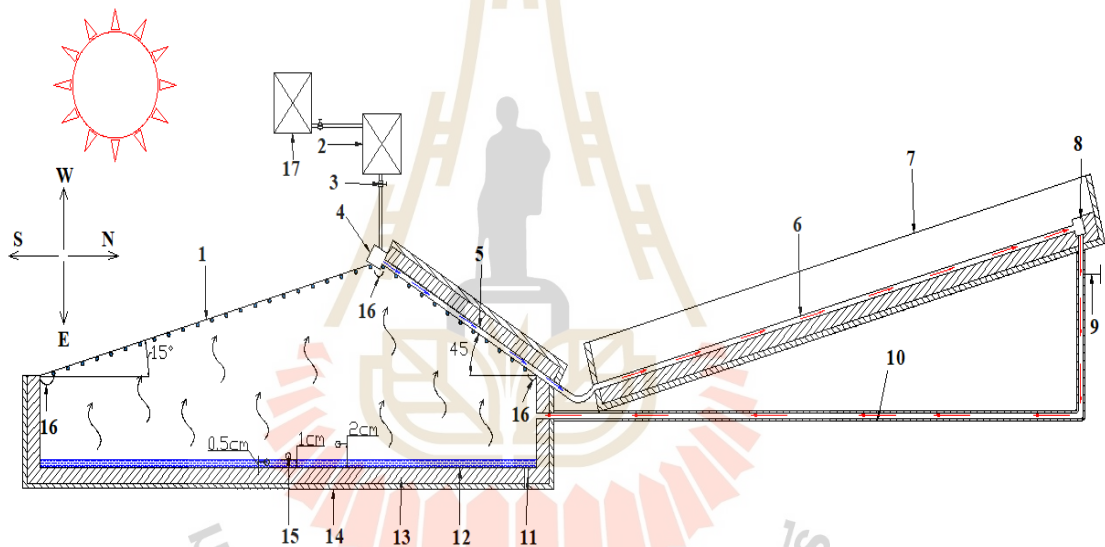
Figure 3.9 Schematic diagrams of Model 3. 1 - Glass cover of solar still; 2 – Water storage tank; 3 - Valve of water tank; 4 - Condenser box; 5 - Condenser tubes; 6 - Receiver tubes; 7 - Glass cover of receiver tubes; 8 - Receiver box; 9 - Valve; 10 - Connecting tube; 11 - Drainage hold; 12 -Basin wall; 13- Foam insulator; 14-Wood cover ; 15- Fresh water collector; 16- Fresh water collector; 17- Feed water reservoir.

Table 3.12 Dimension of different parts of Model 3

Glass cover of collector	- Thickness: 5 mm - Gap between glass and collector tubes: 25 mm - Size: 1000x450x5 mm
Glass cover of solar still	- Thickness: 5 mm - Size: 800x450x5 mm
Condenser and collector tubes	- Inner diameter: 8.5 mm - Outer diameter: 9.5 mm - Length of receiver tubes: 1000 mm - Length of condenser tubes: 450 mm
Box of condenser tubes	- Material: acrylic - Size: 400x30x30 mm
Box of collector tubes	- Material: copper - Size: 400x30x30 mm
Insulation	- Thickness: 25 mm
Wood cover	Thickness: 10 mm

Figure 3.10 Pictorial view of Model 3.

3.1.3.2 Experimental procedure

There are eight type K thermocouples to measure temperature of different parts of Model 3. A thermocouple, T_{wi} is required to measure the temperature of the water in storage tank. One thermocouple measure temperature of condenser's surface. Two thermocouples T_{r1} and T_{r2} at inlet and outlet of the receiver tube are required to measure the temperature of its surface. Another two thermocouples T_{wo} and T_{ws} are required to measure the temperature of hot brackish water out of the receiver and in solar still respectively. One other thermocouple T_b is required to measure temperature of basin. One other thermocouple T_a is required to measure temperature of ambient air. Finally, the humidity sensors measure the temperature of the humid air T_{abs} and relative humidity (RH) in solar still. All thermocouples initially were tested and

calibrated to provide approximately the same reading by exposing them to the ambient temperature and compare them to a mercury-in-glass thermometer. All temperatures were recorded in 10 minutes by a data – logger which connected to a computer. The experiment was conducted between 9 o'clock and 18 o'clock.

The solar radiation was measured by a pyranometer CMP3 supplied by Kipp & Zonen. These data were recorded by a data – logger every 10 minutes and saved in computer.

Before starting experiment, mass flow rate of water is measured by a stop watch and a volume measuring cylinder. The mass flow rate was controlled at 1 L/hour and 0.5 L/hour. The water depths were controlled at 0.5 cm, 1 com and 2 cm for different days when the experiment commenced.

After experiment finish, all water in solar still will flow out through drainage hole. The water storage tank was fulfilled and kept overnight.
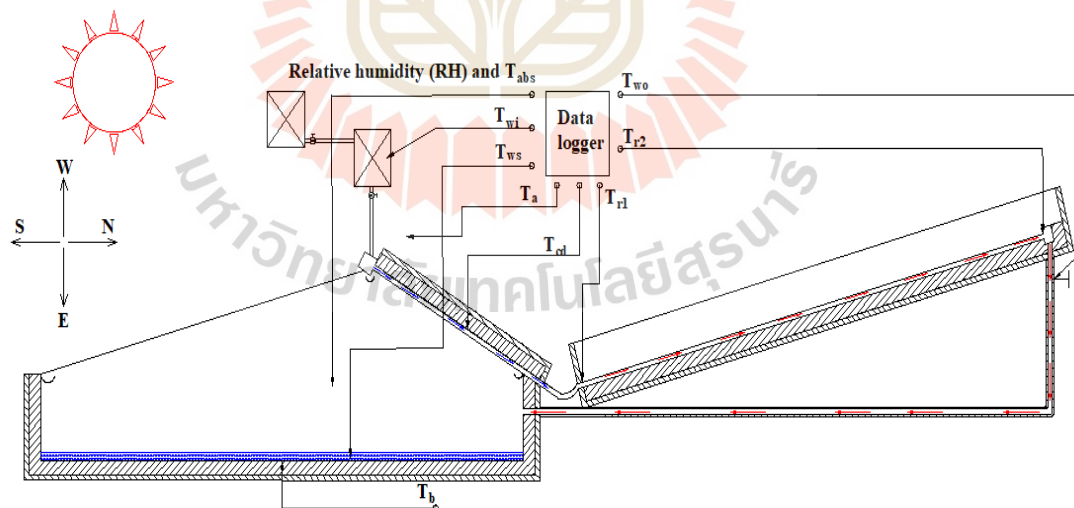

Figure 3.11 Measurement points in Model 3.

3.2 Theoretical analysis

Modeling is one of the most important elements of thermal system design. Theoretical analysis reduces the experiment periods and examines solar still performance at various conditions. In addition, it determines the theoretical reasons for experimental data. In this section, I formulated theoretical analysis for the proposed solar still and the details of them are as follow.

3.2.1 Principle of energy flow in proposed solar still

The heat transfer process in a solar still can be broadly classified into internal and external heat transfer processes based on the energy flow inside and outside of the still. The details of various heat transfers that take place in active solar still are described in figure 5.1. A small part of the solar radiation incident (I(t)) gets absorbed within glass cover ($\alpha_g' I(t)$) and gets reflected, the rest (i.e. large part) is transmitted (τ_gI(t)) into the solar still. This solar radiation is then partially absorbed ($\alpha_w' I(t)$) and reflected (R_w τ_gI(t)) by brackish water. The attenuation of solar intensity in water depends on its absorptivity and level. Most of solar irradiation is finally absorbed by the blackened surface of basin liner which will be converted to heat up the water by convection heat transfer. The current work also takes the effect of water depth on the solar absorption of water and basin. To elaborate, energy transfer from water to humid air by convection and evaporation ($Q_{c_{w-h}}$ and $Q_{e_{w-h}}$) then humid air transfer energy to the glass and condenser tubes by convection ($Q_{c_{h-g}}$ and $Q_{c_{h-cd}}$) and condensation ($Q_{e_{h-g}}$ and $Q_{e_{h-cd}}$) . The radiation heat transferred between water and glass and condenser ($Q_{r_{w-g}}$ and $Q_{r_{w-cd}}$) is also considered. The heat, therefore, absorbed by condenser tubes is transferred to the fluid flow inside tubes by convection ($Q_{c_{cd-f}}$) and

the surrounding by conduction heat (Q_{cd-a}). Meanwhile, the glass loss energy to the air by convection and radiation heat transfer. The heat losses from bottom and sides of basin wall through insulation are counted.
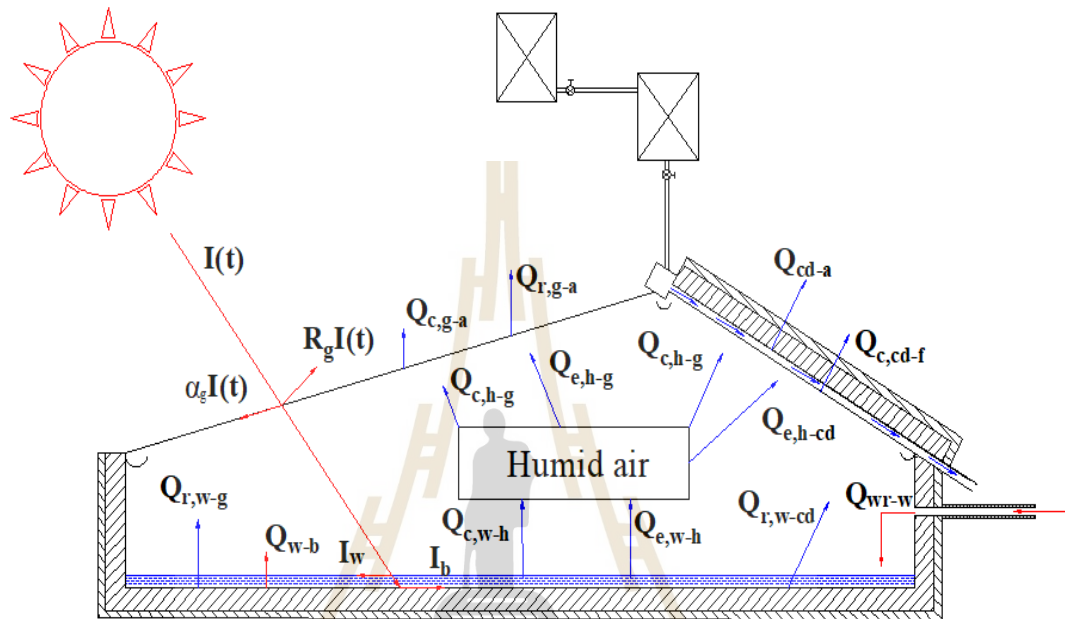
Figure 3.12 The major energy transfer mechanism in solar still

The function of a solar receiver is to absorb solar irradiation, convert it into heat energy and then transfer that heat to the fluid. The collector consists of glass, forty copper tubes, a rectangular copper box and insulation. The thermal loss to the surrounding plays an important role in the study of the performance of a collector. Figure 3.9 shows the energy transfer mechanism in the receiver and considering the solar irradiance on the receiver zone. These energies consist of the radiation heat transfer between the receiver and the glass cover, the convection heat transfer between receiver and air gap, the conduction between the receiver and the insulator and the heat transfers by convection with the fluid flow.
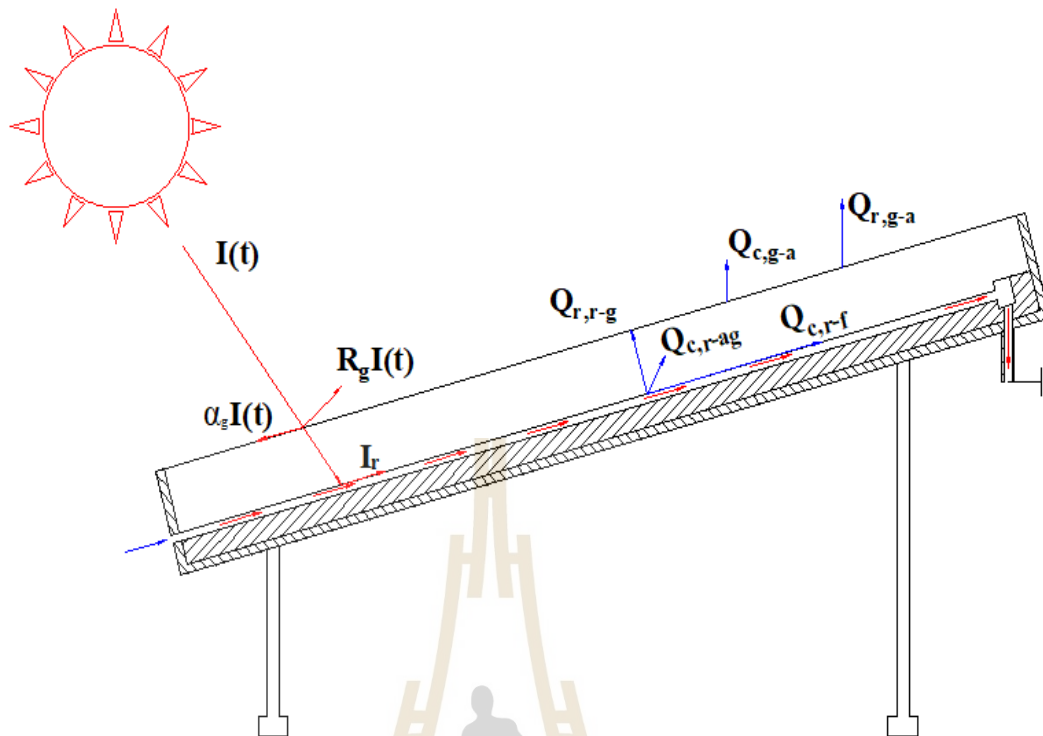
Figure 3.13 The major energy transfer mechanism in solar collector

3.2.2 Energy balance equation

In the analysis of the proposed solar still operation, the following assumption have been made:

- The inclination of glass and condenser tubes are very small

- The device is air vapor tight

- No dry spot in solar still

- The temperature of water in the tank is constant

- The temperature gradient along water mass depth is negligible

Energy analysis is based on the first law of thermodynamics, which is based on the conservation principle of energy in quantity. The energy balance equations at various portions of the solar still are described as follows**:**

3.2.2.1 Energy balance of water in the basin

At the surface of water, the energy is transferred to the humid air above by convection and evaporation and to glass cover and condenser tubes by radiation. Thus, the energy input into and output from the water surface in a given time can be written as:

Energy input = solar energy absorbed by water + energy transferred from basin liner + energy transferred from water outlet of the receiver.

Energy output = evaporation loss from water to humid air + convection energy loss to humid air + radiant energy loss to the glass cover and condenser tubes+ energy loss due to flow over.

Hence, the energy balance expression can be written as:

Increase of energy of the water = Energy in − Energy out

$$\frac{\partial T_w}{\partial t} = \frac{1}{M_w Cp_w}\left(\alpha'_w A_w I(t)_s + Q_{b-w} + \dot{m}Cp_w(T_{f_{ocl}} - T_w) - Q_{c_{w-h}} - Q_{e_{w-h}} - Q_{r_{w-g}} - Q_{r_{w-cd}}\right) \tag{3-1}$$

3.2.2.2 Energy balance of the basin wall

The energy exchange between liner and brackish water can be expressed as:

Energy input = solar energy absorbed by the basin wall

Energy output = convection heat transferred to water + heat loss to ambient.

Therefore,

Increase of energy of the basin wall = Energy in – Energy out

$$\frac{\partial T_b}{\partial t} = \frac{1}{M_b Cp_b}(\alpha'_b A_b I(t)_s - Q_{b-w} - Q_{b-a}) \tag{3-2}$$

3.2.2.3 Energy balance of humid air

The energy incident on and leaving the humid air can be written

as:

Energy input   =   evaporation and convection heat

transferred from water in basin

Energy output   =   convection heat transferred to glass and

condenser tubes + evaporation heat

transferred to glass and condenser tubes.

Therefore,

The increase of energy of the humid air = Energy in – Energy

out

$$\frac{\partial T_h}{\partial t} = \frac{1}{M_h Cp_h}\left(Q_{c_{w-h}} + Q_{e_{w-h}} - Q_{c_{h-g}} - Q_{e_{h-g}} - Q_{c_{h-cd}} - Q_{e_{h-cd}}\right) \tag{3-3}$$

3.2.2.4 Energy balance of glass cover

The condensing top glass cover works as an aperture letting

incident solar radiation enter the distiller and keeping the heat generated inside to meet

the needed heat for evaporation of brackish water. So, the energy balance equation for

the glass cover can be written as follows:

$$\frac{\partial T_g}{\partial t} = \frac{1}{M_g Cp_g}\left(\alpha'_g A_g I(t)_s + Q_{r_{w-g}} + Q_{c_{h-g}} + Q_{e_{h-g}} - Q_{c_{g-a}} - Q_{r_{g-a}}\right) \qquad (3\text{-}4)$$

3.2.2.5 Energy balance of condenser tubes

The condenser tubes receive convection and condensation heat transferred from humid air and radiation heat transferred from water. Meanwhile, it transfers heat to the feed water inside by convection. So, the energy balance equation for the condenser tubes can be given as below:

$$\frac{\partial T_{cd}}{\partial t} = \frac{1}{M_{cd} Cp_{cd}}\left(Q_{r_{w-cd}} + Q_{c_{h-cd}} + Q_{e_{h-cd}} - Q_{c_{cd-f}} - Q_{cd-a}\right) \qquad (3\text{-}5)$$

3.2.2.6 Energy balance of fluid in condenser tubes

The energy balance equation for the fluid flow in condenser tubes can be given as below:

$$\frac{\partial T_{f\_cd}}{\partial t} = \frac{1}{M_{f_{cd}} Cp_{f_{cd}}}\left(Q_{c_{cd-f_{cd}}} - \dot{m}_f Cp_f (T_{wcd} - T_a)\right) \qquad (3\text{-}6)$$

3.2.2.7 Energy balance of receiver tubes

The receiver tubes absorbed solar energy and transferred heat to fluid by convection heat transfer. Thus, the energy input into and output from the receiver tubes can be written as:

Energy input = solar energy absorbed by receiver.

Energy output = convection heat transferred to fluid + convection energy loss to air between

receiver and glass + radiant energy loss to glass cover.

Increase of energy of the receiver = Energy in − Energy out

$$\frac{\partial T_{co}}{\partial t} = \frac{1}{M_r C_r} (\alpha'_r I(t)_s - Q_{c_{r-wr}} - Q_{r_{r-g}} - Q_{c_{r-ag}})$$ (3-7)

3.2.2.8 Energy balance of fluid in receiver

The energy balance equation for the fluid flow in receiver tubes can be expressed as:

$$\frac{\partial T_{wr}}{\partial t} = \frac{1}{M_{wr} C_{wr}} (h_{r-wr} A_r (T_r - T_{wr}) - \dot{m} C p_w (T_{iwr} - T_a))$$ (3-8)

3.2.3 Heat and mass transfer mode in proposed solar still

There are three modes, namely convection, radiation and evaporation processes, by which the heat transfer process of the proposed solar still is governed. The modes of heat transfer occur in solar still and receiver are described briefly in this subsection. The attenuation of solar intensity is also presented below.

3.2.3.1 Solar irradiance

Solar radiation is absorbed by glass, basin liner, water in basin, condenser tubes and receiver tube can be expressed as:

$$I_i = \alpha'_i \times A_{i\times} I(t)$$ (3-9)

i: represent glass, basin liner, water, condenser tubes and receiver tubes.

Actually, solar intensity is attenuated by scattering and absorption by glass, basin liner and water in basin. Therefore, the attenuations of solar energy within them are considered. The solar flux absorbed by glass, basin liner, water and condenser tubes can be calculated as (Tiwari, 2002):

The fraction of solar flux absorbed by glass:

$$\alpha'_g = \left(1 - R_g\right)\alpha_g = 0.045 \tag{3-10}$$

The fraction of solar flux absorbed by condenser tubes:

$$\alpha'_{cd} = \alpha_{cd}\left(1 - \alpha_g\right)\left(1 - R_g\right)R_w = 0.01125 \tag{3-11}$$

The fraction of solar flux absorbed by basin liner:

$$\alpha'_b = \alpha_b\left(1 - \alpha_g\right)\left(1 - R_g\right)\left(1 - R_w\right)\left[\sum \mu_j EXP(\eta_i d_w)\right] = 0.6617 \tag{3-12}$$

The fraction of solar flux absorbed by water mass:

$$\alpha'_w = \alpha_w\left(1 - \alpha_g\right)\left(1 - R_g\right)\left(1 - R_w\right)\left[1 - \sum \mu_j EXP(\eta_i d_w)\right] = 0.161 \tag{3-13}$$

Where: $\sum \mu_j EXP(\eta_i d_w)$ is the attenuation factor and depends on different water levels, and μ_j and η_i are shown in Table 3.13 (Tiwari, 2002).

Additionally, the absorptivity, reflectivity and emissivity of glass, basin water, basin wall, condenser tubes and receiver tubes are described in Table 3.14.

Table 3.13 The value of μ_j and η_i:

j	μ_j	η_i
1	0.237	0.032
2	0193	0.45
3	0.167	3
4	0.179	35
5	0.124	255

Table 3. 14 Absorptivity, reflectivity and emissivity of different components of solar still

Glass	α_g	0.045
	R_g	0.9
	ε_g	0.9
Water	α_w	0.05
	R_w	0.05
	ε_w	0.9
Basin	α_b	0.95
	ε_b	0.9
Condenser and receiver tubes	α_{cd}	0.25
	ε_{cd}	0.93

3.2.3.2 Convective heat transfer inside solar still

Heat transfer occurs across humid air in the distillation by free convection, which is caused by the effect of buoyancy, due to the temperature difference between the water surface and humid air, humid air and the lower tubes or condensing glass. The convection heat transfer strongly depends on fluid properties and geometry and roughness of the involved solid surface.

The convective heat transfer between water and humid air, humid air and glass and humid air and condenser tubes can be defined respectively as following:

$$Q_{c_{w-h}} = h_{c_{w-h}} \times A_w \times (T_w - T_h) \qquad (3\text{-}14)$$

$$Q_{c_{h-g}} = h_{c_{h-g}} \times A_g \times (T_h - T_g) \qquad (3\text{-}15)$$

$$Q_{c_{h-cd}} = h_{c_{h-cd}} \times A_{cd} \times (T_h - T_{cd}) \qquad (3\text{-}16)$$

The corresponding convective heat transfer coefficients are expressed as (Mahdi et al., 2020):

$$h_{c_{w-h}} = \frac{Nu \times k_h}{\dfrac{A_w}{2*(L_w + W_w)}} \qquad (3\text{-}17)$$

$$h_{c_{w-h}} = \frac{Nu \times k_h}{\dfrac{A_w}{2*(L_w + W_w)}} \qquad (3\text{-}18)$$

$$h_{c_{h-cd}} = \frac{Nu \times k_h}{\dfrac{A_{cd}}{2*(L_{cd} + W_{cd})}} \qquad (3\text{-}19)$$

While Nusselt number are given by the following equation (Tanaka et al., 2000):

$$Nu = 0.22 \times Ra^{2/5} \qquad (3\text{-}20)$$

$$Ra = \frac{g \times d_{wg}^3}{\nu_h \alpha_h}\left(\frac{\rho_a}{\rho_{wv}} - 1\right) \tag{3-21}$$

The kinematic viscosity of humid air (ν_h), thermal diffusivity of humid air (α_h), density of dry air (ρ_a), density of water vapor (ρ_{wv}) can be calculated as in Appendix.

3.2.3.3 Irradiative heat transfer inside solar still

The rate of radiative heat transfer inside the solar still equals to the summation of the radiative heat transfer rate from surface water to condenser tubes and the rate of radiative heat transfer from surface water to condensing glass (Tanaka et al., 2000):

$$Q_{r_{w-g}} = h_{r_{w-g}}A_w(T_w - T_g) \tag{3-22}$$

$$q_{r_{w-cd}} = h_{r_{w-cd}}A_w(T_w - T_{cd}) \tag{3-23}$$

$$h_{r_{w-g}} = \frac{\sigma((T_w + 273)^2 + (T_g + 273)^2)(T_w + T_g + 546)}{\frac{1-\varepsilon_w}{\varepsilon_w} + \frac{A_w}{A_g}\left(\frac{1}{\varepsilon_g} - 1\right) + \frac{1}{F_{w-g}}} \tag{3-24}$$

$$h_{r_{w-cd}} = \frac{\sigma((T_w + 273)^2 + (T_{cd} + 273)^2)(T_w + T_{cd} + 546)}{\frac{1-\varepsilon_w}{\varepsilon_w} + \frac{A_w}{A_{cd}}\left(\frac{1}{\varepsilon_{cd}} - 1\right) + \frac{1}{F_{w-cd}}} \tag{3-25}$$

The corresponding shape factors are given by Tanaka et al., (2000):

$$F_{w-g} = \frac{1}{\frac{1-\varepsilon_w}{\varepsilon_w} + \frac{2 \times L_w}{L_w + L_g - L_{cd}} + \frac{1-\varepsilon_g}{\varepsilon_g} \times \frac{L_w}{L_g}} \tag{3-26}$$

$$F_{w-cd} = \cfrac{1}{\cfrac{1 - \varepsilon_w}{\varepsilon_w} + \cfrac{2 \times L_w}{L_w + L_{cd} - L_g} + \cfrac{1 - \varepsilon_{cd}}{\varepsilon_{cd}} \times \cfrac{L_w}{L_{cd}}} \qquad (3\text{-}27)$$

3.2.3.4 Evaporative heat transfer inside solar still

Evaporation occurs at the liquid vapor interface when the vapor pressure is less than the saturation pressure of the liquid at a given temperature. The evaporation heat transfer occurs in the solar still between water and water–vapor interface. The general equation for the total rate of evaporative heat transfer inside solar still is given by:

$$Q_{e_{w-h}} = H_v \times \dot{m}_{e_{w-h}} \times A_w \qquad (3\text{-}28)$$

$$Q_{e_{h-g}} = H_v \times \dot{m}_{e_{h-g}} \times A_w \qquad (3\text{-}29)$$

$$Q_{c_{e-cd}} = H_v \times \dot{m}_{e_{h-cd}} \times A_w \qquad (3\text{-}30)$$

Corresponding molar flux between water and humid air is given by the equation (Mahdi et al., 2020):

$$\dot{m}_{e_{w-h}} = k_m (c_{m,ws} - c_{m,h}) \qquad (3\text{-}31)$$

Mass transfer coefficient (k_m) is expressed as (Mahdi et al., 2020):

$$k_m = \cfrac{Sh \times D_h}{\cfrac{A_w}{2 \times (L_w + W_w)}} \qquad (3\text{-}32)$$

$$Sh = 0.022 \times (Ra \times Le)^{2/5} \tag{3-33}$$

$$Le = \frac{\alpha_h}{D_h} \tag{3-34}$$

The molar concentration at humid air $c_{m,ws}$ and brackish water $c_{m,h}$ can be evaluated from the ideal gas law with gas constant R = 8.314 J mol^{-1} K^{-1} (Mahdi et al., 2020).

$$c_{m,ws} = \frac{P_a}{R \times T_h} \tag{3-35}$$

$$c_{m,h} = \frac{P_{wv}}{R \times T_w} \tag{3-36}$$

We assumed that:

$$A_{w-g} \dot{m}_{e_{w-h}} = A_g \dot{m}_{e_{h-g}} \tag{3-37}$$

$$A_{w-cd} \dot{m}_{e_{w-h}} = A_g \dot{m}_{e_{h-g}} \tag{3-38}$$

3.2.3.5 Convective heat transfer between basin water and basin wall

The convective heat transfer from basin liner to brackish water is also given by the formula (Mahdi et al., 2020):

$$Q_{c_{w-b}} = h_{c_{w-b}} A_b (T_b - T_w) \tag{3-39}$$

$$h_{c_{w-b}} = \frac{k_w}{\sigma_b} Nu = \frac{k_w}{\sigma_b} C(GrPr)^n = 130 \, W/m^2K \qquad (3\text{-}40)$$

$$Gr = \frac{d_f^2 \rho_w^2 g \beta'}{\mu_w^2} \qquad (3\text{-}41)$$

$$Pr = \frac{\mu_w Cp_w}{k_w} \qquad (3\text{-}42)$$

If Gr < 10^5, Nu =1

If 10^5 < Gr < 2 x 10^7, C = 0.54, n = 0.25

If Gr > 2 x 10^7, C = 0.14, n = 0.33

3.2.3.6 Convective heat transfer between condenser tubes and fluid

The convective heat transfer from condenser tubes to inside fluid is also given by as:

$$q_{c_{cd-f}} = h_{c_{cd-f}}(T_{cd} - T_{wi}) \qquad (3\text{-}43)$$

$$h_{c_{cd-f}} = Nu_f \frac{K_f}{d_{in}} \qquad (3\text{-}44)$$

Where the Nusselt number calculated using the empirical Heaton formula suggested by Duffie and Beckman (1991):

$$Nu_f = Nu_\infty + \frac{a\left(Re_f Pr_f \frac{d_t}{L}\right)^m}{1 + b\left(Re_f Pr_f \frac{d_t}{L}\right)^n} \qquad (3\text{-}45)$$

With the assumption that the flow inside of tubes is fully developed, the values of Nu_∞, a, b, m, and n are 4.4, 0.00398, 0.0114, 1.66, and 1.12, respectively, for the constant heat flux boundary condition.

$$Re_f = \frac{V \times d_{in}}{v_f} = \frac{4 \times \dot{m} \times d_{in}}{\pi \times d_{in}^2 \times \mu_f} = \frac{4 \times 2.78 \times 10^{-4}}{\pi \times 0.0085 \times 8.33 \times 10^{-4}} = 50 \tag{3-46}$$

$$Re_f Pr_f \frac{d_t}{L} = 50 \times 5.68 \times \frac{0.0085}{0.3} = 8.046 \tag{3-47}$$

$$Nu_f = 4.4 + \frac{0.00398(8.046)^{1.66}}{1 + 0.0114(8.046)^{1.12}} = 4.51 \tag{3-48}$$

$$h_{c_{cd-f}} = Nu_f \frac{K_f}{d_{in}} = 4.51 \times \frac{0.6125}{0.0085} = 325 \tag{3-49}$$

3.2.3.7 Glass cover loss heat transfer

The heat is lost from the outer surface of the glass to the atmosphere through convection and radiation modes. The glass and atmospheric temperatures are directly related to the performance of the solar still. The temperature of the glass cover is assumed to be uniform because of small thickness. The total top loss heat transfer is defined as:

$$Q_{g-a} = Q_{c_{g-a}} + Q_{r_{g-a}} \tag{3-50}$$

$$Q_{c_{g-a}} = h_{c_{g-a}} A_g (T_g - T_a) \tag{3-51}$$

$$Q_{r_{g-a}} = h_{r_{g-a}} A_g (T_g - T_a) \tag{3-52}$$

Where convective and radiative heat transfer between glass and surrounding air can be calculated (Tiwari, 2002):

$$h_{c_{g-a}} = 2.8 + 3v \tag{3-53}$$

$$h_{r_{g-a}} = \frac{\varepsilon_g \sigma[(T_g + 273)^4 - (T_{sky} + 273)^4]}{T_g - T_a} \tag{3-54}$$

Swinbank (1963) found sky temperature to be correlated to the local air temperature by the relation:

$$T_{sky} = 0.0552 T_a^{1.5} \tag{3-55}$$

3.2.3.8 Condenser tubes loss heat transfer

The heat is lost from condenser tubes to atmosphere through insulation by conduction, convection and radiation processes. The total loss heat transfer coefficient of condensers is defined as (Tiwari, 2002):

$$q_{cd-a} = h_{cd-a}(T_{cd} - T_a) \tag{3-56}$$

$$h_{cd-a} = \left[\frac{\sigma_i}{K_i} + \frac{\sigma_{wc}}{K_{wc}} + \frac{1}{h_{t_{wc-am}}}\right]^{-1} \tag{3-57}$$

$$h_{t_{wc-am}} = 5.7 + 3.8v \tag{3-58}$$

3.2.3.9 Bottom and side loss heat transfer

The heat energy is lost from basin liner to the atmosphere through insulation by conduction, convection and radiation processes (Tiwari, 2002).

$$Q_{b-a} = h_{b-a}A_b(T_b - T_a) \tag{3-59}$$

$$h_{b-a} = \left[\frac{\sigma_i}{K_i} + \frac{\sigma_{wc}}{K_{wc}} + \frac{1}{h_{t_{wc-am}}}\right]^{-1} \tag{3-60}$$

$$h_{t_{wc-am}} = 5.7 + 3.8v \tag{3-61}$$

3.2.4   Radiative heat transfer between receiver and glass

$$Q_{r_{r-g}} = h_{r_{r-g}}A_r(T_r - T_g) \tag{3-62}$$

Radiative heat transfer coefficient between receiver and glass can be expressed (Duffie and Beckman, 1991):

$$h_{r_{w-g}} = \frac{\sigma((T_r + 273)^2 + (T_g + 273)^2)(T_r + T_g + 546)}{\frac{1}{\varepsilon_r} + \frac{1}{\varepsilon_g} - 1} \tag{3-63}$$

3.2.5   Convective heat transfer between receiver and fluid

The convective heat transfer from receiver tubes to inside fluid is also given by as:

$$q_{c_{r-f}} = h_{c_{r-f}}(T_r - T_{wr}) \tag{3-64}$$

$$h_{c_{r-f}} = Nu_f \frac{K_f}{d_{in}} \tag{3-65}$$

Where the Nusselt number calculated using the empirical Heaton formula suggested by Duffie and Beckman (1991):

$$Nu_f = Nu_\infty + \frac{a\left(Re_f Pr_f \frac{d_t}{L}\right)^m}{1 + b\left(Re_f Pr_f \frac{d_t}{L}\right)^n} \tag{3-66}$$

With the assumption that the flow inside of tubes is fully developed, the values of Nu_∞, a, b, m, and n are 4.4, 0.00398, 0.0114, 1.66, and 1.12, respectively, for the constant heat flux boundary condition.

3.2.6 Calculation of yield of proposed solar still

The hourly yield from the solar still can be calculated as:

$$m_{e_t} = \dot{m}_{e_{w-h}} \times 3600 \tag{3-62}$$

The daily yield is also calculated as:

$$M_e = \sum_{1}^{24} m_{e_t} \tag{3-63}$$

3.2.7 Computer simulation of the proposed solar still

In order to solve the nonlinear ordinary differential equations (1) to (8) for finding temperatures glass, condenser tube's surface, receiver tube's surface, outlet water in receiver, humid air, brackish water and basin liner, a computer simulation program (MATLAB ode45 subroutine) was written in MATLAB R2017a. An algorithm of solution is provided in figure 3.14.

From the measured initial values of temperature of glass cover, condenser tubes surface, water in tank, receiver tubes surface, water in receiver, water in basin and basin liner, and by giving the hourly solar irradiance and ambient

temperature, the performance factors of the proposed distiller can be predicted. The solar radiation and ambient Temperature use for simulation were showed in table 3.15.

The calculations were started to calculate thermophysical properties of humid air and brackish water by obtaining equation after giving the initial temperatures of different parts of solar still and data of weather. Having calculated these thermophysical properties, Prandtl, Grashof, Rayleigh, Nusselt, Lewis and Sherwood number can be calculated, from which various heat transfer coefficients, mass transfer coefficients and molar concentrations can be determined. The new temperatures can be calculated, which would be considered as initial values for the next interval time. From the calculation of mass flux of water vapor, the hourly and daily productivity of proposed solar still can be determined.
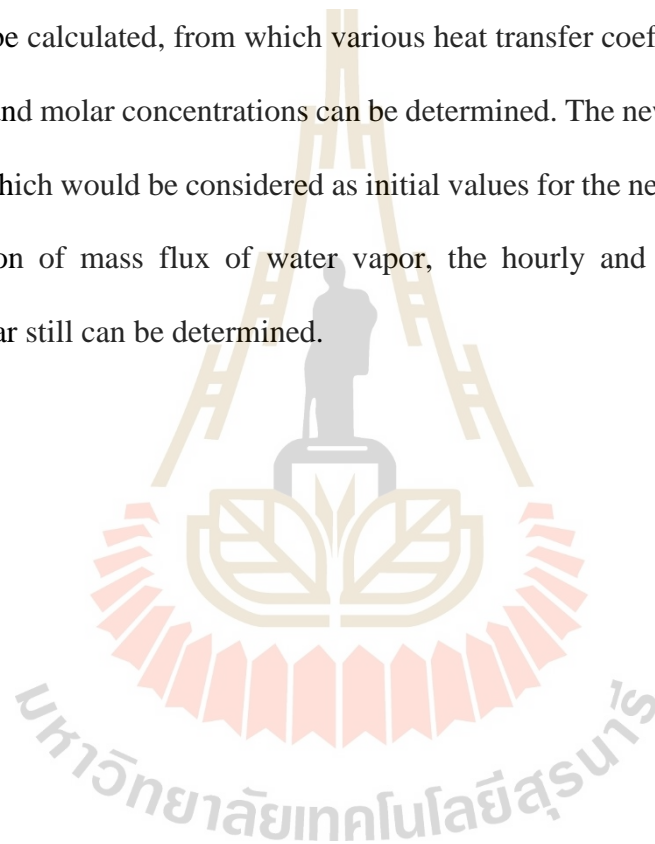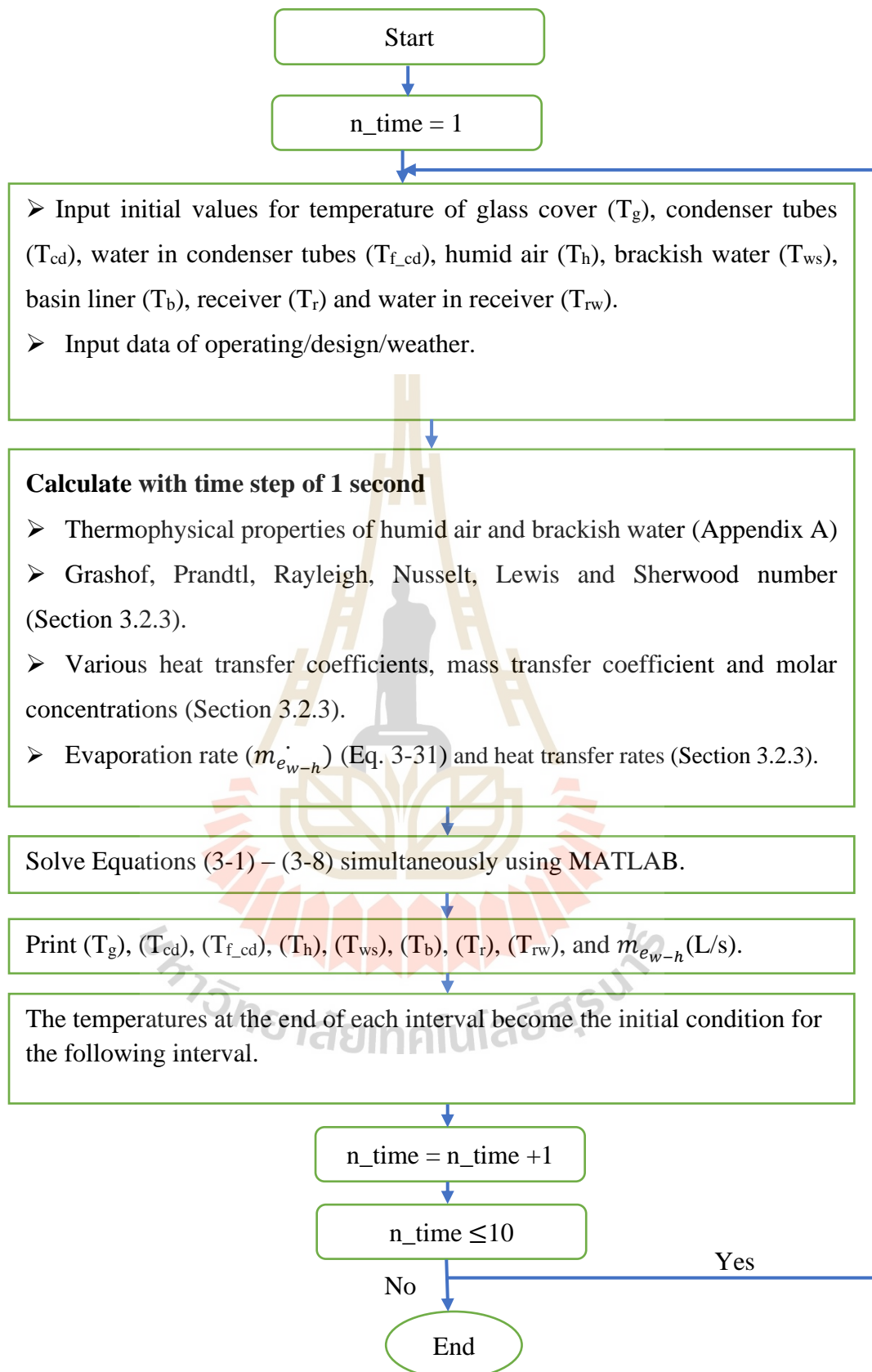
Figure 3.14 The algorithm of solution by the proposed approach of thermal modeling

Table 3.15 Solar radiation and ambient Temperature used for simulation

Time	Solar radiation	Ambient temperature
9	270	30
10	418	32
11	524	34
12	413	36
13	539	40
14	286	39
15	306	35
16	118	33
17	0	30
18	0	29

CHAPTER IV

RESULTS AND DISCUSSION

This chapter is divided into four sections. The first three sections cover the experimental results obtained from Models 1 - 3 which were described in chapter III, whereas the last one covers the theoretical results. All experimental results and theoretical analysis are presented and discussed below.

4.1 Results and Discussion of Model 1

This section presents the results obtained from the experimental work conducted to investigate the performance of Model 1 with different mass flow rates. The experimental results are presented and discussed below.

4.1.1 Experimental Results

Model 1 was tested using 2 different mass flow rates. Therefore, this subsection will begin with the experimental results of Model 1 with a mass flow rate of 1 L/h, including weather conditions on the experimental day. Solar radiation and ambient temperature on the experimental day of a mass flow rate of 1 L/h was described in Figure 4.1 and temperatures value was shown in Table 4.1. Then, the experimental results of Model 1 with mass flow rate 3 L/h was investigated and illustrated in Figure 4.2 and Table 4.2.

As can be seen in Figure 4.1, the solar intensity reached a peak at 12 o'clock at 960 W/m^2 and then reduced gradually. The ambient temperature on the experimental day ranged from 32^{0}C to 38°C.
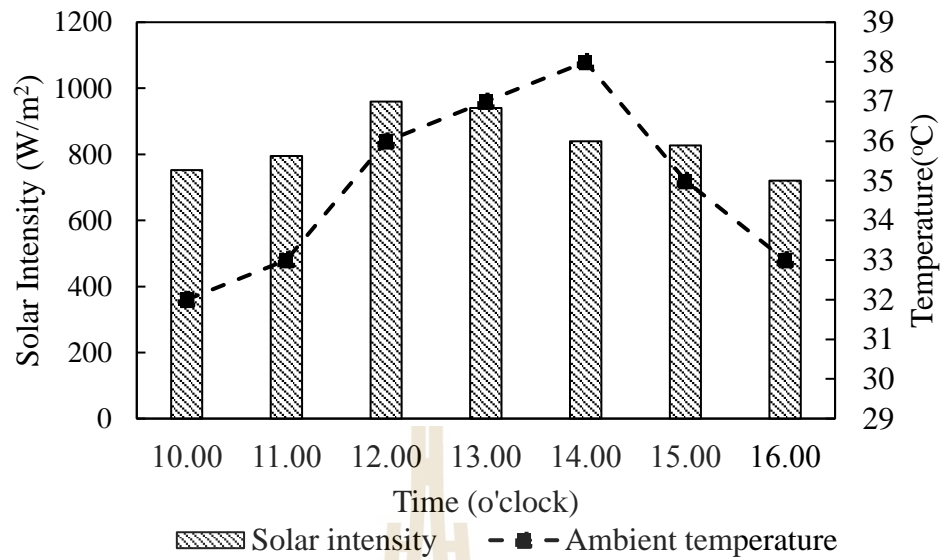
Figure 4.1 Solar radiation and ambient temperature on the experimental day with a mass flow rate of 1 L/h

Table 4.1 The temperature variation in different parts of the Model 1 at the mass flow rate of 1 L/h

Time	T_{wi}	T_{cd1}	T_{cd2}	T_{r1}	T_{r2}	T_{wo}	T_{ws}
10.00	34	30	34	37	40	45	35
11.00	39	41	43	50	60	55	42
12.00	40	41	50	58	63	58	50
13.00	42	44	52	60	70	63	53

Table 4.1 The temperature variation in different parts of the Model 1 at the mass flow

rate of 1 L/h (Continued)

Time	T_{wi}	T_{cd1}	T_{cd2}	T_{r1}	T_{r2}	T_{wo}	T_{ws}
14.00	39	42	48	55	60	53	51
15.00	30	42	45	44	50	46	47
16.00	33	40	40	42	47	45	45
Total productivity: 0.8 L/m² day							

Table 4.1 shows the temperature variation of water, condenser and collector tubes for the mass flow rate of 1 L/h. The highest value of the temperature of outlet water in the receiver (T_{wo}) and receiver's surface (T_{r2}) reached a peak at 63°C and 70°C respectively at 13 o'clock. The difference between the temperature of water in basin and mean temperature of condenser tubes was in the range of 2°C to 7.5°C.
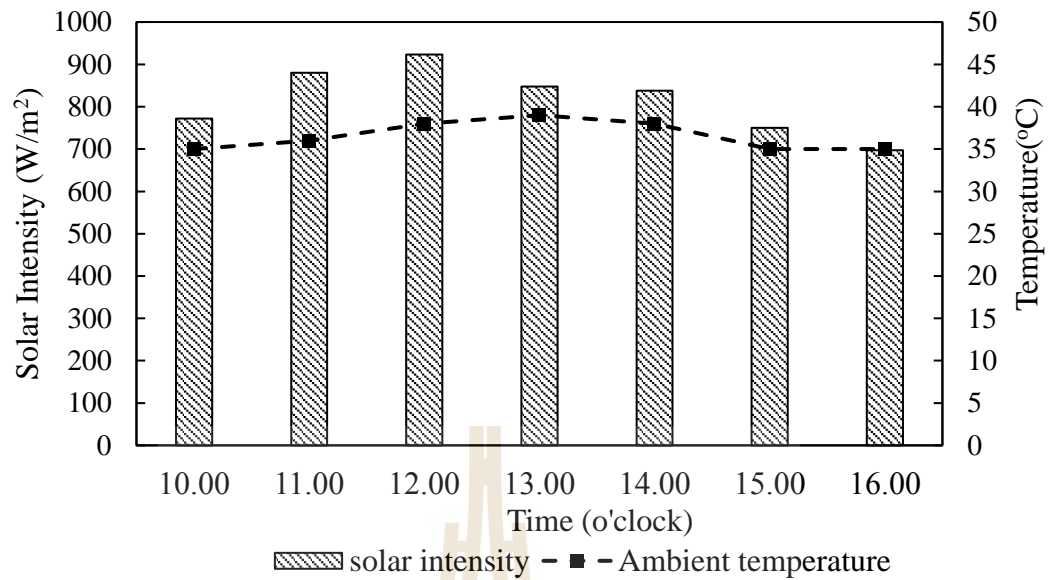
Figure 4.2 Solar radiation and ambient temperature on the experimental day with the

mass flow rate of 3 L/h

Table 4.2 The temperature variation in different parts of the Model 1 at the mass flow

rate of 3 L/h

Time	T_{wi}	T_{cd1}	T_{cd2}	T_{r1}	T_{r2}	T_{wo}	T_{ws}
10.00	36	34	40	43	54	41	35
11.00	38	43	45	55	59	45	43
12.00	35	39	41	53	64	45	42
13.00	36	41	40	51	60	44	44

Table 4.2 The temperature variation in different parts of the Model 1 at the mass

flow rate of 3 L/h (Continued)

Time	T_{wi}	T_{cd1}	T_{cd2}	T_{r1}	T_{r2}	T_{wo}	T_{ws}
14.00	35	41	40	53	58	44	41
15.00	38	36	39	52	55	44	40
16.00	37	36	38	50	53	42	39
Total productivity: 0.1 L/m^2 day							

Solar radiation and ambient temperature on the experimental day of the mass flow rate of 3 L/h were described in Figure 4.2. Table 4.2 shows the temperature variation of water, condenser and collector tubes for mass flow rates of 3 L/h. Higher temperature of outlet water in receiver are obtained during day time at mass flow rate of 1 L/h. The highest value of the temperature of outlet water in the receiver and receiver's surface is reached a peak at 63°C and 70°C respectively at 1 pm. The difference between temperature of water in basin and mean temperature of condenser tubes surface was from 0.5°C to 3.5°C with mass flow rate 3 L/h.

From Tables 4.1 and 4.2, higher temperature of water in solar still and outlet water in the receiver are obtained during day time at mass flow rate 1 L/h. The lower mass flow rate is better for heating feed water.

4.1.2 Discussion of Experimental results

According to Tables 4.1 and 4.2, the total productivity of Model 1 is 0.8 and 0.1 $L/m^2/day$ with mass flow rate of 1 L/h and 3 L/h respectively, which is lower than that of a conventional solar still (around 2.1 $L/m^2/day$). Additionally, the proposed solar still prototype distill much lower productivity than expectation (10 $L/m^2/day$). Three major reasons would be as follow:

1.   According to the temperature measurements, the temperatures of the water in the basin are relatively lower than those at the outlet of the receiver. According to the Equation (1), these changes in temperature of water in basin depends on the difference between energy input and energy output. Figure 4.3 described the major energy transfer mechanism in Model 1. The energy input of water in the still includes heat transferred from outlet water in receiver (Q_{wr-w}) and radiative heat transfer from condenser ($Q_{r(cd-w)}$), while the energy output consists of convection heat transfer between water and basin (Q_{b-w}), convection heat transfer between water and humid air ($Q_{c(w-h)}$) and evaporative heat transfer between water and humid air ($Q_{e(w-h)}$). Figure 4.36 shows that due to convection losses from the water to the basin and evaporation losses to the humid air above the water, the temperature of water raised marginally. Consequently, the obtained temperature of water in solar still (T_{ws}) ranged from 35°C to 53°C. Whereas, as shown in Figure 4.24, the water temperature in conventional solar still was from 35°C to 68°C, which cause higher evaporation rate and better productivity also. The water temperature difference between two stills could be due to absorption rate of basin water.

2.   In the proposed solar still, the temperature of the condenser's surface is not low, especially T_{cd2} (near U-turn position). Generally, during

condensation process, the vapor releases the latent heat of condensation in the condenser. This increases the temperature of condenser tubes and prevents the condensation of subsequent vapor which later reaches the condenser tubes with a temperature of water in basin then when comes in contact with the condenser tubes, it absorbs a latent heat which further increases its temperature. Figure 4.37 shows that heat transfer from tubes to fluid is much less than the heat they gain, which leads to the increased temperature of condenser. Additionally, as can be seen in the Figure 1 in Appendix B, the temperature of the condenser's surface is higher than the dew point temperature from 9 to 11 o'clock, which results in zero productivity in this period time. The water vapor starts to condense into water droplets from 11 o'clock to 17 o'clock. Moreover, the water storage tank is not insulated, which increase temperature of input water to condenser, resulted in low condensation rate. Another reason for the increase in condenser tubes temperature is conduction heat transferred from receiver tubes.

3.   The system is designed so that there is no water flowing out from the basin. The reason of doing this is to keep the useful heat absorbed at the receiver within the system. However, the discussion in section 4.4.4 indicates that productivity reduces when the amount of water increases gradually over time. Increasing of volumetric heat capacity of water requires the increase of heat source. However, the effect of high temperature water from receiver is not significant because the mass of water in the basin is larger than the mass of water supplied from the receiver in most experimental time. Meanwhile, the volume of water in conventional solar still approximately remain unchanged during experimental period, which cause constant volumetric heat capacity of water. As a result, the temperature of basin water increased significantly comparing to Model 1.
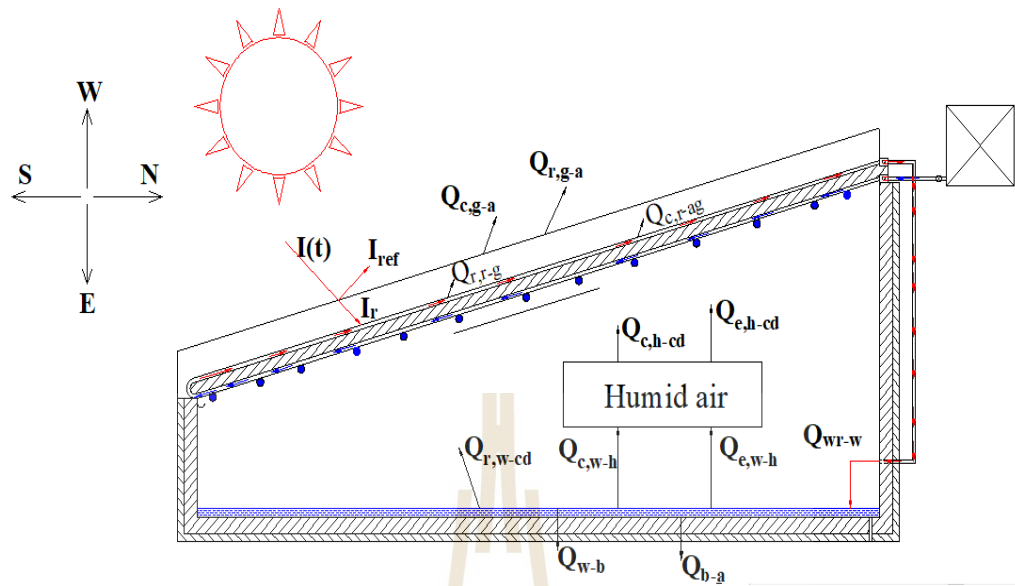
Figure 4.3 The major energy transfer mechanism in Model 1.

4.   As we can see in Figure 4.4, water vapor condensed on the surface of tubes, however, as the droplet increased its size, it became heavier and thus may fall down before reaching to the collector trough.

Figure 4.4 Condensation in solar still

4.2   Results and Discussion of Model 2

4.2.1   Experimental results

The experimental result subsection describes results obtained from two Models 2. It will begin with the performance of "Model 2 without glass". Then, the experimental results of "Model 2 with glass" are shown.

4.2.1.1 Model 2 without glass cover solar still

Figure 4.5 depicts the solar radiation and ambient temperature with respect to time. The solar radiation is measured in the range of 630 W/m^2 to 1103 W/m^2, and the ambient temperature is in the range of 32 °C to 44 °C.
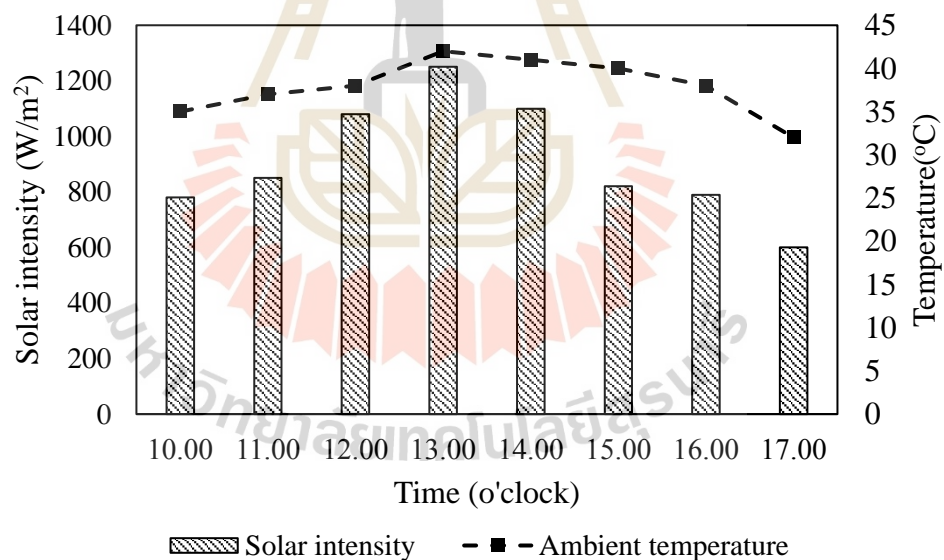
Figure 4.5 Solar radiation and ambient temperature on the experimental day of

"Model 2 without glass"

Table 4.3 The temperature variation in the different parts of the Model 2

Time	T_{wi}	T_{cd}	T_{r1}	T_{r2}	T_{wo}	T_{ws}	T_b
10	34	34	75	83	42	35	30.3
11	37	37	60	69	57	40	37
12	39	40	70	78	74	41	39
13	39	44	90	99	97	47	45
14	35	41	82	88	85	50	47
15	37	40	75	80	77	48	46
16	36	39	68	73	69	44	43
17	34	36	62	69	65	41	41
Total productivity: 1.5 L/m^2 day							

The variation of hourly temperatures is recorded in Table 4.3. The highest temperature of collector and water in the collector are obtained at 2 pm (99°C and 97°C respectively). Nevertheless, the temperature of water in basin still keep in low because of low temperature of the basin. Moreover, the distribution of water in the system is not uniform due to low mass flow rate. The productivity of model 2 is 1.5 L/m^2/day.

4.2.2.2 Model 2 with glass cover solar still

The climatic conditions on the experimental day of Model 2 with glass is given in Figure 4.6. The solar radiation is measured in the range of 630 W/m^2 to 1103 W/m^2 and the ambient temperature is in the range of 32 $^{\circ}$C to 44 $^{\circ}$C.
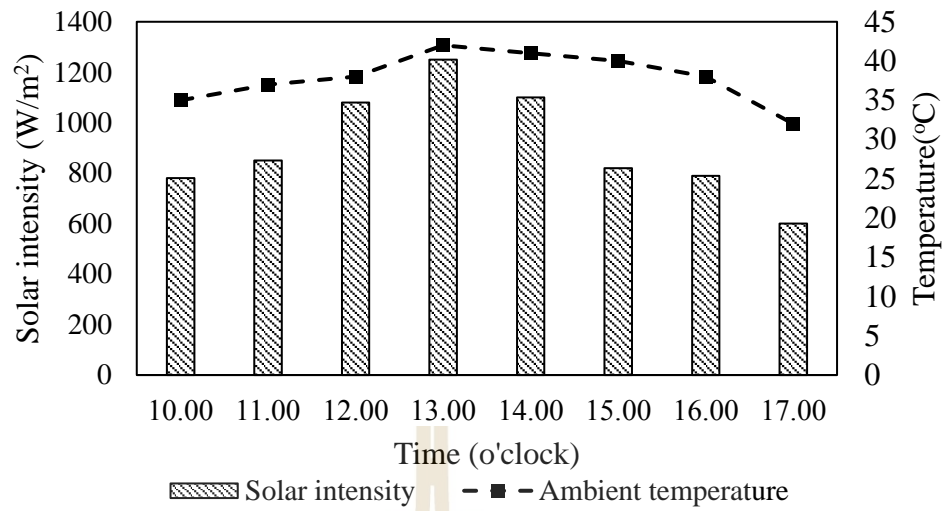
**Figure 4.6** Solar radiation and ambient temperature on the experiment day of Model
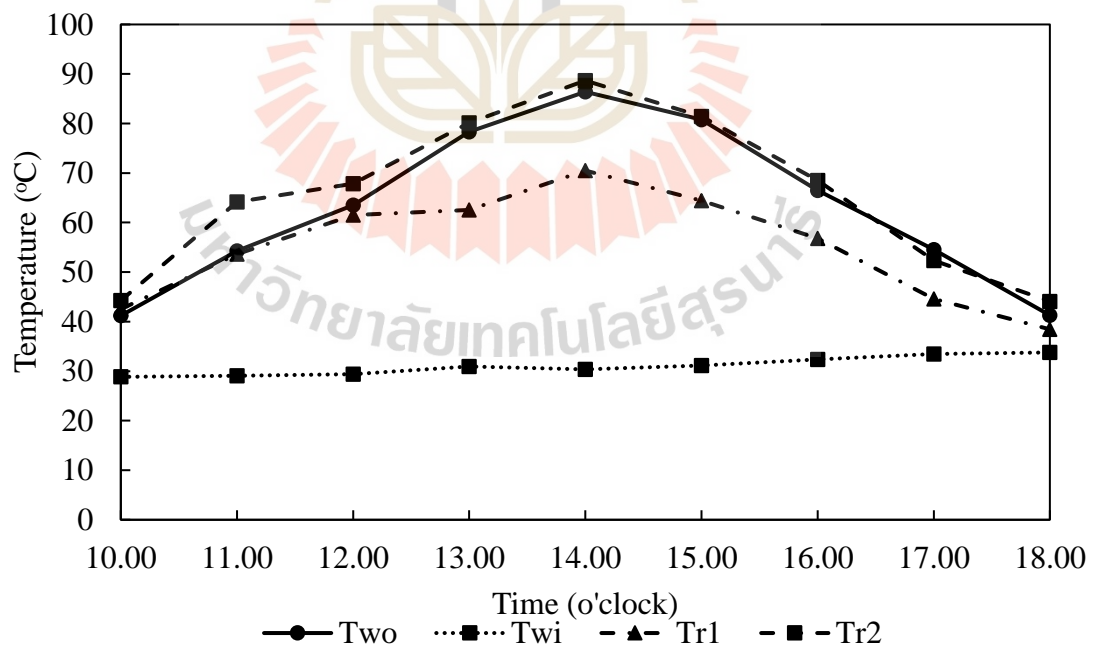
Figure 4.7 The temperature of inlet water (Twi), outlet water (Two) and receiver's

surface (Tr1 and Tr2) of solar still with glasses cover

The collector and the water out collector got the highest temperatures at 2 p.m. at 88.67°C and 86.4°C which are shown in Figure 4.7. It is observed that there is a significant increase in the temperature of water after flowing through the tube system. The temperature of water was then raised by 60°C at 14 o'clock.

Figure 4.8 shows temperature variation of water, humid air and relative humidity inside the still. Relative humidity was remarkably low, below 55% before 15 o'clock and increased significantly in the rest of experimental time due to the temperature increase of the air and the decreased evaporation rate. It was clear that the relative humidity of the humid air was definitely not saturated in the daytime.
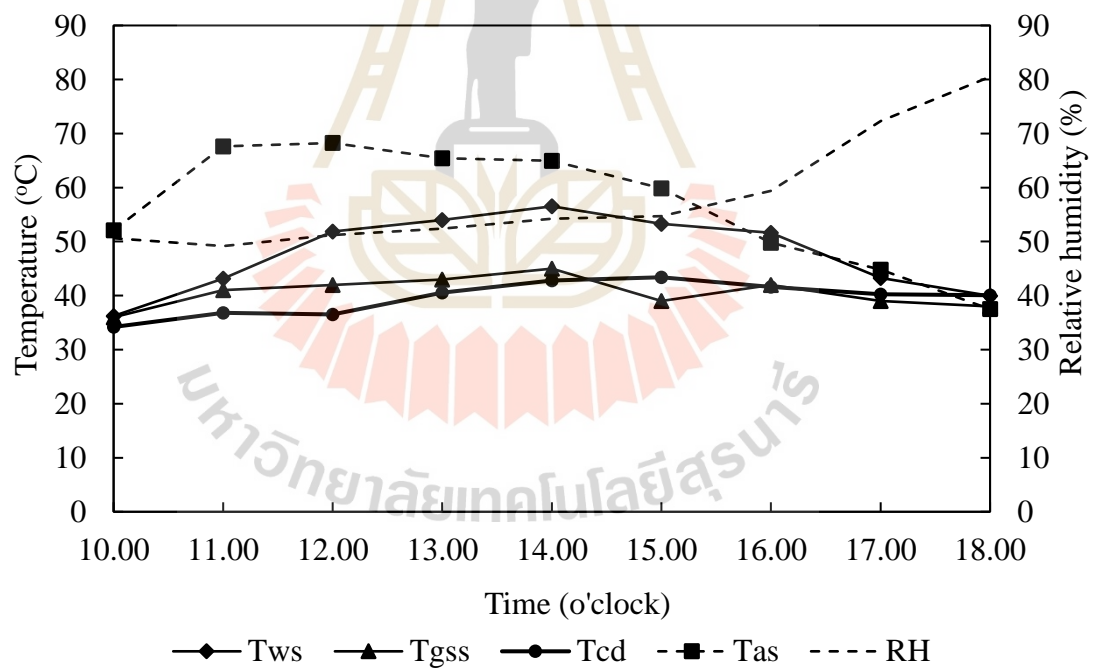
Figure 4.8 The temperature of water in still (Tws), condenser tubes (Tcd), glass of still (Tgss), humid air in solar still (Tas) and Relative humidity (RH).
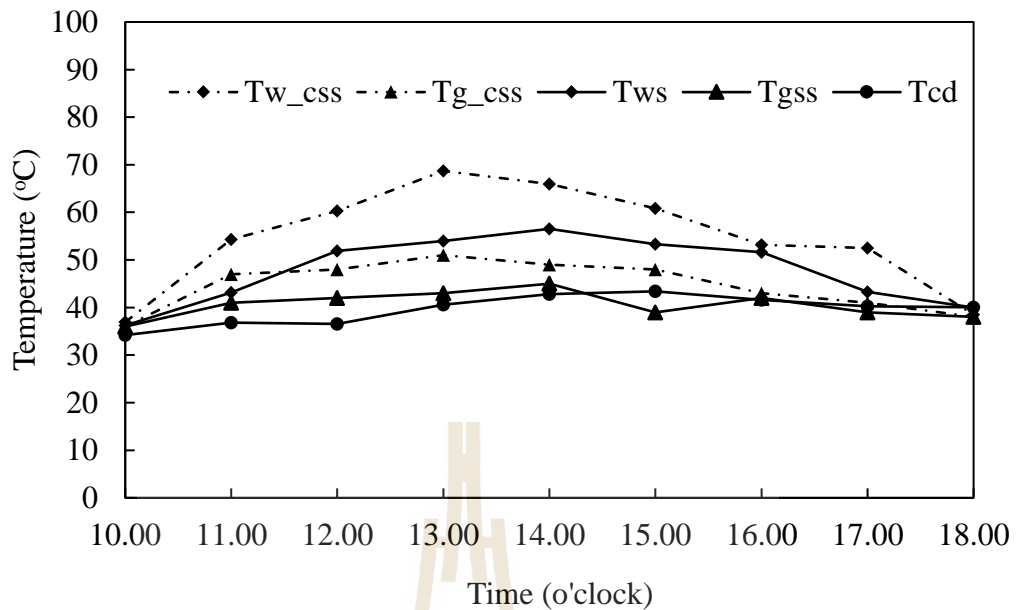
Figure 4.9 The hourly temperature variations of water for Model 2 and the conventional

solar still

Figure 4.9 gives information about the temperature variations of water in Model 2 and the conventional solar still. The temperature of water and glass cover of the conventional solar still were in the range of $36.93 – 73.5^{\circ}$C and $36 – 51^{\circ}$C respectively. Compared to conventional solar still, the temperature of water after flowing out from the collector tubes in Model 2 was higher but it was the opposite for the water temperature in the basin wall. Moreover, from Figure 4.8 and 4.9, the temperature of condenser tubes (in range of 34.2 to 43.4°C) and glass (from 36 to 45°C) in Model 2 is lower than that of glass cover in the conventional solar still (in the range of 36 to 51°C). The yield of conventional solar still was 2.1 L/m^2/day while the accumulated productivity of Model 2 was 2.3 L/m^2/day.

4.2.3   Discussion

It was apparent that the daily productivity of distiller was enhanced when we used glass cover distiller comparing to Model 1 and Model 2 without glass. We believe that this is due to:

- The temperature of water in solar still was increased, which improved the evaporation rate. As discussion in section 4.1, in Model 1, the water transferred heat to basin by convection mode. However, it opposite when we used glass cover in Model 2.

-The change in tilt angle of condenser tubes prevented water droplet falling down to the basin

- The insulation of water tank maintained the water in tank at a low temperature. This lowered the condenser's temperature considerable and enhance condensation process.

However, the temperature of water in proposed distiller was lower than that in the conventional one. This is due to 90$^\text{o}$ angle of glass, which did not maximize the amount of solar radiation absorbed by distiller. In addition, the increase in mass of water was related to the low productivity of Model 2.

4.3   Results and Discussion of Model 3

The experiment of Model 3 was conducted to investigate the influence of water depth in solar still and the mass flow rate of water in condenser and receiver tubes. A conventional solar still with similar basin area was built to compare with Model 3 in the same condition of water depth. This section discusses the experimental results of Model 3, which was illustrated in section 3.3.

4.3.1 Effect of water level in solar still

Figure 4.10 depicts the solar radiation with respect to time on three experimental days. It is observed that solar radiation intensity increased to the highest value at midday and decreased after that gradually. During the test, it was cloudy, which was the reason why the fluctuations appeared in the figure.
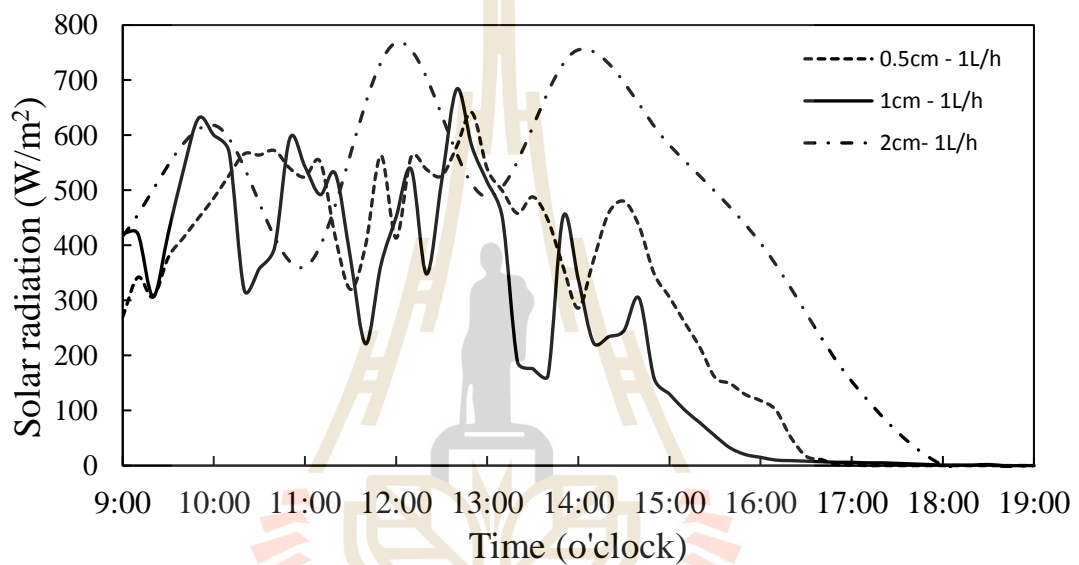

Figure 4.10 Solar radiation on 3 different days for 3 different water depths

The hourly observed water temperatures for different water depths have been shown in Figure 4.11 As can be seen in this figure, the higher temperatures of water are obtained during day time at water depth 0.1 cm. The water temperature peak at 67°C at 14 o'clock, 64°C at 13 o'clock and 62°C at 13 o'clock for 0.5 cm, 1 cm and 2 cm water depth respectively.
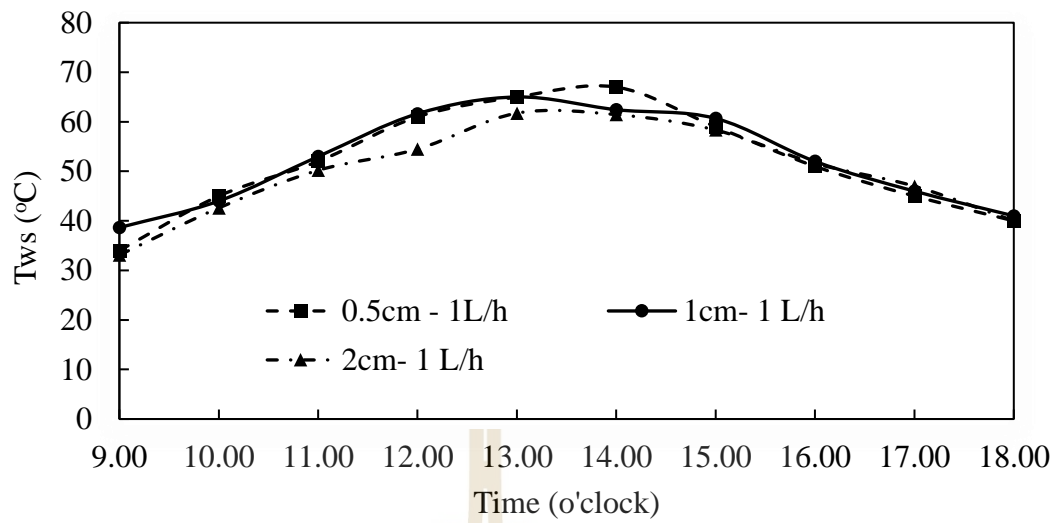
**Figure 4.11** Variation of water temperature for all water depths.
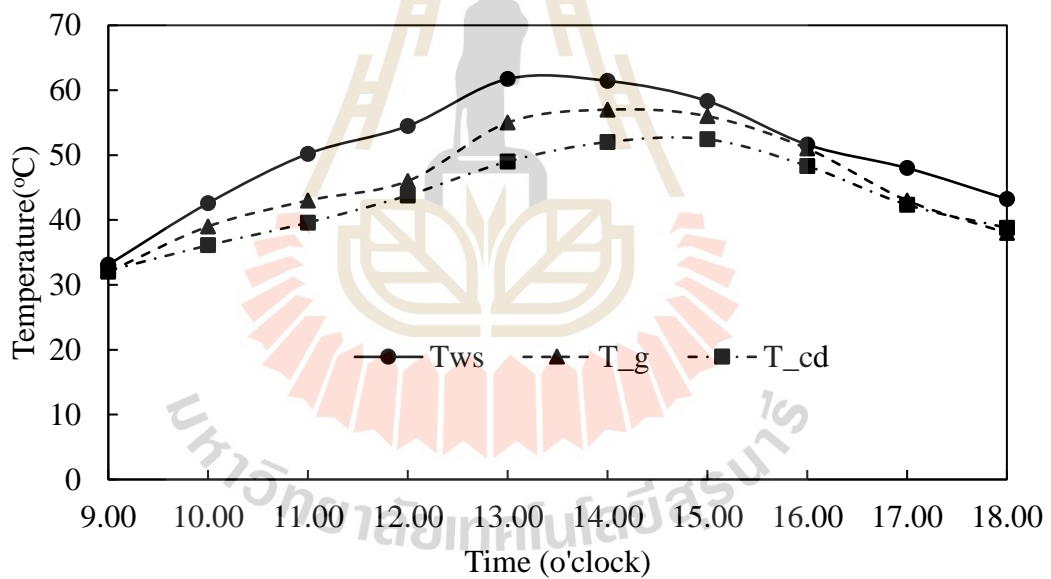
Figure 4.12 Temperature of water, glass and condenser at water level 2 cm
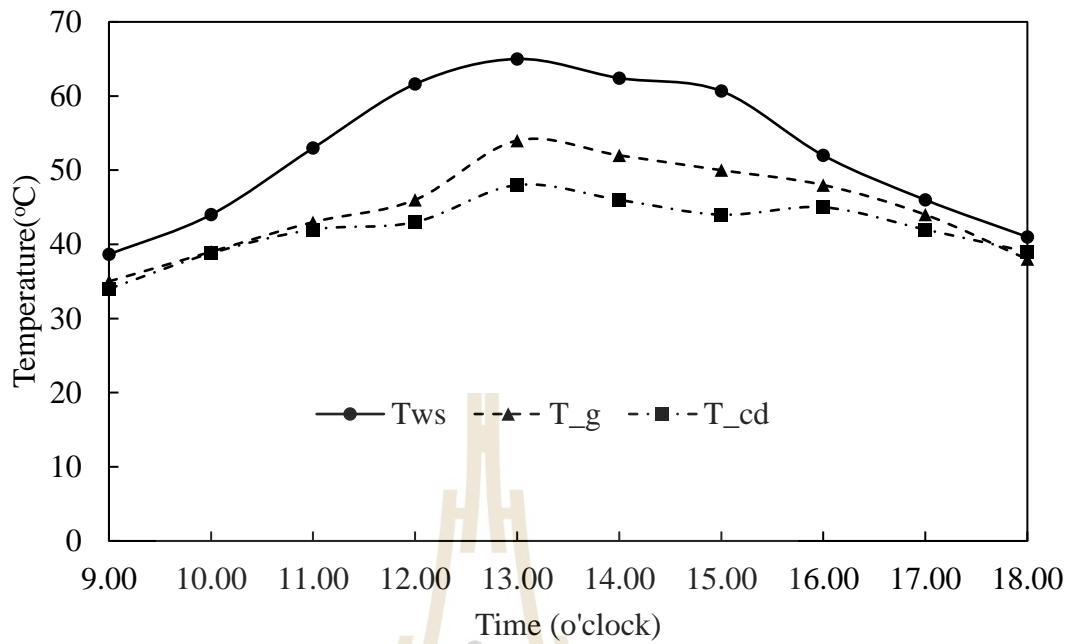
**Figure 4.13** Temperature of water, glass and condenser at water level 1 cm
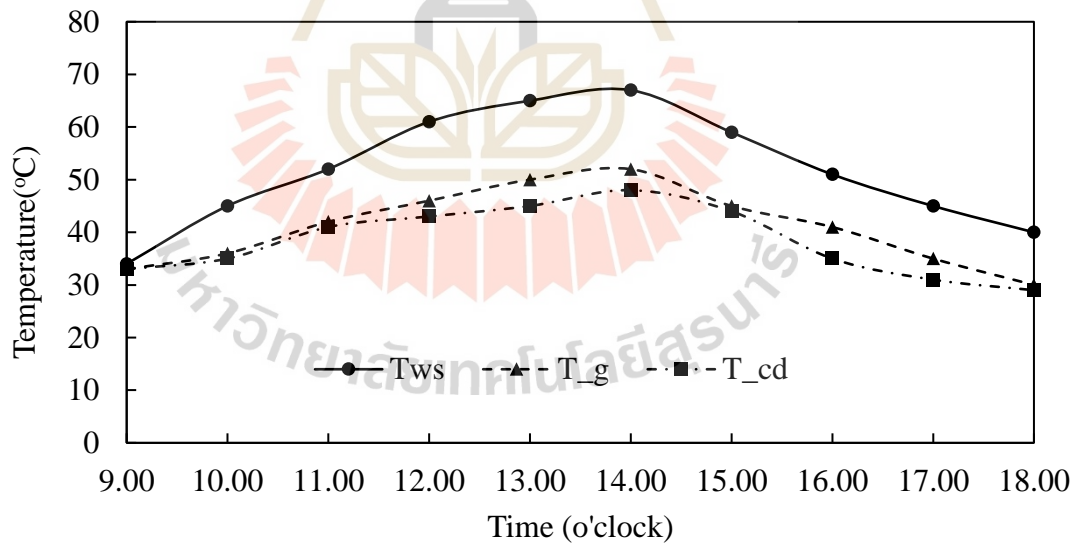
Figure 4.14 Temperature of water in basin, glass and condenser at water level 0.5 cm

The temperature of water in solar still, glass and condenser at water depth 2 cm, 1 cm and 0.5 cm are illustrated in Figure 4.12, 4.13 and 4.14 respectively.

The higher difference in temperature between water and condenser surface (glass and condenser tubes) belongs to water depth 0.5 cm. The temperature difference between water and glass ranges from 1°C to 15°C and between water and condenser tubes from 1°C to 20°C. This is due to the cooling effect of the water flowing in the tubes.

Figure 4.15 compares cumulated productivity from glass, condenser tubes and rectangular box of different water levels. In 3 cases, the productivity from glass is higher than that of the condenser and the box because of its larger area. The highest output is 1310 ml/day (approximate 3.5 L/m^2/day), belonging to water depth 0.5 cm. The productivity of solar still reduces with the increase of water depth.
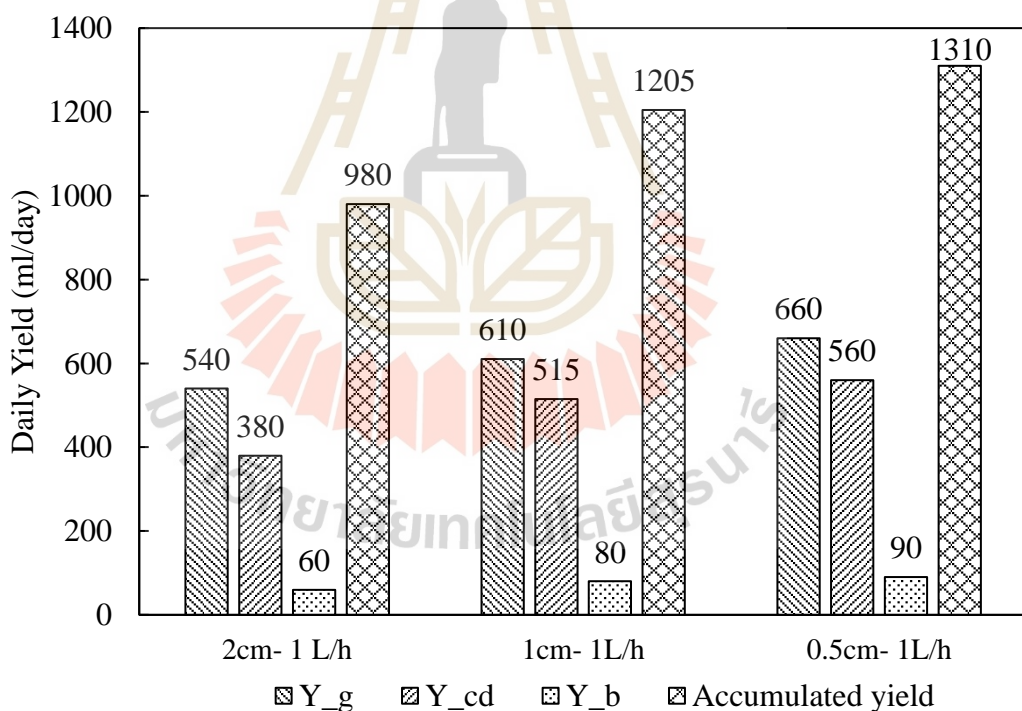

Figure 4.15 Variations of cumulated productivity from glass (Y_g), condenser tubes (Y_cd) and rectangular box (Y_b).
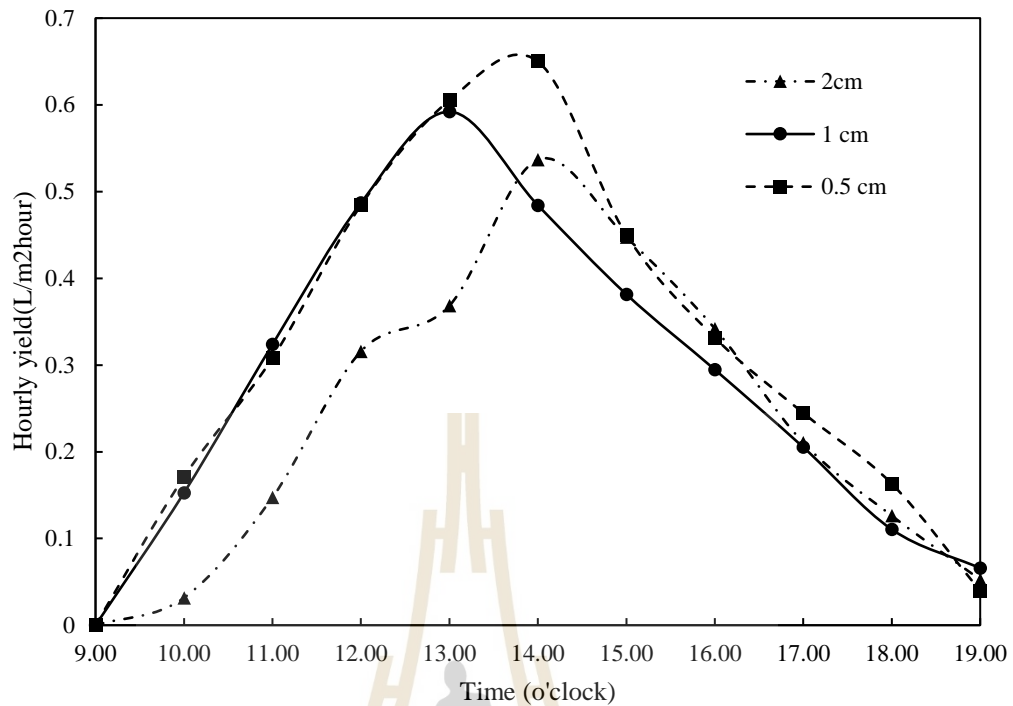
Figure 4.16 Variations of cumulated productivity at different water depths.

4.3.2 Effect of mass flow rate on performance of solar still

In this subsection, attention is drawn to the impact of different mass flow rates on the productivity of Model 3 at the same water depths. Experimental results and discussion are presented as follow.

4.3.2.1 Water depth 0.5 cm

Figure 4.17 illustrates the solar radiation with respect to time on two experimental days of Model 3 at water depth 0.5 cm with different mass flow rates of 1L/h and 0.5 L/h. During the test, it was cloudy, which was the reason of the fluctuations appeared in the figure. It is observed that solar radiation intensity increased to the highest value at midday at 641 W/m^2 and decreased after that gradually
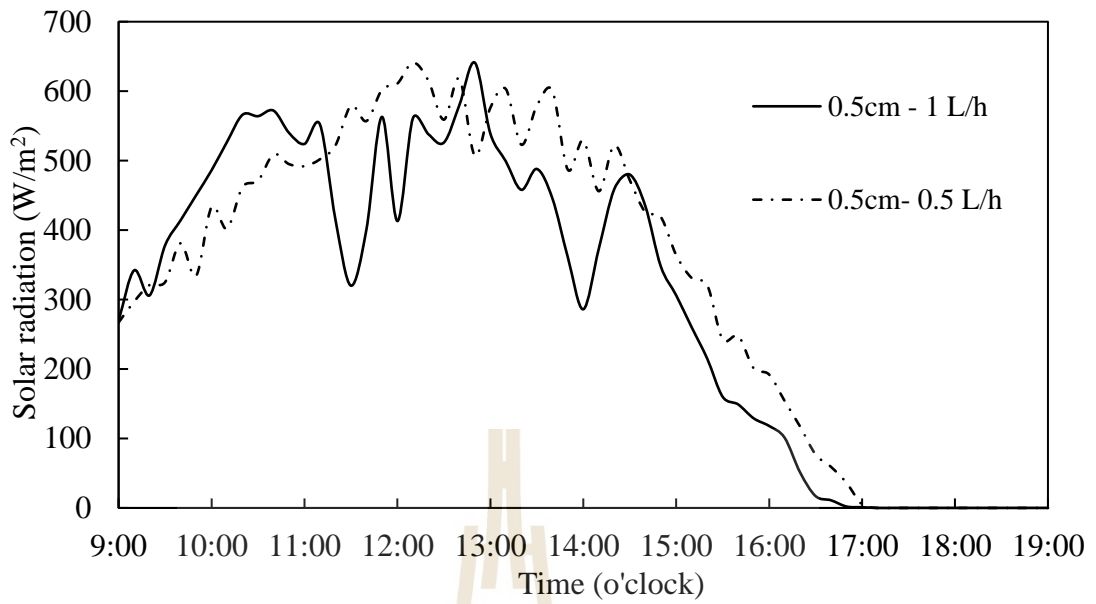
Figure 4.17 Irradiation variation with time on 2 days with different mass flow rates at

water depth of 0.5 cm
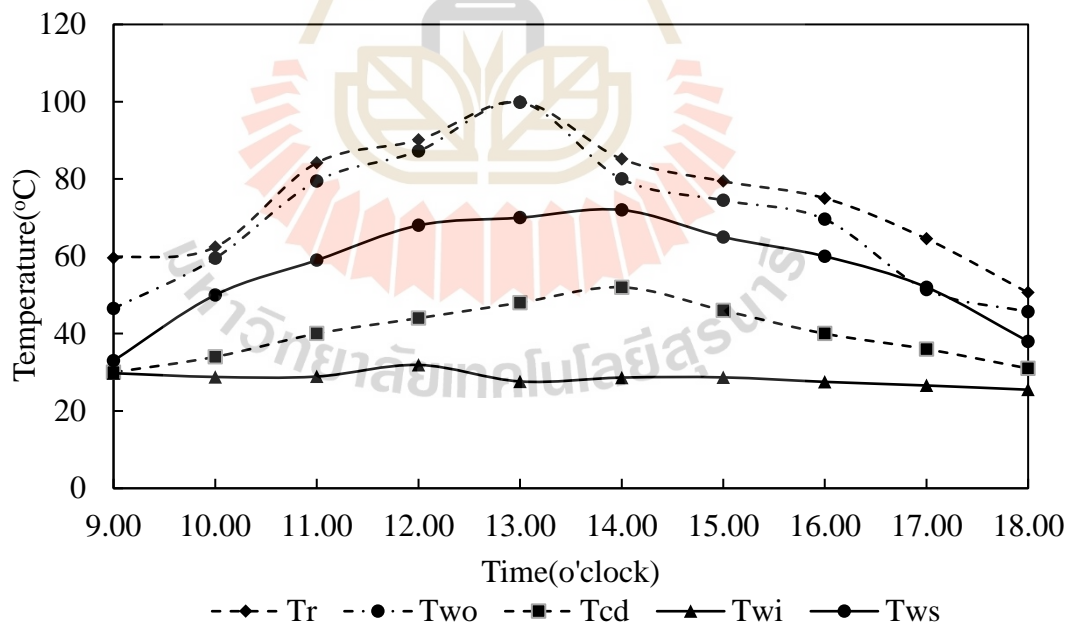
Figure 4.18 Effect of mass flow rate of 0.5 L/h on receiver, condenser and water out
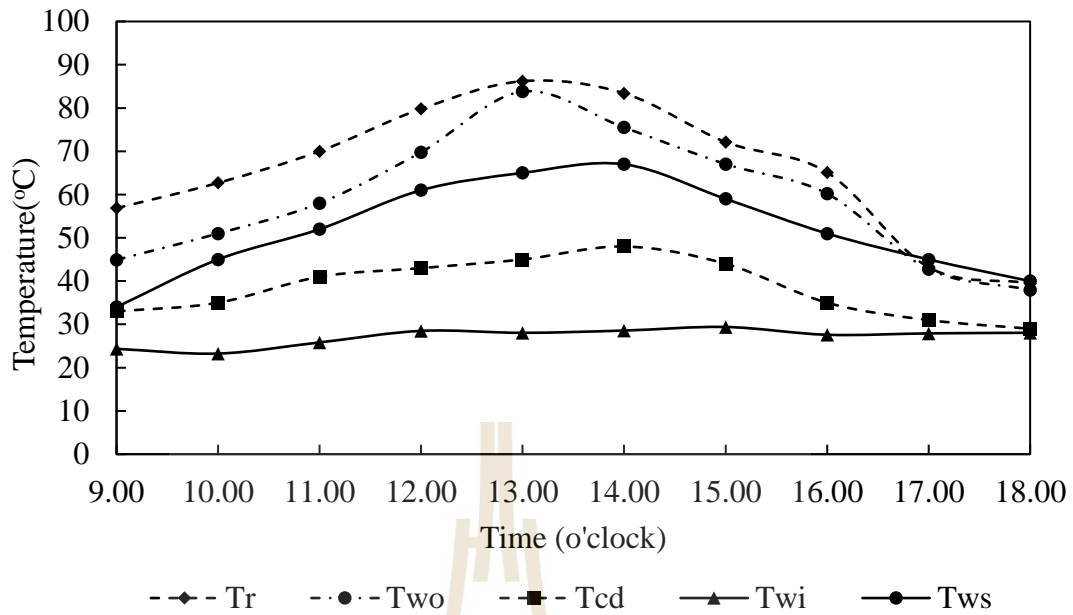
receiver.

Figure 4.19 Effect of mass flow rate of 1 L/h on receiver, condenser and water out

receiver.

The variation of receiver's surface, water out receiver and condenser's surface temperature at the same water depth of 0.5 cm with mass flow rates of 0.5 L/h and 1 L/h are shown in Figure 4.18 and Figure 4.19 respectively. It is observed that the reduction of mass flow rate causes the increase of temperature of receiver, condenser and fluid flow in tubes. The results show that they went up to the highest value at noon and then decreased gradually. Higher water and receiver's temperatures are obtained at mass flow rate of 0.5 L/h, and the maximum temperature is 99.8°C at 13 o'clock. Meanwhile, at mass flow rate of 1L/h, the temperature of receiver and water reach a peak at 86.2°C and 83.8°C at 13 o'clock. Additionally, there is a decrease in the temperature difference between water and condenser when the mass flow rate decline.

4.3.2.2 Water depth 1 cm
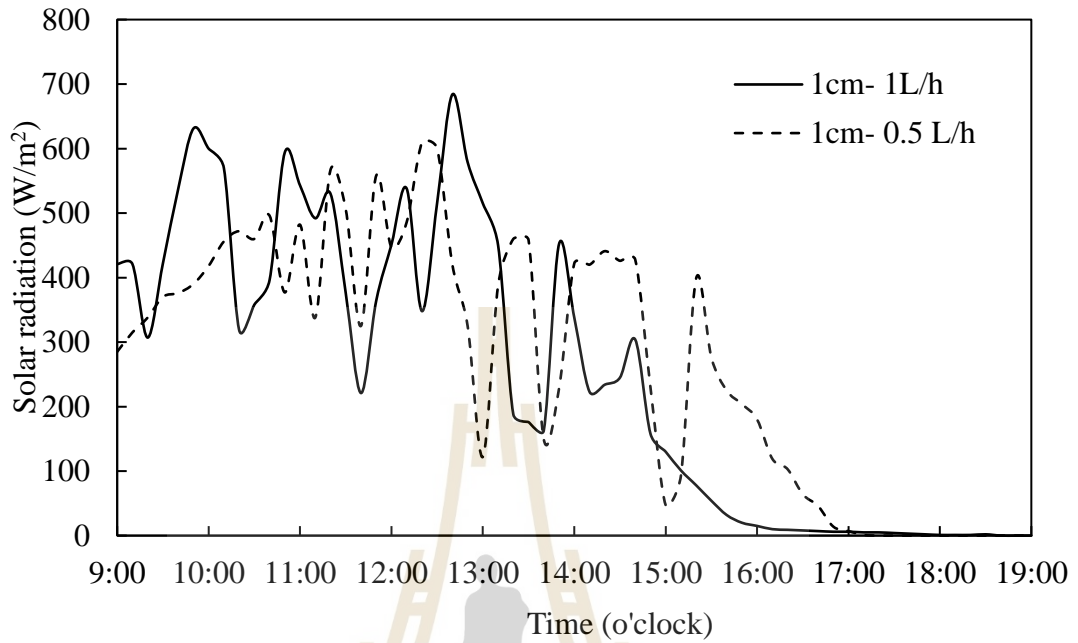
Figure 4.20 Irradiation variations with time on 2 days with different mass flow rates

at water depth of 1 cm
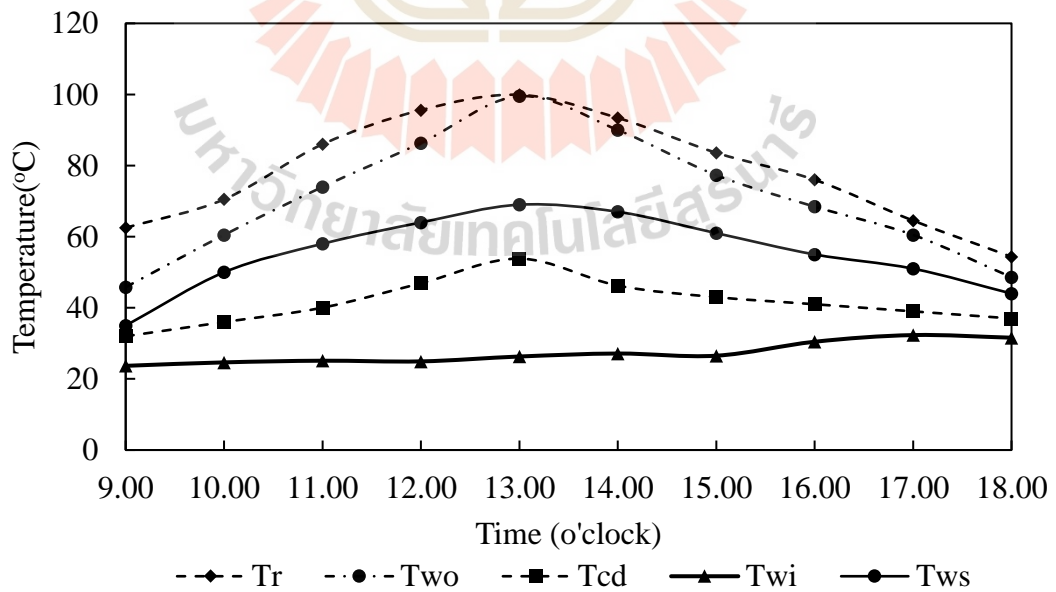
Figure 4.21 Effect of mass flow rate of 0.5 L/h on receiver, condenser and water out

receiver at 1 cm of the basin water depth.
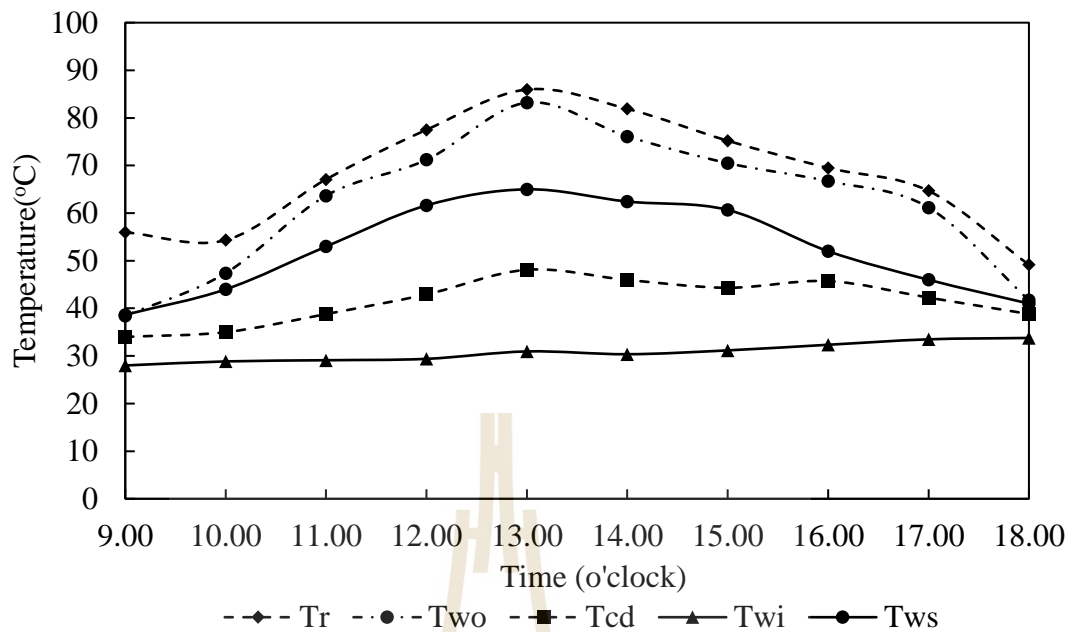
Figure 4.22 Effect of mass flow rate of 1 L/h on receiver, condenser and water out
receiver at 1 cm of the basin water depth.

The effect of the mass flow rate at water depth of 1 cm on Model

3 is similar to that at water depth of 0.5 cm. Figure 4.21 and Figure 4.22 indicate that

when the mass flow rate increases, the temperature of receiver, condenser and outlet

water from receiver. Higher temperature of outlet water from receiver and receiver

surface were obtained at mass flow rate of 0.5 L/h, and the highest temperature is 99.5°C

at 13 o'clock. Meanwhile, at mass flow rate of 1L/h, the temperature of receiver surface

and outlet water of receiver reach a peak at 85.96°C and 83.2°C at 13 o'clock. In

Addition, the temperature difference between water and condenser declined due to the

reduce of the mass flow. Comparing to case of 0.5 cm of water depth, the temperature

of basin water was lower for both mass flow rates.
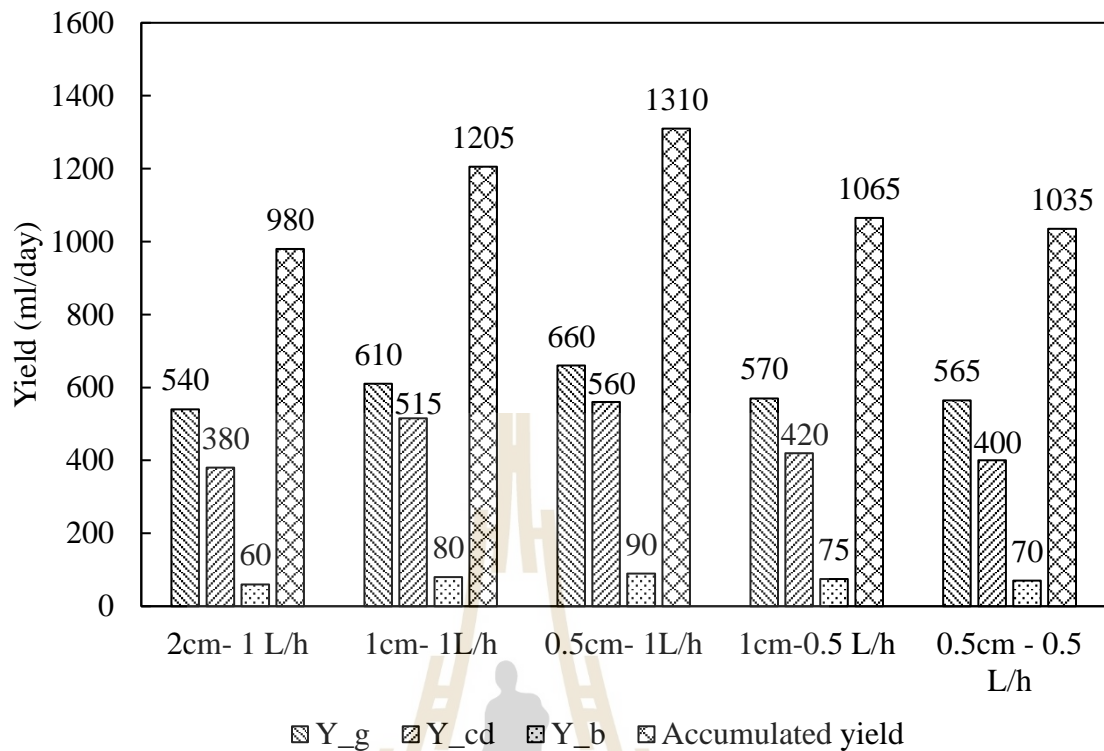
Figure 4.23 Variations of accumulated productivity from glass, condenser tubes and rectangular box with different mass flow rates and water depths

Figure 4.23 shows information about cumulate yield from glass, condenser tubes and rectangular box at different water levels and two mass flow rates. It is interesting that in all cases, although the obtained temperature of glass was lower than that of condenser surface and rectangular box, the distilled water from glass is higher than that of the condenser and the box. The larger area of glass is reason of this result. Moreover, the reduction of mass flow rate resulted in the lower productivity. This is explained that the volume of high temperature outlet water from receiver is much lower than the volume of basin water in case of mass flow rate of 0.5 L/h. The water depth of 1 cm and 0.5 cm have volume of 3.8 liters and 1.9 liters, respectively.

4.3.3 Comparison between Model 3 with the conventional solar still

4.3.3.1 Water depth 1 cm
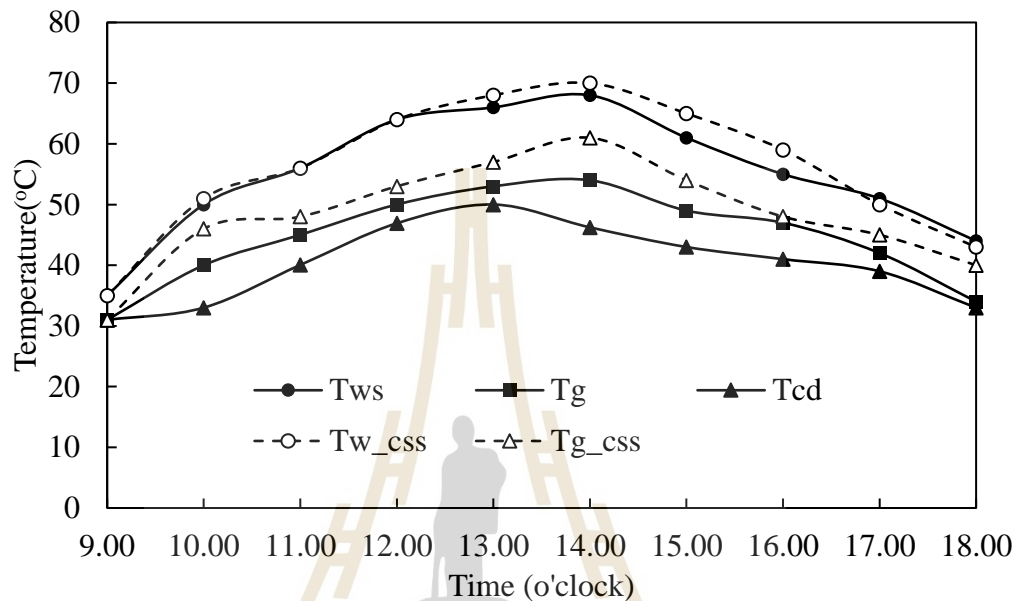
Figure 4.24 Temperature comparison between the Model 3 at 1 cm of water depth and 0.5 L/h of mass flow rate and conventional solar still.

Figure 4.24 compares the temperature of water in basin and condenser's surfaces between Model 3 and the conventional solar still at 1 cm water depth. The temperature of water in single basin solar still ranges from 35°C to 70°C and that of Model 3 is between 35°C to 68°C. The temperature difference between water and glass in the conventional still is 4 to 11°C, while in Model 3, it ranges from 4°C to 14°C (between water and glass) and from 4°C to 21°C (between water and condenser). Due to the higher temperature gradient between water and condenser surfaces, accumulated yield of Model 3 is higher than that of conventional solar still. This is illustrated in Figure 4.25. The accumulated productivity of Model 3 at 1 cm of water

depth and 0.5 L/h of mass flow rate was 2.9 L/m^2/day while that of conventional distiller was 2.1 L/m^2/day.
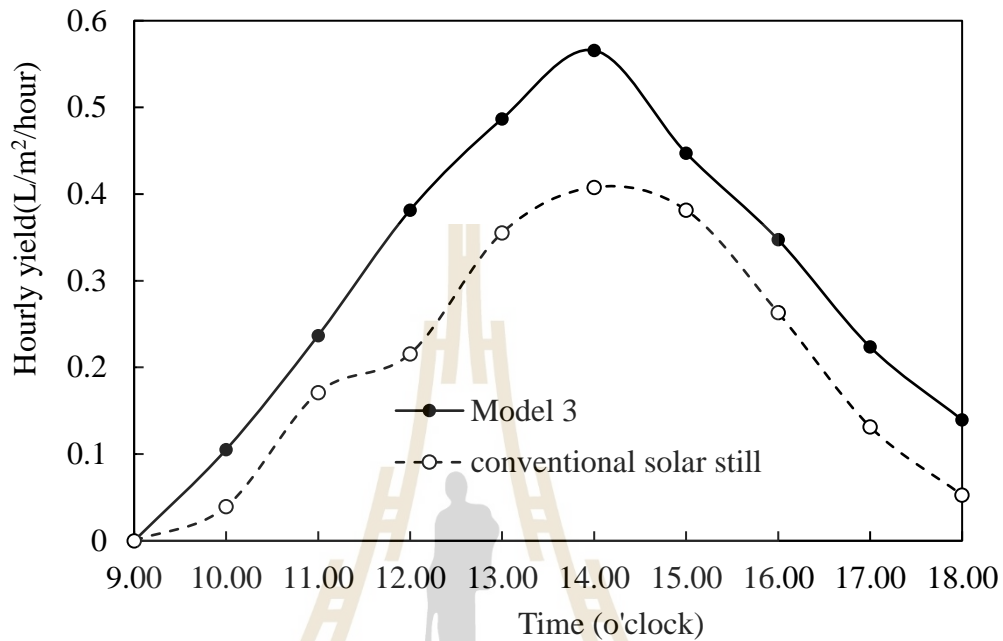
Figure 4.25 Cumulative productivity comparation between the Model 3 at 1 cm of water depth and 0.5 L/h of mass flow rate and conventional solar still.

4.3.3.2 Water depth 0.5 cm

Temperature comparison between the conventional solar still and Model 3 at water depth of 0.5 cm is shown in Figure 4.26. The temperature difference between water and glass of conventional solar still ranges from 2°C to 26°C (at 12 o'clock), while that of Model 3 is 3°C to 17°C (with glass) and 3°C to 20°C (with condenser tubes). However, because there was no additional water source, there were dry spots in the conventional solar still from 13 o'clock, which reduce its productivity. The output of Model 3 at 0.5 cm water depth and 0.5 L/h mass flow rate is 2.7 L/m^2/day, is higher than that of single basin solar still at water depth of 0.5 cm (1.7L/m^2/day).
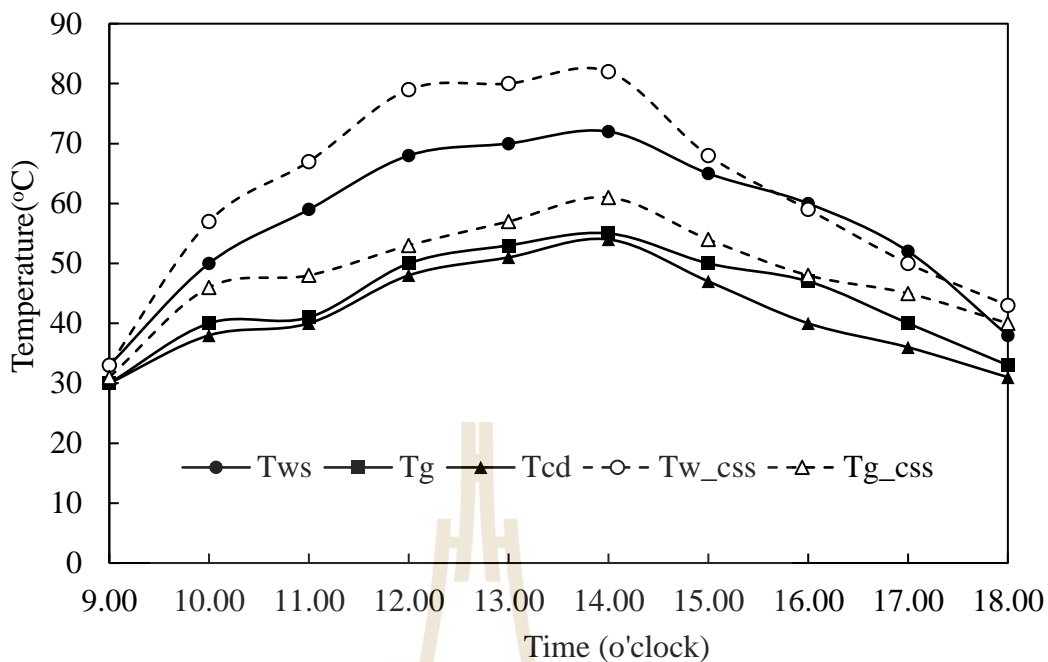
Figure 4.26 Temperature comparison of water and condenser's surface between Model

3 and the conventional solar still.
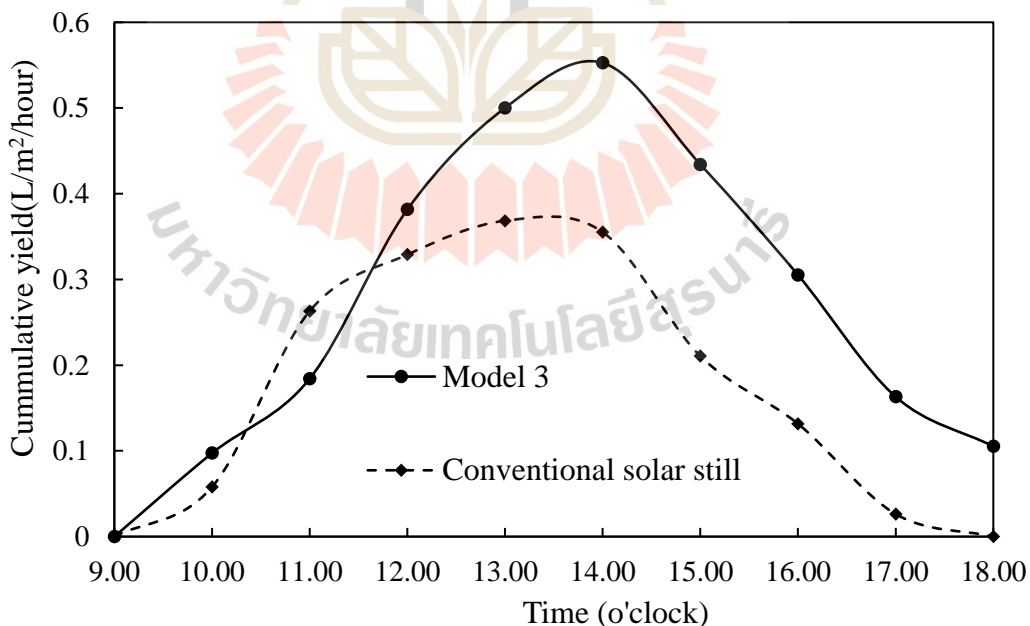
Figure 4.27 Cumulative productivity comparison between Model 3 with a mass flow

rate of 0.5 L/h and the conventional solar still at the same water level.

4.3.4 Comparison of daily productivity between 3 models
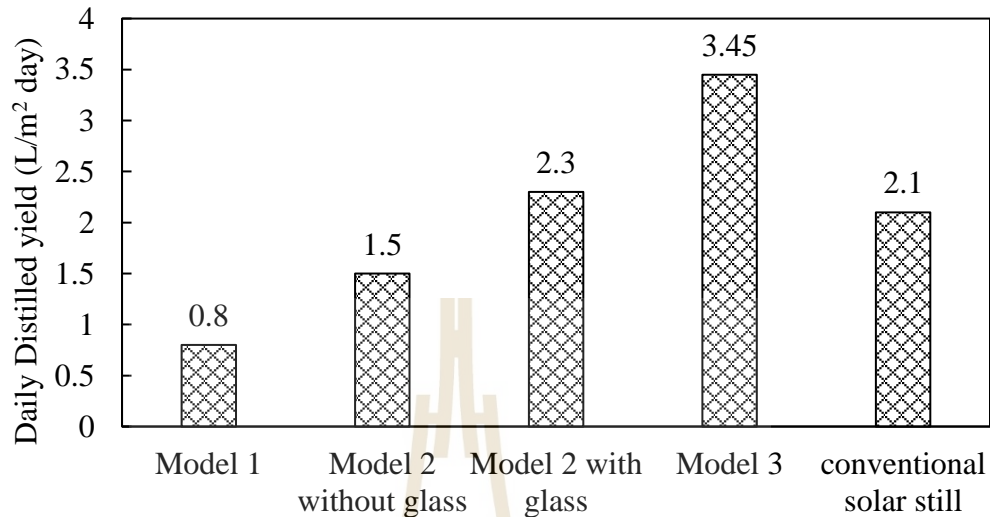
Figure 4.28 Cumulative productivity comparison between Model 3 with 0.5 L/h mass

flow rate and conventional solar still at the same water level

The total daily yield of three Models and the conventional solar

still are put in comparison in Figure 4.28. The highest productivity is 3.45 L/m²/day,

belonging to Model 3 with water level of 0.5 cm and mass flow rate of 1 L/h. Following

it, in descending order are Model 2 with glass, conventional solar still, Model 2 without

glass and Model 1. The productivity of Model 3 improved by 64.3% compared with

conventional solar still.

4.4 Theoretical Results

Numerical calculations were carried out to explore the performance of solar still

based on realistic data of solar insolation and ambient temperature on experimental day

of Model 3. There are 3 cases to be studied and their descriptions are listed as below:

- Case 1 - mass flow rate of 1 L/h, water depth of 0.5 cm, with glass cover, with overflow.

- Case 2 - mass flow rate of 1 L/h, water depth of 0.5 cm, with glass cover, without overflow.

- Case 3 - mass flow rate of 1 L/h water depth of 0.5 cm, without glass cover, without overflow.

The theoretical analysis is used to predict the performance of distiller in cases of no glass and no overflow. The influence of temperature of water in the tank, area of condenser and receiver and water depth on total daily productivity for 3 cases above were predicted and described as below.

4.4.1 Validation of Mathematical Model with Experimental Results

The levels of agreement between the theoretical results and experimental data in terms of temperatures of water in solar still, condenser tubes receiver tubes, glass and the daily productivity of Model 3 at mass flow rate of 1 L/h and water depth of 0.5 cm are illustrated and discussed in this subsection.
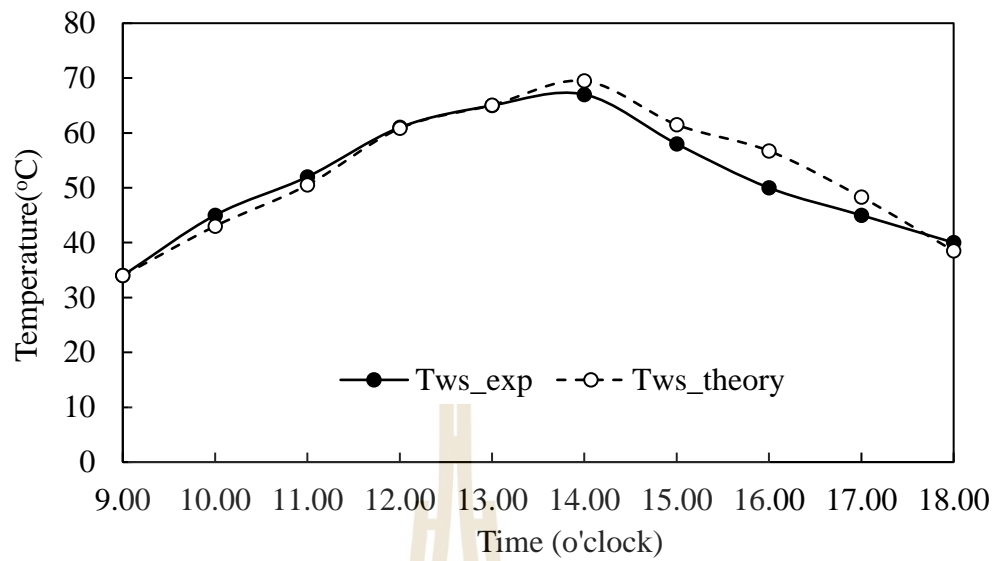
Figure 4.29 Temperature comparison of water in solar still calculated from the
present model with experimental data.
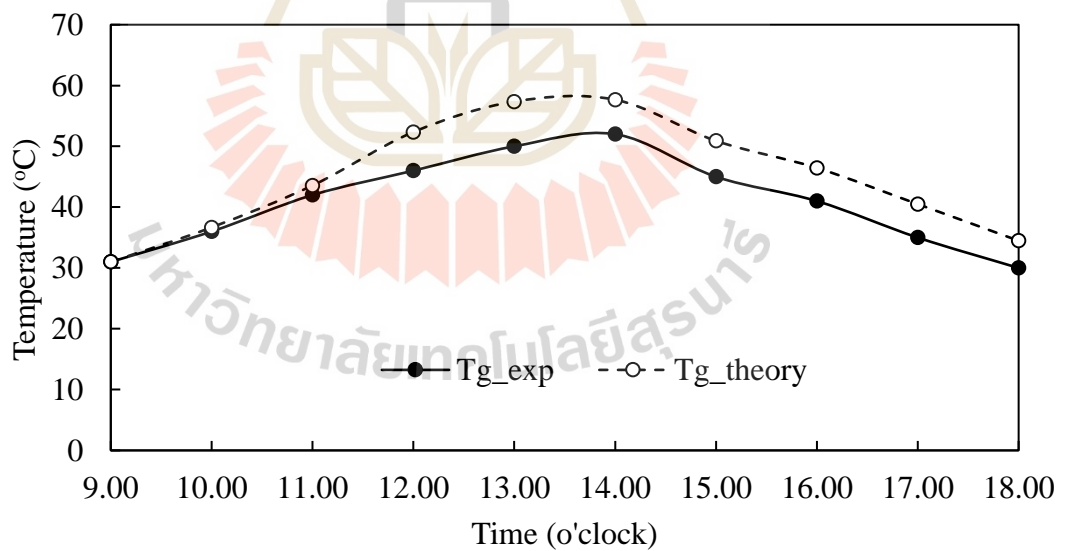
**Figure 4.30** Temperature comparison of glass calculated from the present model with
experimental data.
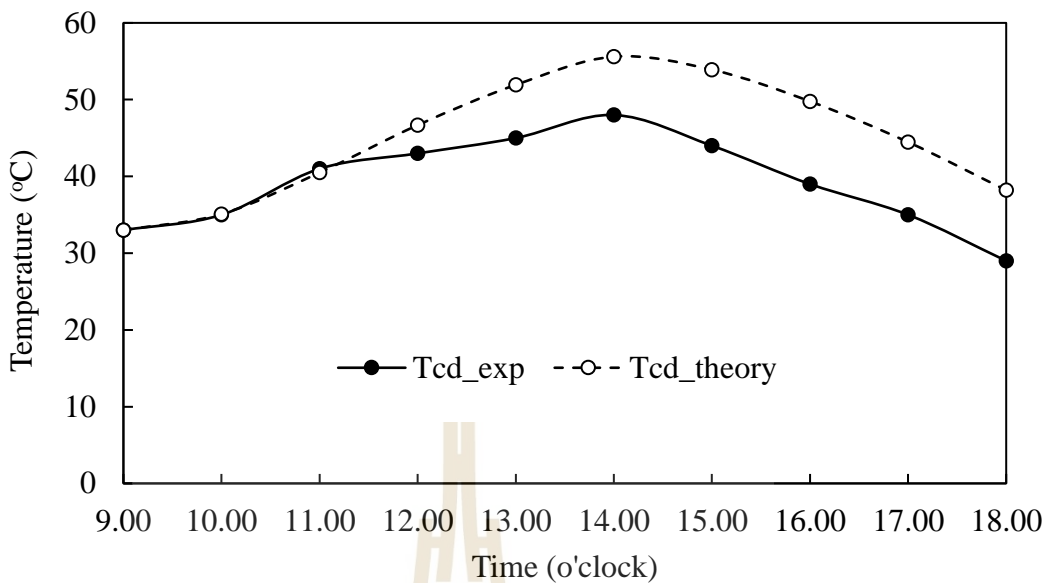
Figure 4.31 Temperature comparison of condenser tubes in solar still calculated from

the present model with experimental data.
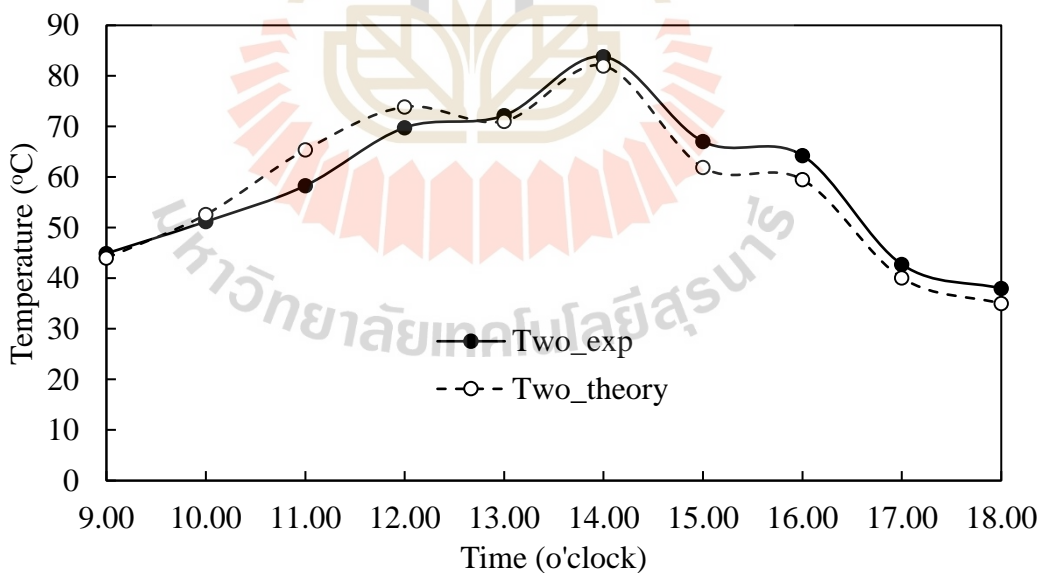
Figure 4.32 Comparison of temperature of outlet water in receiver calculated from the

present model with experimental data.
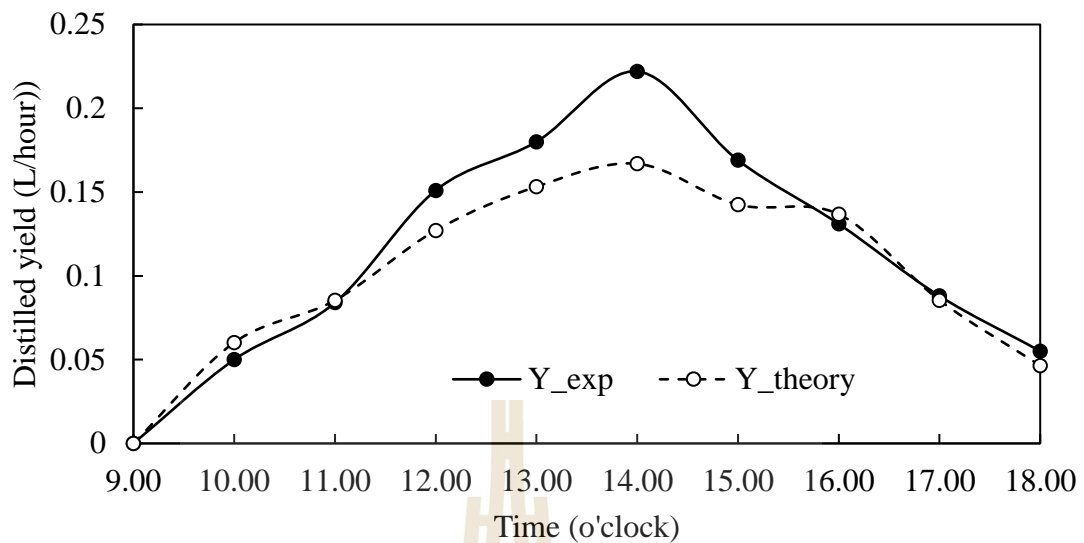
Figure 4.33 Comparison of distilled yield calculated from the present model (Y_theory) with productivity from experimental data (Y_exp).

As can be seen clearly in Figure 4.29 to Figure 4.32, the temperature variations of water in basin, glass cover, condenser tubes and water out collector calculated from the thermal model are close to experimental data. The difference in temperature between the experiment and prediction are observed in ranges from 0 to 6.72°C for brackish water, 0.68°C to 8.3°C for glass, 0.1 to 14.87°C for condenser tubes and 0.9°C to 14.37°C for water out collector. The error percentages between experiment and theoretical analysis are: 0.1 to 10 percent for water in basin, 1.8 to 19.1 percent for glass cover, 0.28 to 30% for condenser tubes, 1.57 to 10.8 percent for water out collector. Figure 4.34 compares the productivity of solar still between theoretical analysis and experimental data. The error percentage between experimental and theoretical yield is 18 percent.

Related to modeling errors, the reason may partly from air velocity and solar intensity, which is considered a constant parameter through time interval. Moreover,

the designed parameters come from the other paper are calculated approximately such as: emissivity, absorptivity, and transmissivity of glass, water, basin liner, copper tubes, mass of condenser, mass of basin, mass of receiver. The effects of aforementioned problems may naturally lead to the errors of calculation.
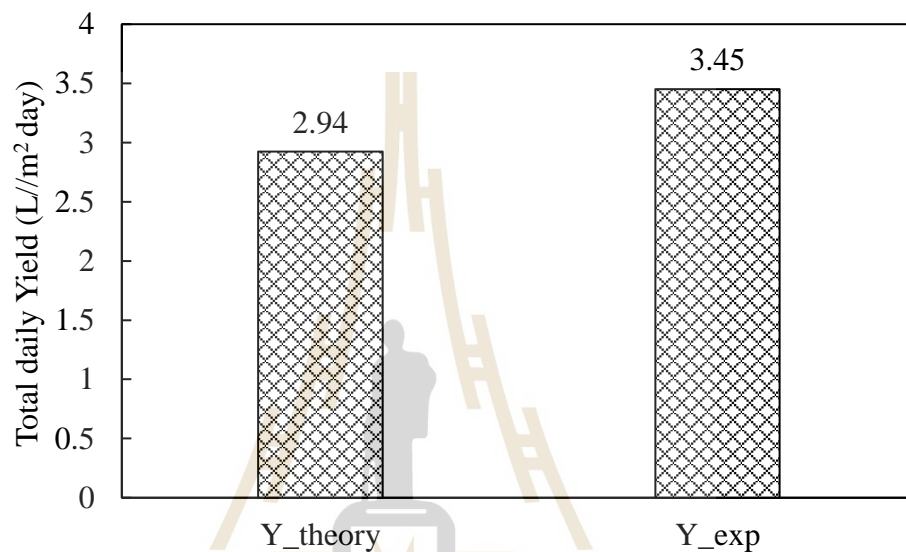
**Figure 4.34** Comparison between theoretical daily productivity (Y_theory) and
experimental daily productivity (Y_exp)

4.4.2 Validation of heat transfer rate in water in basin and condenser tubes

This subsection presents heat transfer rates input into and output from condenser tubes and water in basin in two circumstances with glass and without glass at 1 p.m. Two circumstances symbolize Model 3 and Model 1 respectively.

4.4.2.1 Heat transfer rate in solar still without glass cover
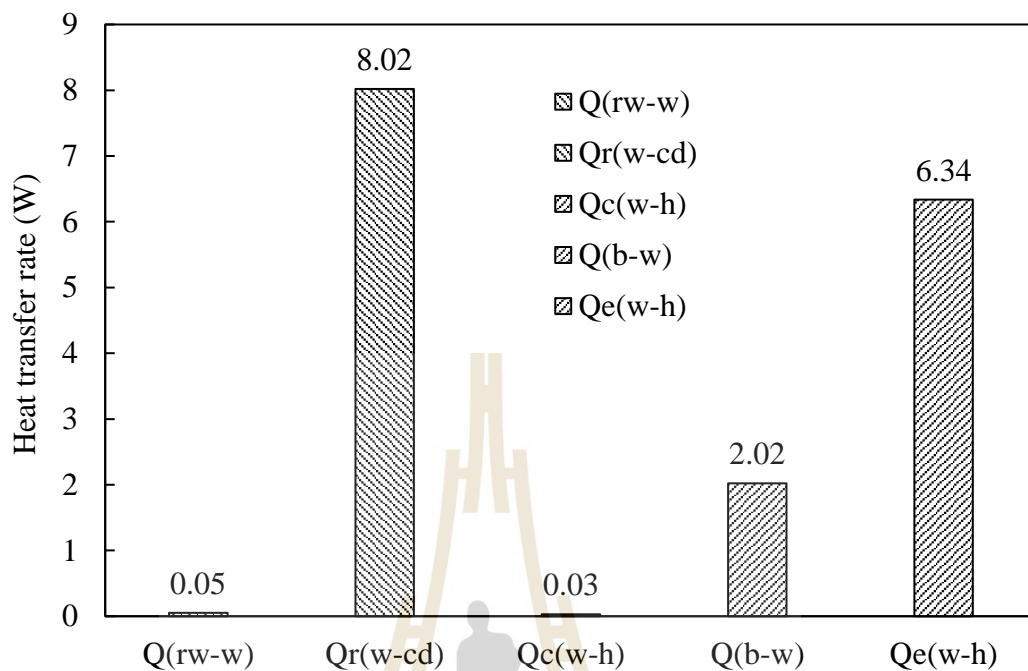
Figure 4.35 Heat transfer rate of water in solar still without glass cover

Figure 4.35 show variation of heat in and out of water in basin without glass cover. brackish water received heat from outlet water in receiver (Q_{rw-w}) and radiative heat transfer from condenser tubes ($Q_{r(w-cd)}$) while it loss heat humid air by convection ($Q_{c(w-h)}$) and evaporation ($Q_{e(w-h)}$), and to basin wall by convection (Q_{b-w}). $Q_{e(w-h)}$ contributes 75.84 percent of heat loss of water, following by Q_{b-w} (24.16 percent) and $Q_{c(w-h)}$. It is observed that total heat in is only 8.07 W, which is proportional to heat for evaporation rate, only 6.34 W.

Figure 4.36 shows heat variation in and out of condenser tubes. Evaporation heat transfer from humid air to condenser tubes ($Q_{c(h-cd)}$) contributes 80.5 percent of the heat absorbed by condenser tubes, convection heat transfer between humid air and condenser (19.5 percent).
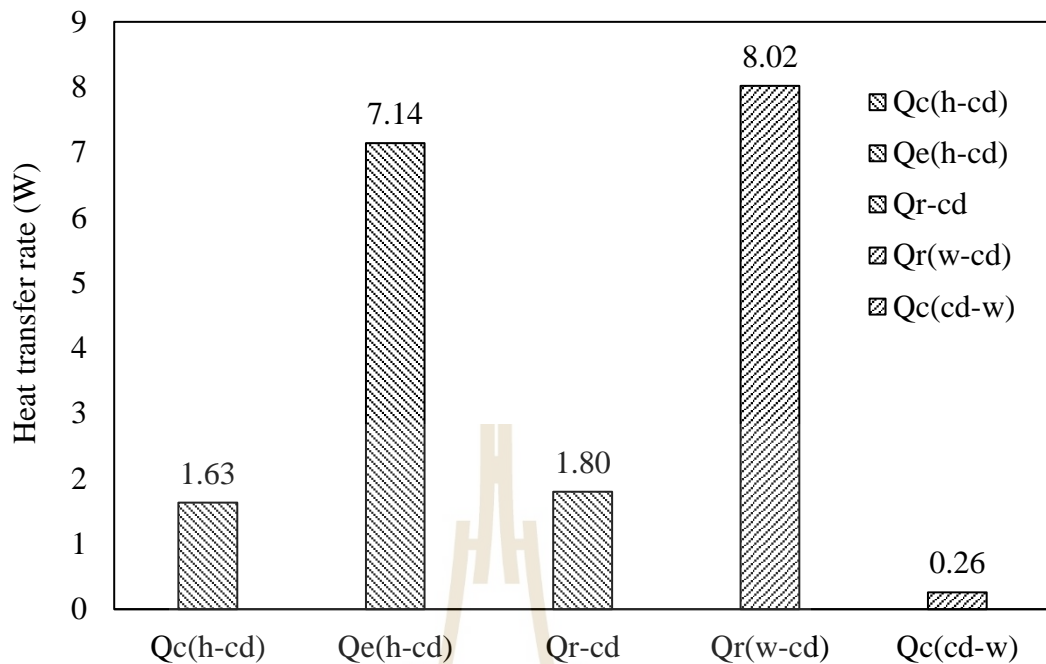
Figure 4.36 Heat transfer rate of condenser tubes in solar still without glass cover

4.4.2.2 Heat transfer rate in solar still with glass cover

Figure 4.37 shows heat variation in and heat out of water in basin with glass cover. As can be seen from the Figure 4.37, evaporative heat transfer from water to humid air ($Q_{e(w-h)}$) contributes 92.2 percent of heat loss of water, following by radiative heat transfer from water to condenser tubes (7.65 percent) and convection heat transfer between water and humid air (0.15 percent). Furthermore, total heat in of Model 3 is 151.44 W, which is 14 higher than that of Model 1. This leads $Q_{e(w-h)}$ increase to 112.15 W, 13 times higher than in Model 1. Hence, I would like emphasize that the glass should be used in proposed solar still.
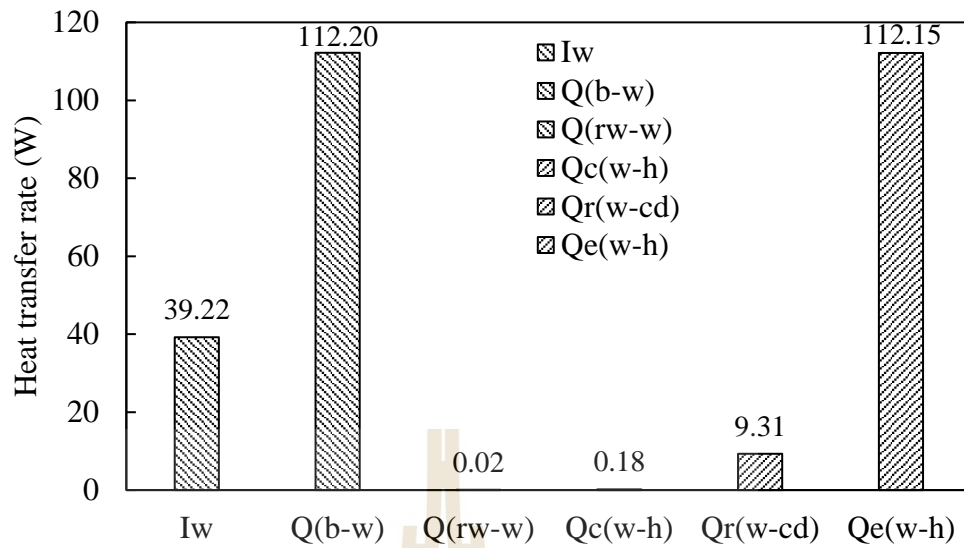
Figure 4.37 Heat transfer rate of water in solar still with glass cover
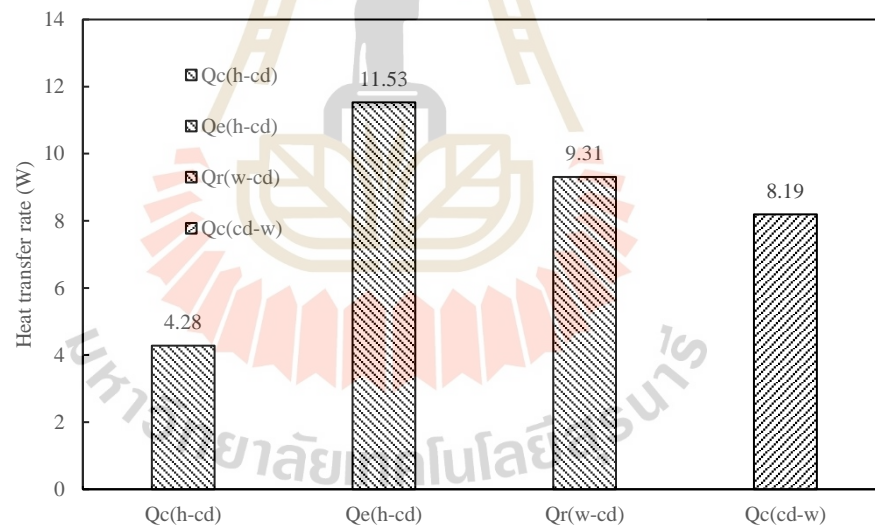
Figure 4.38 Heat transfer rate of condenser tubes with glass cover

Figure 4.38 shows heat variation in and out of condenser tubes. Evaporation heat transfer from humid air to condenser tubes ($Q_{c(h-cd)}$) contributes 57 percent of the heat absorbed by condenser tubes, following by radiative heat transfer

from water to condenser tubes (21.81 percent) and convection heat transfer between humid air and condenser (21.19 percent).

4.4.3 Parameters affecting the solar still productivity

The performance of the proposed solar distillation system is influenced by several parameters. The effect of water depth and mass flow rate on Model 3's performance have been investigated by experimental results, which are presented and discussed in section 4.3. Therefore, this subsection pays attention to the impact of temperature of inlet water, area of condenser and receiver, water depths and mass flow rates theoretically in different conditions of no glass cover, no overflow and normal case.

4.4.3.1 Effect of temperature of water in tank on productivity
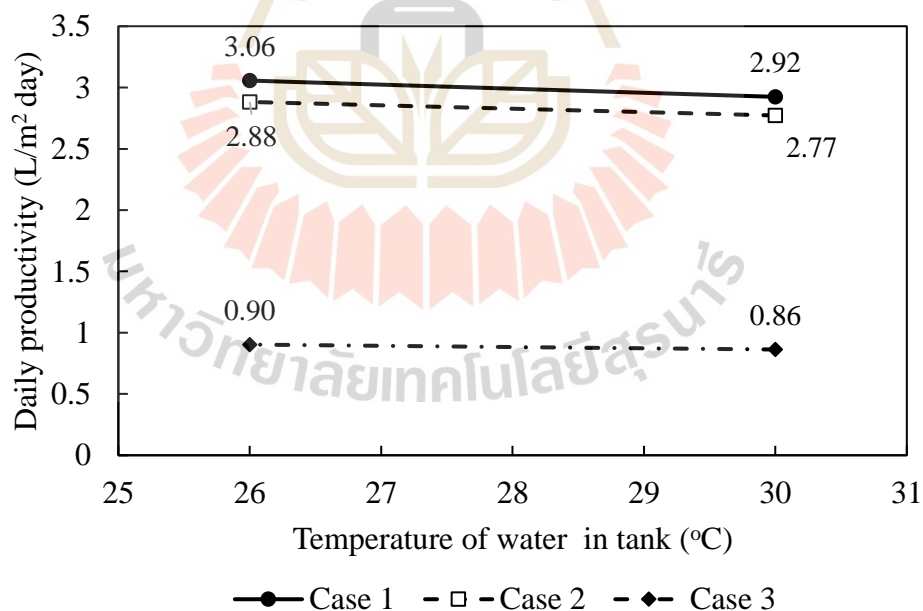
Figure 4.39 Theoretical valuation of temperature of water in tank on productivity

The effect of input water temperature on productivity of proposed solar still for 3 cases were shown in Figure 4.39. It was observed that the cumulated yield decreased with the increase of temperature of inlet water for all 3 cases. The increase of input water will rise temperature of condenser tubes, which reduce condensation rate of water vapor. More apparently, the daily distilled yield of Case 1 is 3 times higher than that of Case 3, which indicated that employing glass have more advantage than solar sill without glass. Therefore, we suggested that basin wall need absorb solar energy in future study related to solar still.

4.4.3.2 Effect of area of condenser and receiver tubes on productivity
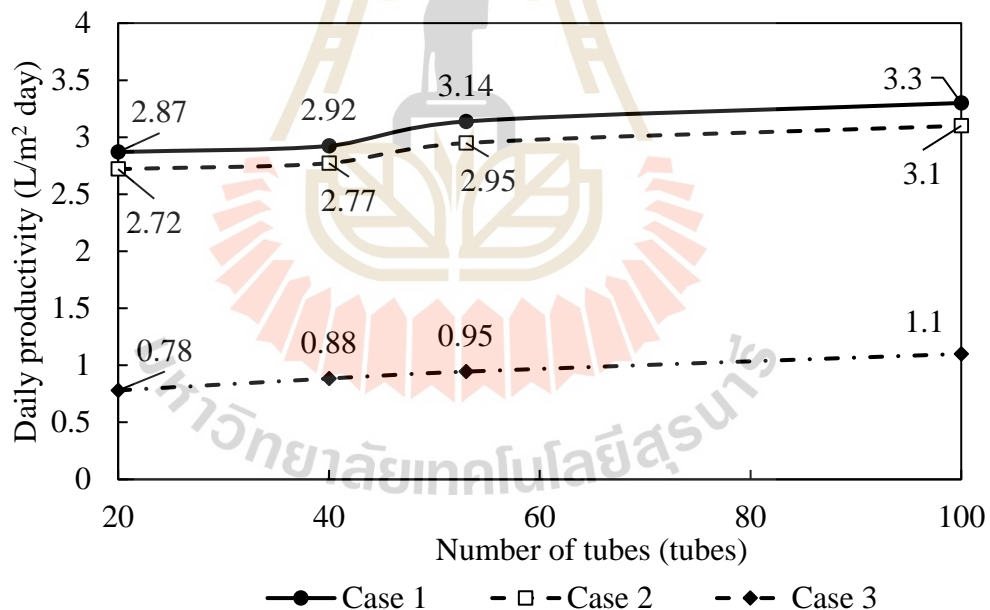
Figure 4.40 Theoretical valuation of number of condenser and receiver tubes on productivity

Figure 4.40 shows the prediction of the daily yield with the change in area of condenser and receiver. It is observed that the daily yield of solar still

is proportional with the number of tubes. The increase of condenser surface's area enhances condensation rate, and the temperature of feed water improves with a larger area of receiver.

4.4.3.3 Effect of water depth on productivity
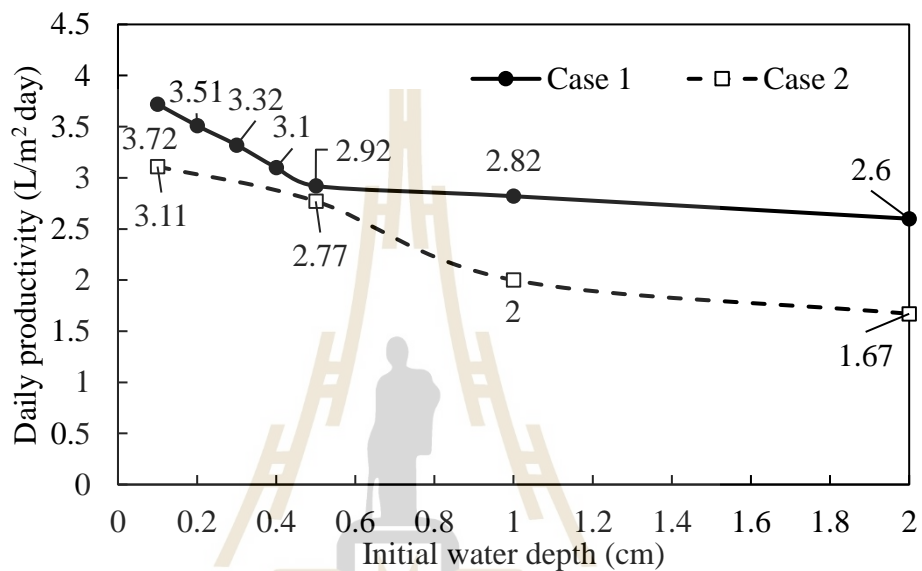
Figure 4.41 Theoretical valuation of water depth of basin water on productivity

The basin water depth is having a considerable impact on the productivity of solar still. Prediction shows that water depth is inversely proportional to the productivity of still. When the depth of water in basin increases, its volumetric heat capacity also increases, which reduces the water temperature for the given solar radiation input. Consequently, the evaporation rate decline resulted in the decrement of productivity. The daily productivity decreases significantly in the case of no overflow due to much higher volumetric heat capacity of basin water. According to the Figure 4.41, we recommend low level of basin water in the proposed solar still.

4.3.4.4 Prediction performance of Model 3 with different mass flow rate and different water depth
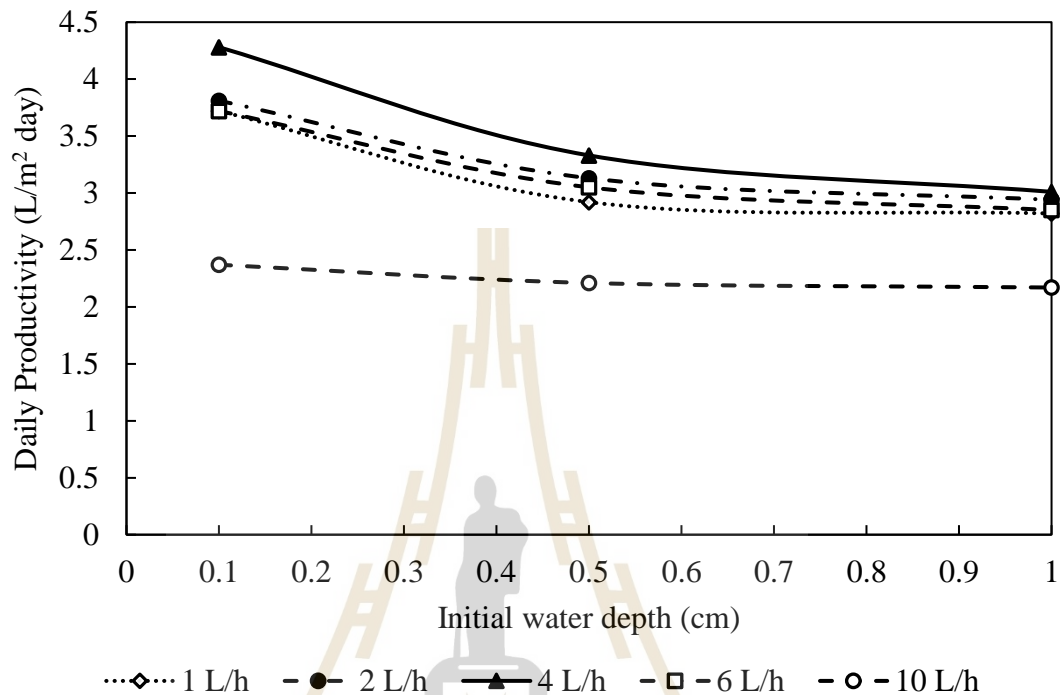
Figure 4.42 Daily distiller yield of Model 3 at different mass flow rates of water in tubes and different basin water depths

        Figure 4.42 shows the accumulate productivity prediction of Model 3 at variation of mass flow rates and water depths. The accumulate yield of Model 3 is predicted to get 4.28 L/m²/day at water depth of 0.1 cm and mass flow rate of 4 L/h. It can be explained that the increase of mass flow rate reduces the temperature of condenser tubes, which improve condensation rate while evaporation rate is anticipated to be the highest among different water levels due to higher temperature of basin water. The theoretical temperature of basin water and outlet water from the receiver with the mass flow rate of 4L/h and 6L/h are shown in the Figure 4.43 and

Figure 4.44, respectively. The temperature of water in basin is predicted to peak at 68.1ºC and 64.68ºC, while the prediction of the temperature of outlet water from receiver reach a peak at 76.1ºC and 70.32ºC. It is apparent that the temperature difference between basin water and outlet water from receiver reduce with the increase of mass flow rate, which lead to reductant of evaporation rate in solar still. Especially, proposed solar still with mass flow rate of 10 L/h has low yield, which is approximate the productivity of a conventional solar still. As shown in Figure 4.45, temperature of water out receiver evenly is lower than that of basin water, which causes the low temperature of water in basin. As a result, it is suggested that in order to get high productivity in Model 3, the water depth should be kept low and mass flow rates is not over 4 L/h.
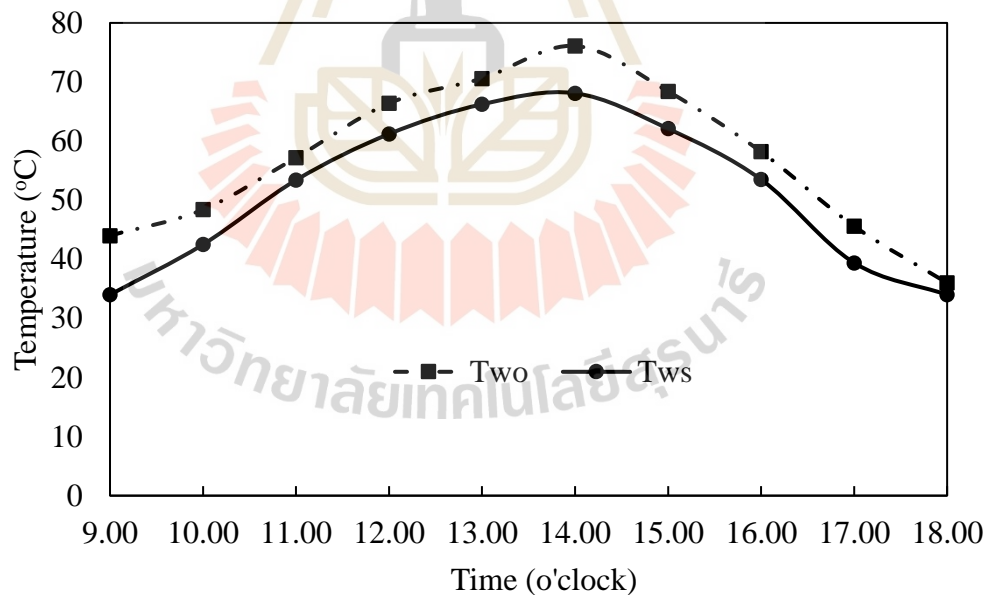
Figure 4.43 Theoretical temperature of outlet water in receiver (Two) and basin water (Tws) at the mass flow rate of water in receiver of 4 L/h and the water depth of basin water of 0.5 cm.
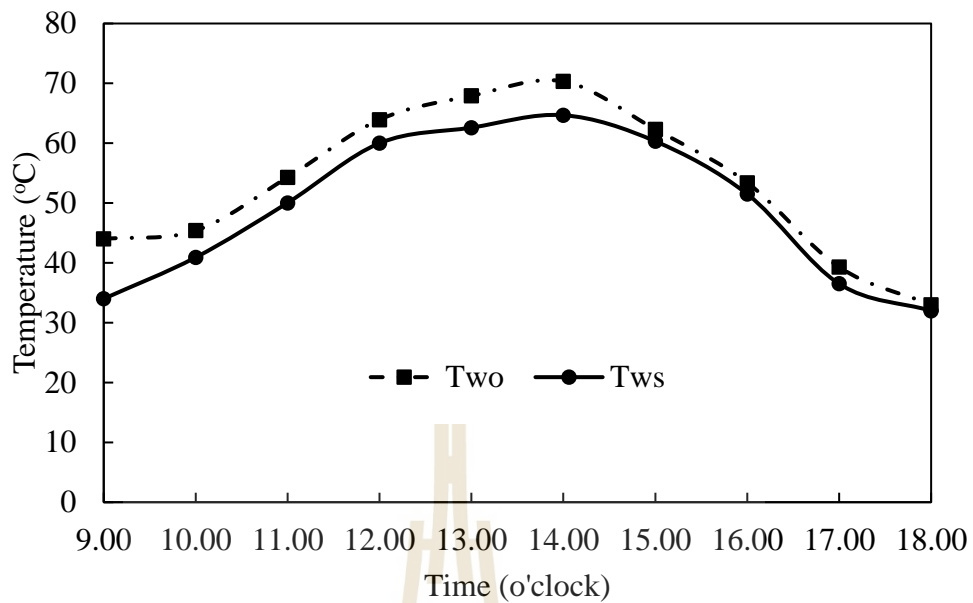
Figure 4.44 Theoretical temperature of outlet water in receiver (Two) and basin water

(Tws) at the mass flow rate of water in receiver of 6 L/h and the water

depth of basin water of 0.5 cm.
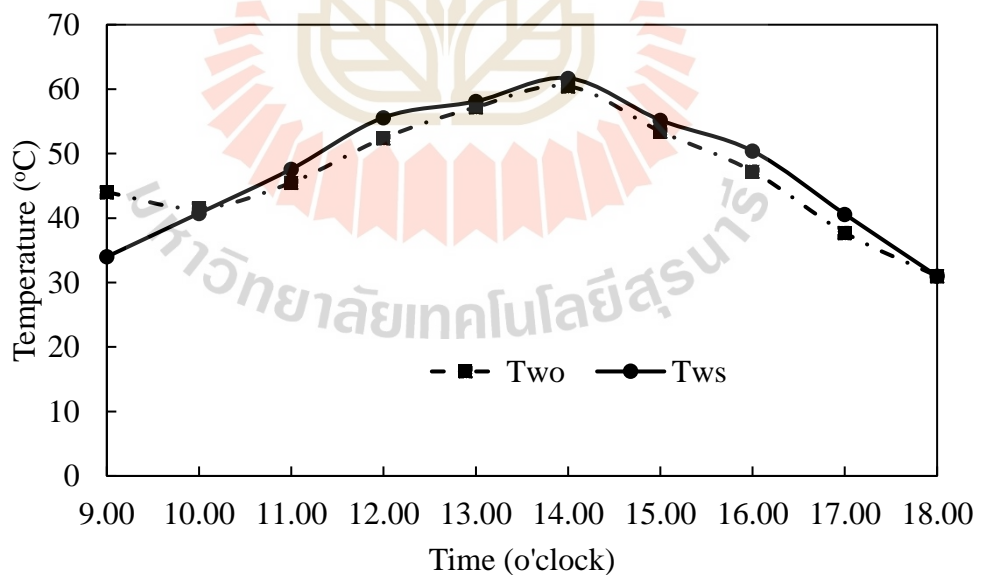

Figure 4.45   Theoretical temperature of outlet water in receiver (Two) and basin water

(Tws) at the mass flow rate of water in receiver of 10 L/h and the water

depth of basin water of 0.5 cm.

CHAPTER V

CONCLUSIONS AND RECOMMENDATIONS FOR

FUTURE WORK

The major conclusions and findings from this study are presented in this chapter. Recommendations for further improvements that should be introduced in theoretical and experimental investigations of the dynamic multi-effect solar water still are highlighted.

5.1   Conclusions

In this research, based on reviews and concept design, the fabrication, implementation and evaluation of three models under the climatic conditions of Nakhon Ratchasima, Thailand have been presented. The analysis of the experimental data enables to underline the following conclusion:

(a)   The effect of mass flow rate was studied in Model 1 and found that the temperature of water and productivity was higher with the mass flow rate of 1 Liter per hour.

(b)   The using of glass cover for 3 sides of Model 2 improve its productivity.

(c)   There is a significant increase in water temperature after flowing through tubes system, especially in Models 2 and 3, even it reaches boiling point at mass flow rate of 0.5 L/h. However, the temperature of water in the still is not as high as expectation in Model 1 and Model 2.

(d)   The effect of water depth and mass flow rate was conducted in Model 3. The results indicate that the decrease of water depth causes the higher temperature of water in solar still and improve the productivity. However, it is opposite with mass flow rate of 0.5 L/h.

(e)   The output of Model 3 declined with the decrease of water mass flow rate.

(f)   The performance of the Model 2 with glass cover and Model 3 were improved compare with conventional solar still. Especially, the yield of Model 3 at water depth 0.5 cm and mass flow rate of 1 L/h increase 67% (3.5 L/h compare to 2.1 L/h of single basin solar still).

(g)   Comparisons of the theoretical and experimental results showed that the developed mathematical model can accurately predict the performance of the proposed solar still.

5.2   Recommendations for future work

The experimental prototype of proposed still can be further modified to provide better performance and higher productivity. Recommendations for improvements to be carried out in future work can be summarized as follows:

(a)   Although Model 1 provided low productivity, it is a promising device for distill brackish water. Further experimental investigation on the performance of Model 1 should be conducted with consideration of water depth in basin. I believe that Model 1 can be improved with some modifications such as: increase thickness of insulator, reduce gap between water in basin and condenser tubes and water depth of water in basin is very thin.

(b)   The productivity of Model 3 can be enhanced when the temperature of glass and condenser tubes reduce. It can be done if we use cooling air and or water flow on their surface. The mass flow rate of cooling fluid on glass's surface and condenser tubes surface should be considered to maximize productivity of Model 3.

REFERENCES

Al -Hinai. H., Al-Nassri, M. S., and Jubran B. A., (2002), Effect of climatic, design and operational parameters on the yield of a simple solar still. Energy Conservation Managerment, 43: 1639 – 50.

Arunkumar, T., Iayaprakash, R., Denkenberger, D., Amimul Ashan, Okundamiya, M. S., Kumar Sanjay, Hiroshi Tanakaand and Aybar, H. S. (2012), An experimental study on hemispherical solar still. Desalination; 286:342–8.

Arunkumar, T., Vinothkumar, K., Amimul Ahsan, Jayaprakash, R., and Sanjay Kumar, (2012), Experimental Study on Various Solar Still Designs. International Scholarly Research Network ISRN Renewable Energy, Volume 2012, Article ID 569381, 10 pages.

Arunkumar, T., Jayaprakash, R., Ahsan Amimul, Denkenberger, D. and Okundamiya MS. (2013). Effect of water and air flow on concentric tubular solar water desalting system, Applied Energy, vol.103, pp. 109–115.

Bassam A.K Abu-Hijleh, (1996), Enhanced solar still performance using water film cooling of the glass cover. Desalination, 107: 235-244

Dhiman Naresh, K., (1988), Transient analysis of a spherical solar still. Desalination, 69(1): 47–55.

Duffie J. and Beckmann W. (1991). Solar engineering of thermal processes, 2nd edition, Wiley Interscience, New York.

Dunkle., R. V., (1962). Solar water distillation the roof type still and a multiple effect diffusion still, paper presented in International Heat Transfer Conference, University of Colorado, Boulder, Colorado, U.S.A.

El-Bahi, A., and Inan., D., (1999), Analysis of a parallel double glass solar still with separate condenser. Renewable Energy, 17: 509-521.

El-Sebaii, A. A., (2000), Effect of wind speed on some designs of solar stills. Energy Conversion & Management, 41: 523-538.

Gnanadason, M. K, Kumar, P. S., Wilson, V. H., and Kumaravel, A., (2014), Productivity enhancement of a-single basin solar still. Desalination and Water treatment, 55: 1998–2008, http://dx.doi.org/10.1080/19443994.2014.930701.

Gnanadason, M. K., Kumar, P. S., Wilson, V. H., Kumaravel, A., and Jebadason., B., (2013), Comparison of performance analysis between single basin solar still made up of copper and GI. International Journal of Innovative Research in Science, Engineering and Technology, 2: 3175–3183.

Hashim, A. Y., Al-asadi, J. M., and Taha., W. A., (2009), Experimental investigation of symmetrical double slope single basin solar stills productivity with different insulation.   Journal of KUFA – PHYSICS, 1: 26–32.

Hiroshi Tanaka and Yasuhito Nakatake. (2006). Theoretical analysis of a basin type solar still with internal and external reflectors. Desalination, 197: 205–216.

Horace McCracken and Joel Gordes, (1985), Understanding solar stills. Volunteers in Technical Assistance (VITA). 37: 9/85

Julio R. Hirschmann, (1975), Solar distillation in Chile. Desalination, Volume 17, Issue 1, Pages 31-67.

Kabeel, A.E., 2009. Performance of solar still with a concave wick evaporation surface. Energy, Elsevier. vol. 34(10), pages 1504-1509.

Khalifa Abdul Jabbar, N., Hamood Ahmad, M., (2009), Effect of insulation thickness on the productivity of basin type solar still: an experimental verification under local climate. Energy Conversation Management, 50: 2457 – 61.

Lawrence, S. A., Gupta S. P., and Tiwari G. N., (1990), Effect of heat capacity on the performance of solar still with water flow over the glass cover. Energy Conversation Management, 30(3): 85-277.

Lobo P. C. and Araujo S. R. D., (1977). Design a simple multi -effect basin type solar still. In: Proceedings international solar energy congress. New Delhi, P 2026.

Mahdi H. , Faramarz S. , Adrian P., (2020), A detailed thermal modeling of a passive single-slope solar still with improved accuracy. Ground water for Sustainable Development. 11: 100384.

Nafey A. S., Abdelkader, M., Abdelmotalip, A. and Mabrouk A. A., (2000), Parameters affecting solar still productivity. Energy Conservation Management, 41: 1797 – 809.

Phadatare, M. K., and Verma, S. K., (2007), Influence of water depth on internal heat and mass transfer in a plastic solar still. Desalination, 217(1–3):267–75.

Rai, S. N., and Tiwari G. N., (1983), Single basin solar still coupled with flat plate collector. Energy Conversion and Management, 23(3): 145–9

Sampathkumar, K., Arjunan, T. V., Pitchandi, P., and Senthilkumar, P., (2010). Active solar distillation - A detailed review. Renewable and Sustainable Energy Reviews, 14: 1503–1526.

Shanmugan, S., Rajamohan, P. and Mutharasu, Performance, D., (2008), Study on an acrylic mirror boosted solar distillation unit utilizing seawater. Desalination, 230:281–7.

Sharqawy, M.H., Lienhard, J.H., Zubair, S.M., (2010), Thermophysical properties of seawater: a review of existing correlations and data. Desalination and water Treat. 16 (1–3): 354–380.

Shiv Kumar, Aseem Dubey and Tiwari, G. N., (2014), A solar still augmented with an evacuated tube collector in forced mode, Desalination, 347: 15–24.

Singh, R. V., Kumar, S., Hasan, M. M., Khan, M. M., and Tiwari G. N., (2013), Performance of a solar still integrated with evacuated tube collector in natural mode. Desalination, 318: 25–33.

Swinbank. (1963). Longwave radiation from clear skies, Quart J. Roy Metorol Soc. 89, 539.

Sodha, M. S., Nayak, J. K., Tiwari, G. N., and Kumar, A. (1980). Double basin solar still. Energy Conversion and Management, 20(1), 23-32.

Taamneh Yazan and Taamneh Madhar, (2012), Performance of pyramid-shaped solar still: experimental study. Desalination, 291:65–8.

Tanaka, H., Nosoko, T. and Nagata, T., (2000), A highly productive basin-type-multiple-effect coupled solar still. Desalination, 130 (3), 279–293.

Thirugnanasambandam, M., Iniyan, S. and Goic, R. (2010). A review of solar thermal technologies. Renewable and Sustainable Energy Reviews. 14(1): 312-322.

Tiwari, A. N., and Tiwari, G. N., (2005), Effect of inclination of condensing cover and water depth in solar still for maximum yield: in winter climatic condition. Solar Energy, 130: 27-33

Tiwari Anil, Kr. and Tiwari, G. N., (2007), Thermal modeling based on solar fraction and experimental study of the annual and seasonal performance of a single slope passive solar still: the effect of water depths. Desalination, 217: 267 – 75.

Tiwari, G. N., (2002). Solar Energy Fundamentals, Design, Modeling and Applications. Alpha Science International Ltd, Pangbourne England.

Tiwari, G. N., Singh, H. N., and Tripathi, R., (2003), Present status of solar distillation. Solar energy, 75(5), 367-373.

Tiwari. G.N., Dimri Vimal, Singh Usha, Chel Aravind and Sarkar Bikash, (2007), Comparative thermal performance evaluation of an active solar distillation system. International Journal of Energy Research, 31: 82-1465.

Tiwari, G. N., and Bapeshwara Rao, V. S. V., (1984), Transient performance of a single basin solar still with water flowing over the glass cover. Desalination, 9: 41-231.

Tripathi, R. and Tiwari, G. N., (2005), Effect of water depth on internal heat and mass transfer for active solar distillation. Desalination, 173: 187 – 200.

Vimal Dimri, Bikash Sarkar, Usha Singh and Tiwari., G. N., (2008), Effect of condensing cover material on yield of an active solar still: an experimental validation. Desalination 227: 178-189.

Yacoub Yousef Ahmad Alotaibi. (2015). Desalination technology; economy and simplicity. International Journal of Engineering Research and Applications. 5: 109-116.

Yousef H. Zurigat and Mousa K. Abu-Arabi, (2004). Modelling and performance analysis of a regenerative solar desalination unit, Applied Thermal Engineering, 24: 1061–1072.

Zaki, G. M., Dali, T. E. I., and Shafiey, H. E. I., (1983), Improved performance of solar stills, paper presented in Solar Energy and the Arab World: Proceedings of 1st Arab International Solar Energy Conference, Kuwait.

Zeinab S. Abdel-Rehim and Ashraf Lasheen, (2007), Experimental and theoretical study of a solar desalination system located in Cairo, Egypt. Desalination 217: 52–64.
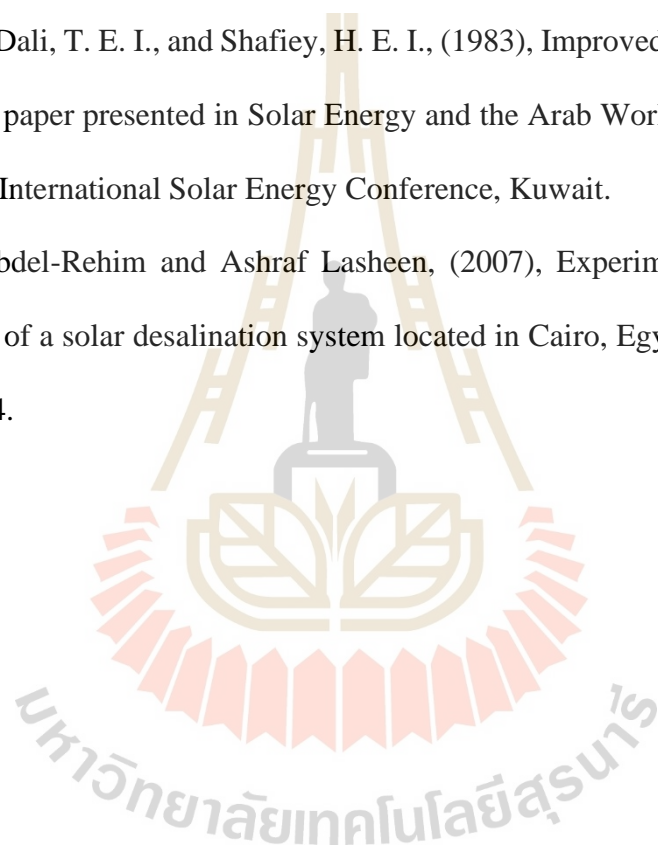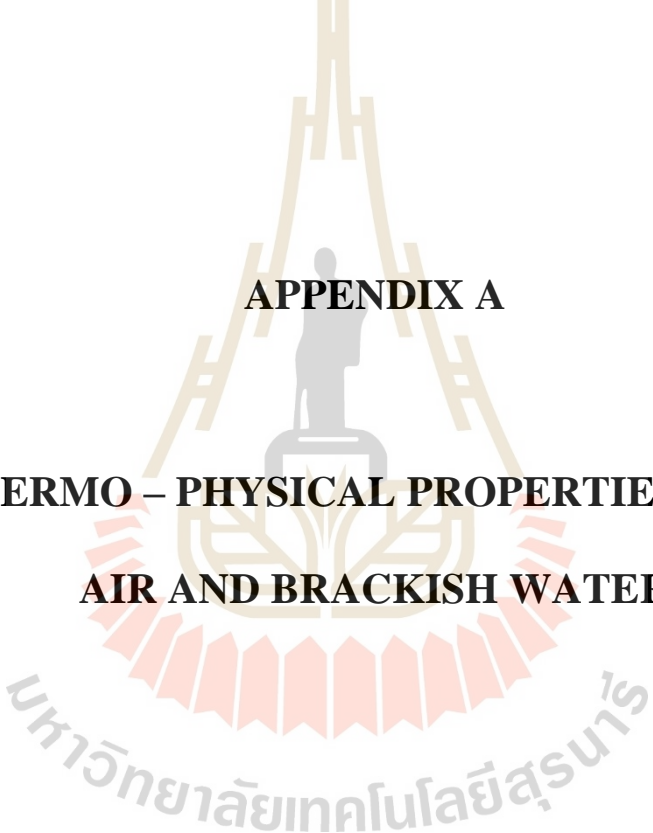
APPENDIX A

THE THERMO – PHYSICAL PROPERTIES OF HUMID

AIR AND BRACKISH WATER

1.   Thermo physical properties of humid air

All values of the thermo-physical properties of the vapor-air mixture can be estimated as follows:

- Dynamic viscosity (kg m^{-1} s^{-1}) is expressed (Poling et al., 2001):

$$\mu_h = \frac{y_a \mu_a}{y_a + y_{wv} A_{a-wv}} + \frac{y_{wv} \mu_{wv}}{y_a A_{wv-a} + y_{wv}} \tag{A-1}$$

While

$$y_a = \frac{P_a}{P} \tag{A-2}$$

$$y_{wv} = \frac{P_{wv}}{P} \tag{A-3}$$

$$A_{a-wv} = \frac{\left(1 + \left(\frac{\mu_a}{\mu_{wv}}\right)^{0.5} \left(\frac{M_{wv}}{M_a}\right)^{0.25}\right)^2}{\left(8\left(1 + \frac{M_a}{M_{wv}}\right)\right)^{0.5}} \tag{A-4}$$

$$A_{wv-a} = \frac{\mu_{wv}}{\mu_a} \frac{M_a}{M_{wv}} A_{a-wv} \tag{A-5}$$

$$P = P_a + P_{wv} \tag{A-6}$$

$$M_a = 28.982 \left(\frac{g}{mol}\right) \tag{A-7}$$

$$M_{wv} = 18.016 \left(\frac{g}{mol}\right) \tag{A-8}$$

$$P_a = exp\left(25.317 - \frac{5144}{T_w + 273}\right) \tag{A-9}$$

$$P_{wv} = exp\left(25.317 - \frac{5144}{(T_g + T_{cd})/2 + 273}\right) \tag{A-10}$$

$$\mu_a = -6.725 \times 10^{-6} + 0.1145 \times 10^{-6} T_h - 1.0 \times 10^{-10} T_h^2 \tag{A-11}$$

$$\mu_{wv} = 5.364286 \times 10^{-6} + 1.25 \times 10^{-9} T_h + 4.642857 \times 10^{-11} T_h^2 \tag{A-12}$$

- Density (kg/m^3)

$$\rho_h = \frac{352.6 \times (1 - 0.378\frac{P_{wv}}{P})}{T_h} \tag{A-13}$$

- Thermal conductivity (W m^{-1} K^{-1})

$$k_h = \frac{y_a k_a}{y_a + y_{wv}A_{a-wv}} + \frac{y_{wv}k_{wv}}{y_a A_{wv-a} + y_{wv}} \tag{A-14}$$

Where

$$k_a = 0.851 \times 10^{-3} + 9.555 \times 10^{-5}T_h - 3.75 \times 10^{-8}T_h^2 \tag{A-15}$$

$$k_{wv} = 1.0843 \times 10^{-3} - 2.314286 \times 10^{-5}T_h + 1.619048 \times 10^{-7}T_h^2 \tag{A-16}$$

- Diffusivity of water vapor in air (m^2/s):

$$D_h = 0.187 \times 10^{-9}T_h^{2.072} \tag{A-18}$$

- Specific heat (J kg^{-1} K^{-1})

$$C_{p,h} = \frac{C_{p,a} + C_{p,wv} \times x}{1 + x} \tag{A-19}$$

While

$$x = 0.622 \times (\frac{P}{P_{wv}} - 1) \tag{A-20}$$

$$C_{p,a} = 1055.05 - 0.3475T_h + 6.25 \times 10^{-4}T_h^2 \tag{A-21}$$

$$C_{p,a} = 3399.476 - 10.83929T_h + 1.916667 \times 10^{-2}T_h^2 \tag{A-22}$$

- Thermal diffusivity (m^2/s)

$$\alpha_h = \frac{1}{\rho_h C_{p,h}} \tag{A-23}$$

2.   Thermo physical properties of brackish water

All values of the thermo-physical properties of brackish water can be expressed as follows (Sharquawy et al., 2010):

- Thermal conductivity (W m^{-1} K^{-1})

$$k_\mathrm{w} = 0.5536 + 2.38 \times 10^{-3} \times T_w - 9.87 \times 10^{-2} T_w^2 \qquad \text{(A-24)}$$

- Density (kg/m^3)

$$\rho_\mathrm{w} = (a_1 + a_2(T_w - 273) + a_3(T_w - 273)^2 + a_4(T_w - 273)^3 \qquad \text{(A-25)}$$
$$+ a_5(T_w - 273)^4) + (b_1 S + b_2 S(T_w - 273)$$
$$+ b_3 S(T_w - 273)^2 + b_4 S(T_w - 273)^3$$
$$+ b_5 S^2(T_w - 273)^4)$$

Where:

$a_1 = 9.999$ x 10^{-2}; $a_2 = 2.304$ x 10^{-2}; $a_3 = $ -6.162 x 10^{-3}; $a_4 = 2.261$ x 10^{-5}; $a_5 = $ -4.657 x 10^{-8};

$b_1 = 8.02$ x 10^2; $b_2 = $ -2.001; $b_3 = 1.677$ x 10^{-2}; $b_4 = $ -3.06 x 10^{-2}; $b_5 = $ -1.613 x 10^{-5}; for $273 < T_w < 453.15$ K and $10 < S < 160$ (g kg^{-1})

- Dynamic viscosity (kg m^{-1} s^{-1})

$$\mu_\mathrm{w} = \mu_{pw}(1 + A \times S + B \times S^2) \qquad \text{(A-26)}$$

Where:

$$A = 1.541 + 1.998 \times 10^{-2}(T_w - 273) - 9.52 \times 10^{-5}(T_w - 273)^2$$

$$B = 7.974 - 7.561 \times 10^{-2}(T_w - 273) + 4.724 \times 10^{-4}(T_w - 273)^2$$

$$\mu_{pw} = 4.2844 \times 10^{-5} + (0.157(T_w - 208.157)^2 - 91.296)^{-1} \qquad \text{(A-27)}$$

for $273 < T_w < 453.15$ K and $0 < S < 150$ (g kg^{-1})

- Specific heat (kJ kg^{-1} K^{-1})

$$C_{pw} = A + B \times T_w + C \times T_w^2 + D \times T_w^3 \qquad \text{(A-28)}$$

A = 5.328 - 9.76 x 10^{-2} S + 4.04 x 10^{-4} S^2

B = -6.913 x 10^{-3} + 7.351 x 10^{-4} S - 3.15 x 10^{-6} S^2

C = 9.6 x 10^{-6} – 1.927 x 10^{-6} S + 8.23 x 10^{-9} S^2

D = 2.5 x 10^{-9} + 1.666 x 10^{-9} S – 7.125 x 10^{-12} S^2

for $273 < T_w < 453.15$ K and $0 < S^2 < 180$ (g kg^{-1})

- Latent heat of vaporization (J kg^{-1})

$$H_v = H_{v,pw} \times \left(1 - \frac{S}{1000}\right) \qquad \text{(A-29)}$$

$$
\begin{aligned}
H_{v,pw} = {} & 2.501 \times 10^6 - 2.369 \times 10^3 (T_w - 273) \qquad \text{(A-30)} \\
& + 2.678 \times 0.1 (T_w - 273)^2 \\
& - 8.103 \times 10^{-3} (T_w - 273)^3 \\
& - 2.079 \times 10^{-5} \times (T_w - 273)^4
\end{aligned}
$$

APPENDIX B

OTHER FIGURE AND TABLE
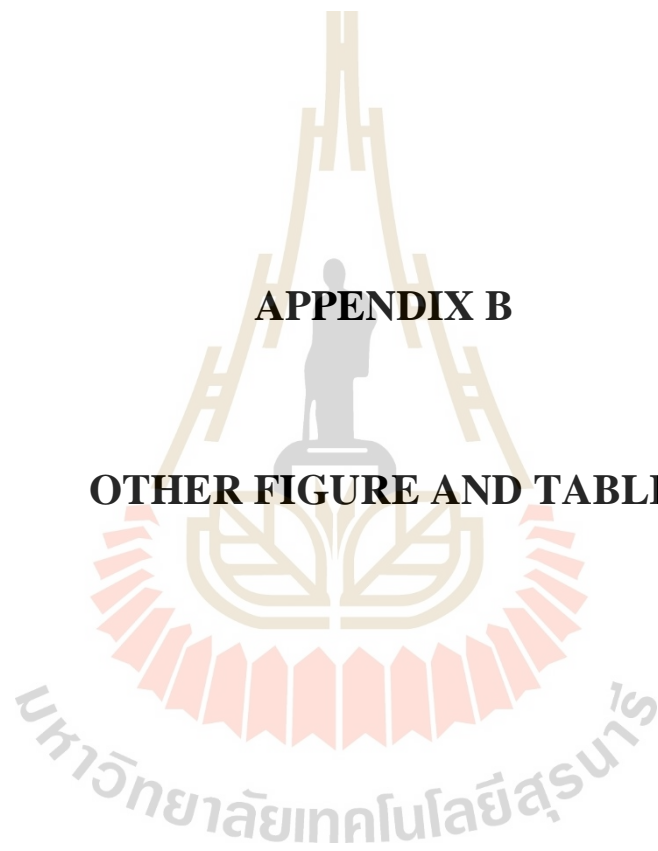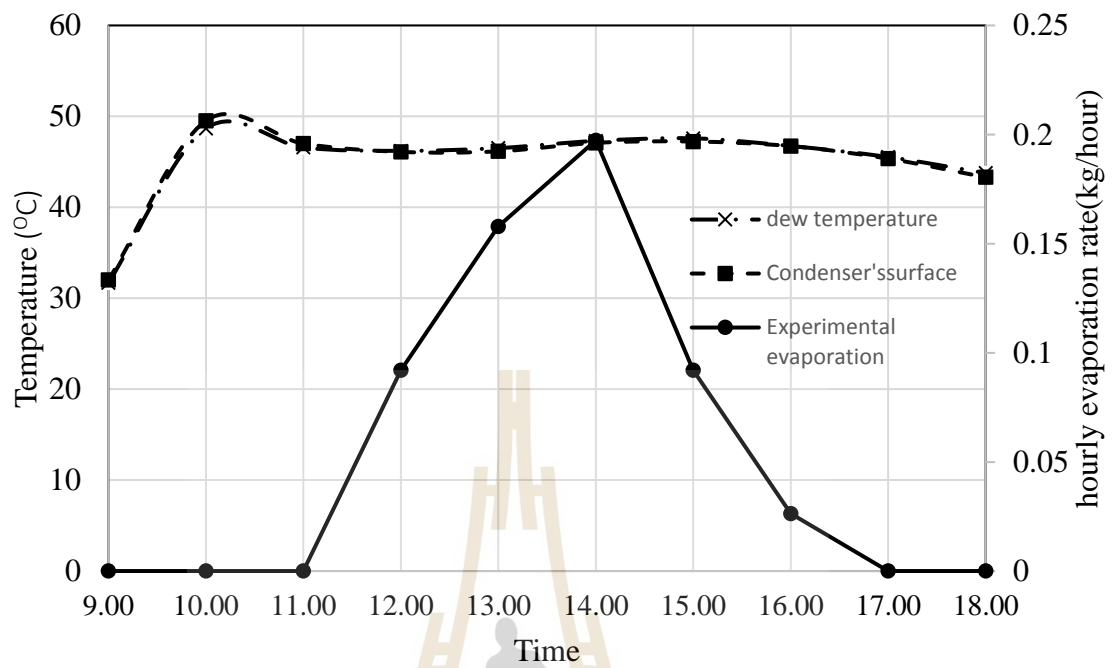
Figure B.1. Theoretical dew point temperature and condenser's surface temperature in

case of solar still without glass and no overflow.

APPENDIX C

MATLAB CODE

```
function  [f,mdot_w_h,f6_1,f6_2,f6_3,f6_4,f6_5,f6_7,f1_1,f1_2,f1_3,f1_4,f1_5,q1] =
f_hieu_ode45_moutput(t,Tf)
[m1,m2]=size(Tf);
if m1>8
   T = Tf(m1,:);
else
   T = Tf;
end
T;
% cd - condenser - T1
% cdw - water in condenser - T2
% r - receiver - T3
% rw - water in receiver - T4
% g - glass - T5
% w - water in basin - T6
% b - basin - T7
% h - humid air - T8
Ng=1;
Acd = 0.18;                      %Area of condenser
Ar = 1.19;                       %Area of receiver
Ag = .304;                       %Area of glass
Aw =.38;                         %Area of water
Ab = .38;                        %Area of basin
%
m_cd = 5;                        %mass of condenser
m_cdw = 0.000289*998;            %mass of water in condenser
m_r = 13;                        %mass of receiver
m_rw = 0.0007225*998;            %mass of water in receiver
m_g = 4.2;                       %mass of glass
m_w = 1.9;                       %mass of water
m_b = 15;                        %mass of basin
m_h = 0.0944*1.12;               %mass of humid air

cp_cd = 390;                     %Heat capacity of condenser
cp_cdw = 4186;                   %Heat capacity of water in condenser
cp_r = 390;                      %Heat capacity of receiver
cp_rw = 4186;                    %Heat capacity of water in receiver
cp_g = 840;                      %Heat capacity of glass
cp_w = 4186;                     %Heat capacity of water in basin
cp_b = 900;                      %Heat capacity of basin
cp_h = 1006;                     %Heat capacity of humid air

alphap_r=0.8;
alphap_g=0.0475;
alphap_w=0.161;
alphap_cd=0.01125;
alphap_b=0.661;
%%%%%%%%%%%%%%%%%%%%%%%%%%%%%%%%%%%%%%%%
```

```
mdot_w = 1/(1000*3600);
Tamb = 31;
q2p = 270;
%%%%%%%%%%%%%%%%%%%%%%%%%%%%%%%%
Lw=1;
Ww=0.38;
Lg=1*10^-3;
Wg=0.38;
Lcd=1;
Wcd=0.38;
V_air=2;
g=9.81;
dwg=0.165;

%%%%%%%%%%%%%%%%%%%%%%%%%%%%%%%%
P_a=exp(25.317-5144/(T(6)+273));
P_wv=exp(25.317-5144/(T(1)+273));
P=P_a+P_wv;
y_a=P_a/P;
y_wv=P_wv/P;
M_a=28.982;
M_wv=18.016;
mu_a=-6.725*10^-6+0.1145*10^-6*(T(8)+273)-1*10^-10*(T(8)+273)^2;
mu_wv=5.364286*10^-6+1.25*10^-9*(T(8)+273)+4.642857*10^-11*(T(8)+273)^2;
A_awv=(1+(mu_a/mu_wv)^0.5*(M_wv/M_a)^0.25)^2/(8*(1+M_a/M_wv))^0.5;
A_wva=(mu_wv/mu_a)*(M_a/M_wv)*A_awv;
mu_h=y_a*mu_a/(y_a+y_wv*A_awv)+y_wv*mu_wv/(y_a*A_wva+y_wv);
ro_a=353/(T(8)+273);
ro_wv=352.6*(1-0.378*P_wv/P)/(T(8)+273);
ro_h=352.6*(1-0.378*P_wv/P)/(T(8)+273);
nu_h=mu_h/ro_h;
Cp_a=1055.05-0.3475*(T(8)+273)+6.25*10^-4*(T(8)+273)^2;
Cp_wv=3399.476-10.83929*(T(8)+273)+1.916667*10^-2*(T(8)+273)^2;
x=0.622*(P/P_wv-1);
Cp_h=(Cp_a+Cp_wv*x)/(1+x);
alpha_h=1/(ro_h*Cp_h);
Ra_h=g*dwg^3*(ro_a/ro_wv-1)/(nu_h*alpha_h);
Nu_h=0.22*Ra_h^(2/5);
k_a=0.851*10^-3+9.555*10^-5*(T(8)+273)-3.75*10^-8*(T(8)+273)^2;
k_wv=1.0843*10^-3-2.314286*10^-5*(T(8)+273)+1.619048*10^-7*(T(8)+273)^2;
k_h=y_a*k_a/(y_a+y_wv*A_awv)+y_wv*k_wv/(y_a*A_wva+y_wv);

%convective heat transfer coefficient between water and humid air
hc_w_h=Nu_h*k_h/(Aw/(2*Lw+2*Ww));

%convective heat transfer coefficient between humid air and glass
hc_h_g=Nu_h*k_h/(Ag/(2*Lg+2*Wg));
```

```
%convective heat transfer coefficient between humid air and condenser
%hc_h_cd = Nu_h*k_h/(Acd/(2*Lcd+2*Wg));
hc_h_cd = Nu_h*k_h/(0.0095*40/2);

%convective heat transfer coefficient between condenser and water in condenser tubes
hc_cd_cdw = 325;

%convective heat transfer coefficient between glass and ambient
hc_g_amb =2.8+3*V_air ;

%convective heat transfer coefficient between basin and water
k_w=0.5536+2.238*10^-3*T(6)-9.87*10^-2*T(6)^2;
mu_w=4.2844*10^-5+(0.157*(T(6)+273-208.157)^2-91.296)^-1;
ro_w=9.999*10^-2+2.034*10^-2*T(6)-6.162*10^-3*T(6)^2+2.261*10^-5*T(6)^3-
4.657*10^-8*T(6)^4;
nu_w=mu_w/ro_w;
betap_w=1/(T(6)+273);
Cp_w=5.328+(-6.913)*10^-3*(T(6)+273)+9.6*10^-6*(T(6)+273)^2+2.5*10^-
9*(T(6)+273)^3;
Gr_w=betap_w*g*ro_w^2*(T(7)-T(6))/(nu_w^2);
Pr_w=Cp_w*nu_w/k_w;
if Gr_w<10^5
  Nu_w=1;
elseif 10^5 < Gr_w < 2*10^7
  Nu_w=0.54*(Gr_w*Pr_w)^0.25;
elseif Gr_w > 2*10^7
  Nu_w=0.14*(Gr_w*Pr_w)^(1/3);
end
hc_b_w = Nu_w*k_w/(Aw/(2*(Lw+Ww)));

%hc_b_w =130;
%radiative heat transfer coefficient between water and condenser
e_w=0.9;
e_g=0.9;
e_cd=0.95;
e_r=0.95;
s=5.67*10^-8;                          %Stefan-Bolzman constant
F_w_cd=((1-e_w)/e_w+2*Lw/(Lw+Lcd-Lg)+((1-e_cd)*Lw/(Lcd*e_cd)))^-1;
hr_w_cd = s*((T(6)+273)^2+(T(1)+273)^2)*(T(6)+T(1)+273*2)/((1-
e_w)/e_w+Aw*(1-e_cd)/(Acd*e_cd)+1/F_w_cd);
%radiative heat transfer coefficient between water and condenser
F_w_g=((1-e_w)/e_w+2*Lw/(Lw+Lcd-Lg)+((1-e_g)*Lw/(Lg*e_g)))^-1;
hr_w_g=s*((T(6)+273)^2+(T(5)+273)^2)*(T(6)+T(5)+273*2)/((1-e_w)/e_w+Aw*(1-
e_g)/(Ag*e_g)+1/F_w_g);

%radiative heat transfer coefficient between glass and sky
Tsky = 0.0552*(Tamb^1.5);
hr_g_sky = s*e_g*((T(5)+273)^2+(Tsky+273)^2)*(T(5)+Tsky+273*2);
```

```
% Ub = 1.2;
% Ub = (s_i/k_i+s_wc/k_wc+1/(5.7+3.8*V_air))^-1;
%Receiver
%convective heat transfer coefficient between receiver and air gap
%delta_a = 0.02; % airgap thickness between receiver and glass
%beta = 15; % tilt angle of receiver
%Nu_a=1+1.44*(1-1708*sin(1.8*beta))^1.6)*(1-
1708/Ra_a*cos(beta))+((Ra_a*cos(beta))^(1/3)-1);
%hc_r_amb=Nu_a*ka/delta_a;
%hc_r_amb = 6;
%convective heat transfer coefficient between receiver and water in receiver
hc_r_rw = 325;
%radiative heat transfer coefficient between receiver and glass of receiver
hr_r_rg = s*(T(3)^2+T_rg^2)*(T(3)+T_rg)/(1/e_g+1/e_r-1)
%hr_r_rg = 10;
%Total heat loss
UL=10;
s_i=0.025;
k_i=0.034;
s_wc=0.01;
k_wc=0.106;
Ub = (s_i/k_i+s_wc/k_wc+1/(5.7+3.8*V_air))^-1;
U_cd=(s_i/k_i+s_wc/k_wc)^-1;
Hv=2.501*10^6-2.369*10^3*T(6)+2.678*0.1*T(6)^2-8.103*10^-3*T(6)^3-
2.079*10^-5 * T(6)^4;
%mdot_w_h = (mdot_h_cd*Acd + mdot_h_g*Ag)/Aw;
D_h=0.187*10^-9*(T(8)+273)^2.072;
Le_h=alpha_h/D_h;
Sh=0.022*(Ra_h*Le_h)^(2/5);
k_m=Sh*D_h/(Aw/(2*Lw+2*Ww));
R=8.314;
cm_w=P_a/(R*(T(8)+273));
cm_h=P_wv/(R*(T(6)+273));

mdot_w_h =k_m*(cm_w-cm_h); %
mdot_h_cd = Aw*mdot_w_h/Acd;
mdot_h_g = Aw*mdot_w_h/Ag;
f = zeros(8,1);

%Condenser
f1_1 = Hv*mdot_h_cd*Acd;
f1_2 = hc_h_cd*Acd*(T(8) - T(1));
f1_3 = hr_w_cd*Acd*(T(6) - T(1));
f1_4 = hc_cd_cdw*Acd*(T(1) - T(2));
%f1_4 = hc_cd_cdw*pi()*0.0085*0.4*40*(T(1) - T(2))
%f1_5 = U_cd*Acd*2*(T(1)-Tamb);
f1_5=U_cd*Acd*(T(3)-T(1));
f(1) = (f1_1 + f1_2 + f1_3 - f1_4-f1_5)/(m_cd*cp_cd);
```

```
%Water in condenser
f2_1 = hc_cd_cdw*Acd*(T(1) - T(2));
f2_2 = mdot_w*cp_cdw*(T(2) - Tamb);
f(2) = (f2_1 -f2_2)/(m_cdw*cp_cdw);

%Receiver
f3_1 = alphap_r*q2p*Ar;
f3_2=UL*Ar*(T(3)-Tamb);
%f3_2 = hc_r_amb*Ar*(T(3) - Tamb);
%f3_3 = hr_r_sky*Ar*(T(3) - Tsky);
f3_4 = hc_r_rw*Ar*(T(3) - T(4));
f(3) = (f3_1 - f3_2 - f3_4)/(m_r*cp_r);

%Water in receiver
f4_1 = hc_r_rw*Ar*(T(3) - T(4));
f4_2 = mdot_w*cp_rw*(T(4) - T(2));
f(4) = (f4_1 - f4_2)/(m_rw*cp_rw);

%Glass
f5_1 = alphap_g*q2p*Ag*Ng;
f5_2 = Hv*mdot_h_g*Ng;
f5_3 = hc_h_g*Ag*(T(8) - T(5))*Ng;
f5_4 = hr_w_g*Aw*(T(6) - T(5))*Ng;
f5_5 = hc_g_amb*Ag*(T(5) - Tamb)*Ng;
f5_6 = hr_g_sky*Ag*(T(5) - Tsky)*Ng;
f(5) = (f5_1 + f5_2 + f5_3 + f5_4 - f5_5 - f5_6)/(m_g*cp_g);

%Water in basin
f6_1 = alphap_w*q2p*Aw*Ng;
f6_2 = hc_b_w*Aw*(T(7) - T(6));
f6_3 = mdot_w*cp_w*(T(4)-T(6));
f6_4 = hc_w_h*Aw*(T(6) - T(8));     %convective heat transfer between water and
                                    humid air
f6_5 = Hv*mdot_w_h*Aw;
f6_6 = hr_w_g*Aw*(T(6) - T(5))*Ng;
f6_7 = hr_w_cd*Aw*(T(6) - T(1)); %Radiative heat transfer between water and
                                 condenser
f(6) = (f6_1 + f6_2 + f6_3 - f6_4 - f6_5 - f6_6- f6_7)/(m_w*cp_w);

%Basin
f7_1 = alphap_b*q2p*Ab*Ng;
f7_2 = hc_b_w*Aw*(T(7) - T(6));
f7_3 = Ub*Ab*(T(7) - Tamb);
f(7) = (f7_1 - f7_2 - f7_3)/(m_b*cp_b);

%Humid air
f8_1 = hc_w_h*Aw*(T(8) - T(6));
```

```
f8_2 = Hv*mdot_w_h*Aw;
f8_3 = Hv*mdot_h_cd*Acd;
f8_4 = Hv*mdot_h_g*Ag*Ng;
f8_5 = hc_h_g*0.794*(T(8) - T(5))*Ng;
f8_6 = hc_h_cd*Acd*(T(8) - T(1));
f(8) = (-f8_1 + f8_2 - f8_3 - f8_4 - f8_5 - f8_6)/(m_h*cp_h);
q1=mdot_w*cp_w*T(4);


clear
clc
% cd - condenser - T1
% wcd - water in condenser - T2
% r - receiver - T3
% wr - water in receiver - T4
% g - glass - T5
% w - water in basin - T6
% b - basin - T7
% h - humid air - T8


%9h-I=270, Ta=31
%T0 = [32 30 56 44 31 44 44 32];
%10h-I=418 Ta=32
%T0 = [35.1 30 52.59 52.59 36.7 41 41.82 40.91];
%11h-I=524 Ta=36
%T0 = [40.56 30 65.37 65.37 43.61 50.62 52 50.54];
%12h-I=561 Ta=38
%T0 = [47.8 30 77.85 77.85 54.32 62.24 63.94 62.19];
%13h-I=641 Ta=40
%T0 = [53.59 30 82.85 82.85 53.7 66.76 69.04 66.72];
%14h-I=361 Ta=39
%T0 = [57.7 30 91.23 91.23 57.8 72.4 75 72.35];
%15h-I=306 Ta=35
%T0 = [56.39 30 68 68 53.23 65.45 67.32 65.36];
%16h-I=118 Ta=33
%T0 = [51.61 30 59.52 59.52 47.57 58.64 60.27 58.56];
%17h-I=0
%T0 = [45.4 30 42.52 42.52 40.63 48.27 49.23 48.27];
%18h-T0=[38.39 38.4 30.0649 30.0656 33.34 37.97 38.43 37.9]


[t,T] = ode45(@f_hieu_ode45_moutput,[0:3600],T0);
T(3599,:)
[f,mdot_w_h,f6_1,f6_2,f6_3,f6_4,f6_5,f6_7,f1_1,f1_2,f1_3,f1_4,f1_5,q1] =
f_hieu_ode45_moutput(t,T);
```

List of Publications

ARTICALES IN JOURNALS

Le, T. H., Chitsomboon, T., and Koonsrisuk, A. (2020). **Solar distillation of water using inclined metal tubes as condenser and receiver**, Accepted to be published by Suranaree Journal of Science and Technology (In press for Vol. 27, No. 4, 6 PP, October-December 2020).

Le, T. H., Chitsomboon, T. and Koonsrisuk, A. (2020). **Development of solar water distiller with a receiver and condenser**, Accepted to be published by IOP Conference Series: Material Science and Engineering (TSME-ICOME2019) Vol. 886, 7 PP, DOI:10.1088/1757-899X/1/012042.

ARTICALES IN CONFERENCES

Le, T. H., Chitsomboon, T. and Koonsrisuk, A. (2019). **Solar distillation of water using inclined tubes as receiver and condenser**: In Proceeding of the 14th Conference on Energy, Heat and Mass Transfer in Thermal Equipment and Processes, Krabi, Thailand, February 20th - 21st, 2019, 5 PP.

Le, T. H., Chitsomboon, T. and Koonsrisuk, A. (2019). **Solar distillation of water using inclined tubes as receiver and condenser**: In Proceeding of the 15th Conference of Energy Network of Thailand, KhaoYai, Thailand, 21st - 24th May,2019, 6 PP.

Le, T. H., Chitsomboon, T. and Koonsrisuk, A. (2020). **Effect of water feed rate and water depth in the basin on solar water distillation**: in Proceeding of the 15th Conference on Energy, Heat and Mass Transfer in Thermal Equipment and Processes, Chantaburi, Thailand, March 12th - 13th, 2020, 5 PP.

Le, T. H., Chitsomboon, T. and Koonsrisuk, A. (2019). **Development of solar water distiller with a receiver and condenser**: The 10th TSME International Conference on Mechanical Engineering, Pattaya, Thailand, 10th - 13rd December 2019, 7 PP.

BIOGRAPHY

Mr. Hieu Tri Le was born on the 28th of September 1989 in Hai Phong province, Vietnam. He graduated Bachelor degree of Marine Engine Engineering at Ship Building Department, Vietnam Maritime University (VMU) on February 2012. He started his work on June 2012 as a lecture at Division of Automotive Engineering, Mechanical Engineering Institute, Vietnam Maritime University, Vietnam. In 2014, he got a scholarship from Suranaree University of Technology, Thailand for Ph.D. degree in the program "SUT-Ph.D scholarship for ASEAN countries". He studied in the field of Mechanical Engineering at School of Mechanical Engineering, Institute of Engineering, Suranaree University of Technology, Thailand. He studied with the thesis title "Solar distillation of water using inclined U-turn metal tubes as receiver and condenser" under the supervision of Assist. Prof. Dr. Atit Koonsrisuk